KfK 2555
Januar 1978

On Parameter Optimization for a Linear Accelerator

— A High Current Deuteron Linear Accelerator —

K. Mittag
Institut für Kernphysik

Kernforschungszentrum Karlsruhe

KERNFORSCHUNGSZENTRUM KARLSRUHE

Institut für Kernphysik

KFK 2555

On Parameter Optimization for a Linear Accelerator

- A High Current Deuteron Linear Accelerator -

K. Mittag

Kernforschungszentrum Karlsruhe GmbH, Karlsruhe

Abstract

On Parameter Optimization for a Linear Accelerator
- A High Current Deuteron Linear Accelerator -

This report presents an analytical method to determine the main parameters of a high current linear accelerator. First, the basic theory on particle dynamics in linear accelerators is reviewed. Particular emphasis has been given to include the space charge effect. Second, the theory is applied to estimate the acceptances of a high current deuteron linear accelerator. The main assumption underlying this approach is that the accelerator structure consists of a sequence of periodic subdivisions.

Zusammenfassung

Parameteroptimierung eines Linearbeschleunigers
- Ein Linearbeschleuniger mit großer Stromstärke für Deuteronen -

Dieser Bericht referiert eine analytische Methode zur Bestimmung der wesentlichen Parameter eines Hochstromlinearbeschleunigers. Zunächst wird ein Überblick über die grundlegenden Aspekte der Theorie der Teilchendynamik in Linearbeschleunigern gegeben, wobei insbesondere die Raumladungseffekte berücksichtigt werden. Dann wird die Theorie angewendet, um die Akzeptanzen eines Deuteronenlinearbeschleunigers mit großem Strahlstrom abzuschätzen. Eine wesentliche Annahme, die dieser Methode zugrunde liegt, ist, daß die Beschleunigungsstruktur aus einer Folge von periodischen Elementen besteht.

Contents

1. Introduction

This report presents an analytical method to determine the main parameters of a linear accelerator. Many books and reports have been written on accelerator theory. This article contains no basic new ideas, but rather unifies methods of various authors into a self consistent approach. A basic assumption underlying this approach is that the accelerator structure consists of a sequence of strictly periodic subdivisions. The validity of this has been discussed in [2),3),4)]. Special emphasis has been given to include an estimate of space charge effects. The method is applied to the design of a high current deuteron linac, as part of a study for an intensive neutron source (INKA) [32)].

2. Basic Formulas

First we recollect some basic formulas from relativistic particle dynamics and from electrodynamics. The definitions of the symbols used in this report are given in Appendix 3. MKS units are used. The coordinate system x, y, z, t is the laboratory system. The z-axis is identical with the axis of the linear accelerator.

2.1 Relativistic particle dynamics [1)]

$$v = \frac{dz}{dt} \; ; \qquad \beta = \frac{v}{c} = \frac{\sqrt{\gamma^2 - 1}}{\gamma} \; ; \qquad \gamma = \frac{1}{\sqrt{1-\beta^2}} \tag{1}$$

$$\frac{d\beta}{d\gamma} = \frac{1}{\beta\gamma^3} \; ; \qquad \frac{d(\gamma\beta)}{dt} = \gamma^3 \frac{d\beta}{dt} = c\,\frac{d\gamma}{dz} \tag{2}$$

$$\vec{p} = m\gamma\vec{v} \; ; \quad W = m\gamma c^2 = \sqrt{(pc)^2 + (mc^2)^2} \; ; \quad \frac{dW}{d(pc)} = \beta \tag{3}$$

$$E_{kin} = mc^2(\gamma - 1)$$

2.2 Maxwell's equations and Lorentz forcce [1)]

$$\nabla \cdot \vec{D} = \varrho \; ; \qquad \nabla \times \vec{H} = \vec{J} + \frac{\partial \vec{D}}{\partial t} \tag{4}$$

$$\nabla \times \vec{E} + \frac{\partial \vec{B}}{\partial t} = 0 \; ; \qquad \nabla \cdot \vec{B} = 0 \tag{5}$$

$$\vec{D} = \varepsilon_0 \vec{E} + \vec{P} \; ; \qquad \vec{H} = \frac{\vec{B}}{\mu_0} - \vec{M} \tag{6}$$

$$\frac{d\vec{p}}{dt} = q\left(\vec{E} + \vec{v} \times \vec{B}\right) \tag{7}$$

$$\frac{dW}{dt} = q\,\vec{v} \cdot \vec{E} \tag{8}$$

$$\mu_0 = 4\pi \cdot 10^{-7}\ \frac{Vs}{Am} \; ; \qquad \varepsilon_0 = 8.8542 \cdot 10^{-12}\ \frac{As}{Vm}$$

$$c = \frac{1}{\sqrt{\varepsilon_0 \mu_0}} = 2.9979 \cdot 10^8\ \frac{m}{s}$$

3. Accelerating field in the beam hole region [2),3),4)]

3.1 Wave equation

In order to arrive at some handy equations, one has to start **right** away with approximations. These are chosen to be valid for acceleration by a sequence of rf gaps having cylindrical symmetry around the beam axis. Examples for this are the Alvarez-, Wideroe- or iris type accelerators. The symmetry of the helical structure is more complicated, and so are the fields, although the accelerating E_z - wave turns out to be identical for both cases [5),6),7)].

Polar coordinates (z, r, ϑ) are used from now on.

Assumptions: [2)]

$\frac{\partial}{\partial \vartheta} = 0$ (rotational symmetry) (9)

$\vec{P} = 0, \quad \vec{M} = 0$ (vacuum)

$\rho = 0, \quad \vec{J} = 0$ (the beam current is treated later in first order perturbation theory)

$B_z = 0$ (TM field only, TE field neglected)

Using Maxwells equations one obtains [2)]

$$\frac{\partial^2 E_z}{\partial z^2} + \frac{1}{r}\frac{\partial E_z}{\partial r} + \frac{\partial^2 E_z}{\partial r^2} = \frac{\partial^2 E_z}{c^2 \partial t^2} \quad \text{(wave equation)} \tag{10}$$

$$\frac{1}{r}\frac{\partial (r E_r)}{\partial r} = -\frac{\partial E_z}{\partial z}; \quad E_\vartheta = 0; \quad \frac{\partial E_x}{\partial x} = \frac{\partial E_y}{\partial y} = -\frac{1}{2}\frac{\partial E_z}{\partial z} \tag{11}$$

$$-c^2 \frac{\partial B_\vartheta}{\partial z} = \frac{\partial E_r}{\partial t}; \quad B_r = 0 \tag{12}$$

To obtain E_r and B_ϑ from E_z the relation $\int xI_o(x)dx = xI_1(x)$ turns out to be useful (I_o, I_1 are modified Bessel functions).

3.2 Space harmonics [3]

We are looking for stationary solutions only, and therefore assume a harmonic dependence on time. We choose a standing wave field as we are mainly concerned with standing wave accelerators:

$$E_z(z,r,t) = E_z(z,r) \cos \omega t \; ; \quad \omega = 2\pi f \; ; \quad c = \lambda f \qquad (13)$$

The accelerator structure is assumed to consist of geometrically strictly periodic accelerating cells of length L (see Fig. 1). We choose the origin of our coordinate system to be in the center of such a cell. We expand the z-dependence of $E_z(z,r)$ into a Fourier series. The various terms of this series are called space harmonics, if they are written in the travelling wave form.

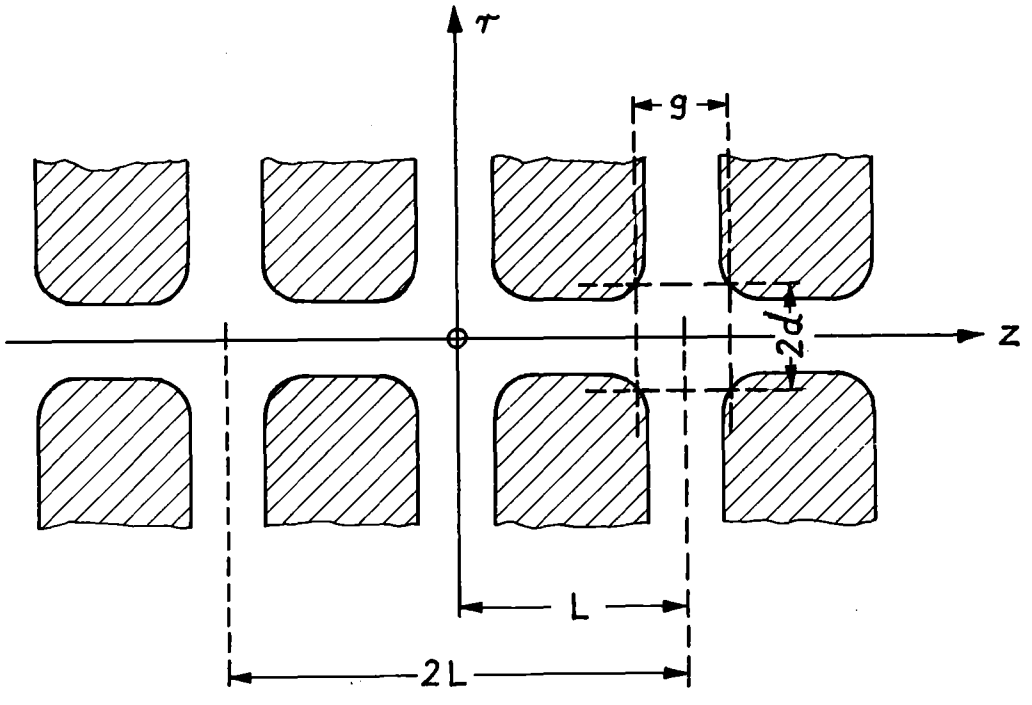

Fig. 1: Geometry close to the beam axis

$$E_z(z,r) = \sum_{m=0}^{\infty} \left[a_m(r) \cos \frac{m\pi z}{L} + b_m(r) \sin \frac{m\pi z}{L} \right] \qquad (14)$$

$$a_0(r) = \frac{1}{2L} \int_{-L}^{L} E_z(z,r)\, dz$$

$$a_m(r) = \frac{1}{L} \int_{-L}^{L} E_z(z,r) \cos \frac{m\pi z}{L}\, dz ; \qquad m \neq 0$$

$$b_m(r) = \frac{1}{L} \int_{-L}^{L} E_z(z,r) \sin \frac{m\pi z}{L}\, dz$$

For this expansion we take a geometrical period of a length of 2 L, which includes two accelerating cells, and therefore two gaps. In this manner structures operating in the π-mode can be treated easily as well. In the π-mode two cells form one electrical period. We assume the field to be symmetric about the center of a cell:

$$E_z(z,r) = E_z(-z,r) \qquad (15)$$

Therefore: $b_m = 0$, and

$$E_z(z,r,t) = \sum_{m=0}^{\infty} a_m(r) \cos \frac{m\pi z}{L} \cos \omega t \qquad (16)$$

This expansion must satisfy the wave equation for E_z. From this one gets conditions for the coefficients $a_m(r)$:

$$\sum_{m=0}^{\infty} \left[\frac{\partial^2 a_m(r)}{\partial r^2} + \frac{1}{r} \frac{\partial a_m(r)}{\partial r} - k_m^2 a_m(r) \right] \cos \frac{m\pi z}{L} = 0 \qquad (17)$$

Applying the orthogonality relations of the trigonometric functions (23) we find that each $a_m(r)$ must satisfy Bessel's modified differential equation:

$$a_m(r) = A_m I_0(k_m r) \tag{18}$$

$$E_z(z,r,t) = \sum_{m=0}^{\infty} A_m I_0(k_m r) \cos\frac{m\pi z}{L} \cos\omega t \tag{19}$$

$$k_m^2 = \left(\frac{2\pi}{\lambda}\right)^2 \left[\left(\frac{m\lambda}{2L}\right)^2 - 1\right] \tag{20}$$

From this the other field components can be derived to be:

$$E_r(z,r,t) = \sum_{m=0}^{\infty} \frac{A_m m\pi}{k_m L} I_1(k_m r) \sin\frac{m\pi z}{L} \cos\omega t \tag{21}$$

$$B_\varphi(z,r,t) = -\sum_{m=0}^{\infty} \frac{A_m \omega}{k_m c^2} I_1(k_m r) \cos\frac{m\pi z}{L} \sin\omega t \tag{22}$$

A main reason for writing the fields as a Fourier series is that particles having the same velocity as one of the space harmonics see on the average only the field of this single space harmonic. The mathematical reason for this is the property of the orthogonality relations of the trigonometric functions:

$$\int_{-L}^{L} \sin\frac{m\pi z}{L} \sin\frac{n\pi z}{L}\, dz = \begin{cases} L & \text{if } m = n \neq 0 \\ 0 & \text{if } m = n = 0 \text{ or if } m \neq n \end{cases} \tag{23}$$

$$\int_{-L}^{L} \cos\frac{m\pi z}{L} \cos\frac{n\pi z}{L}\, dz = \begin{cases} L & \text{if } m = n \neq 0 \\ 2L & \text{if } m = n = 0 \\ 0 & \text{if } m \neq n \end{cases}$$

$$\int_{-L}^{L} \sin\frac{m\pi z}{L} \cos\frac{n\pi z}{L}\, dz = 0 \qquad \text{m and n are integers.}$$

The coefficients A_m of the field expansion can be found in terms of the field on the accelerator axis from (14) and (18):

$$A_o = \int_{-L}^{L} E_z(z,r)\,dz \Big/ \left(2L\,I_o(k_o r)\right)$$

$$A_m = \int_{-L}^{L} E_z(z,r)\cos\frac{m\pi z}{L}\,dz \Big/ \left(I_o(k_m r)\,L\right), \qquad m \neq 0 \tag{24}$$

A_s A_m does not depend on r we get:

$$A_o = \int_{-L}^{L} E_z(z,r=0)\,dz \Big/ (2L)$$

$$A_m = \int_{-L}^{L} E_z(z,r=0)\cos\frac{m\pi z}{L}\,dz \Big/ L, \qquad m \neq 0 \tag{25}$$

3.3 Estimate of amplitude of space harmonics [3),4)]

For many types of accelerating structures the following approximation is reasonable:

$$E_z(z,r=d) = \frac{E_o L}{g} = \text{const., for } -\frac{g}{2} \leq z \leq \frac{g}{2}$$

$$E_z(z,r=d) = (-1)^p \frac{E_o L}{g} \text{ for } \pm L - \frac{g}{2} \leq z \leq \pm L + \frac{g}{2} \tag{26}$$

$$p = 0,\ 1,\ 2,\ 3,\ \ldots\ldots$$

$$E_z(z,r=d) = 0 \text{ elsewhere.}$$

$p\pi$ gives the phase shift of the field from one cell to the next. One says that the structure is operated in the $p\pi$-mode. Inserting the boundary conditions (26) into (24), (25) one obtains:

$$A_0 = \frac{E_0}{I_0(k_0 d)}\,; \quad A_m = \frac{2E_0 \sin\frac{m\pi g}{2L}}{I_0(k_m d)\,\frac{m\pi g}{2L}}\,, \qquad \text{if p+m is even} \qquad (27)$$

$$A_m = 0, \qquad \text{if p+m is odd}$$

Also: $$E_0 = I_0(k_0 d)\int_{-L/2}^{L/2} E_z(z, r=0)\,dz \,/\, L \qquad \text{if p is even}$$

Generally $$I_0(k_0 d) = J_0\left(\frac{2\pi d}{\lambda}\right) \approx 1 \qquad (28)$$

$$E_0 = \int_{-L/2}^{L/2} E_z(z, r=d)\,dz \,/\, L \approx \int_{-L/2}^{L/2} E_z(z, r=0)\,dz \,/\, L, \quad \text{if p is odd,}$$

and if the penetration of fields through the drift tube can be neglected: $\vec{E}(z = L/2, r) \approx 0$. E_0 can be determined by numerical methods, e. g. by the LALA-, CLASL- or SUPERFISH-programs [8),9),10)]. The gap distance g (see Fig. 1) has to be determined at that radius r = d at which E_z does not depend on z **($g \approx g_i + 0.85\ r_i$; r_i is the inner corner radius of the drift tube bore and g_i the geometrical gap distance)** [11),12)].

3.4 Synchronous condition

The standing wave field (19) written as a sum of travelling waves (space harmonics) looks like:

$$E_z(z, r, t) = \sum_{m=0}^{\infty} \frac{A_m}{2} I_0(k_m r)\left[\cos\left(\frac{m\pi z}{L} - \omega t\right) + \cos\left(\frac{m\pi z}{L} + \omega t\right)\right] \qquad (29)$$

We consider only the case in which the relative change of particle velocity due to acceleration is small, so that the assumption of a constant particle velocity is justified for each accelerator period:

$$1/v = \int_{-L}^{L} \frac{dz}{v(z)} \,/\, 2L \qquad (30)$$

Synchronism between a particle of a velocity v_s and the space harmonic number p is fullfilled if v_s equals the phase velocity v_w of that space harmonic:

$$V \approx v_s = v_w = \frac{\omega L}{p\pi} \tag{31}$$

This synchronous condition can be written as

$$L = \frac{p\beta_s\lambda}{2} \tag{32}$$

Let φ be the phase of the particle relative to the field, then:

$$\omega t + \varphi \approx \frac{\omega z}{v_s} + \varphi = \frac{p\pi z}{L} + \varphi \tag{33}$$

Other important relations are:

$$k_p = \frac{2\pi}{\gamma_s\beta_s\lambda} \tag{34}$$

and if the approximations of section 3.3 are allowed:

$$A_p \approx 2E_oT \tag{35}$$

In this equation we have introduced the transit time factor T:

$$T = \frac{\sin(\pi g/\beta_s\lambda)}{(\pi g/\beta_s\lambda)I_o(k_pd)} \tag{36}$$

This relation does not depend explitely on p, although to obtain it, synchronism between particle and the p-th space harmonic was essential.

3.5 Acceleration and defocussing by a standing wave

We now calculate the longitudinal energy gain of a particle synchronous to space harmonic number p over one accelerator period:

$$q\int_{-L}^{L} E_z(z,r,t+\varphi)\,dz = q\sum_{m=0}^{\infty} A_m I_0(k_m r)\int_{-L}^{L}\cos\frac{m\pi z}{L}\cos\left(\frac{p\pi z}{L}+\varphi\right)dz$$

$$= q A_p L I_0(k_p r)\cos\varphi$$

$$\approx q\,2E_0 L T I_0(k_p r)\cos\varphi \qquad (37)$$

Now we turn to the energy gained in transverse direction, again over one accelerator period. Using for the fields the expressions (21), (22) we get:

$$q\int_{-L}^{L}\left[E_r(z,r=\text{const},t+\varphi) - v\,B_\vartheta(z,r=\text{const},t+\varphi)\right]dz$$

$$= -q L A_p \frac{I_1(k_p r)}{\gamma}\sin\varphi$$

$$\approx -q\,2E_0 L T \frac{I_1(k_p r)}{\gamma}\sin\varphi \qquad (38)$$

The result of our calculation is that on the average the energy gain of the particle both longitudinally and transversely results from the influence of the p-th space harmonic only. To obtain this result it was essential to assume that the radial position of the particle does not change over one period. Due to strong focussing, rf defocussing and space charge forces this is strictly not true. However, handy equations are obtained by this averaging procedure, which therefore will be used in the following treatment.

3.6 Smooth approximation for the rf field

We are now looking for a single travelling wave which gives over one accelerator period the same energy gain in longitudinal and transverse direction as the standing wave field of section 3.2. Using the approximations of section 3.3 it can be written as:

$$E_z(z,r,t) = E_0 T I_0(k_p r)\cos\left(\omega t - \frac{\omega z}{\beta_w c}\right)$$

$$E_r(z,r,t) = -\gamma_w E_0 T I_1(k_p r)\sin\left(\omega t - \frac{\omega z}{\beta_w c}\right) \qquad (39)$$

$$B_\vartheta(z,r,t) = -\frac{\beta_w \gamma_w}{c} E_0 T I_1(k_p r)\sin\left(\omega t - \frac{\omega z}{\beta_w c}\right)$$

$$E_0 = \frac{\int_{-L/2}^{L/2} E_z(z,r=0)\,dz}{L}\ ; \qquad k_p = \frac{2\pi}{\gamma_w \beta_w \lambda} \qquad (40)$$

$$T = \frac{\sin(\pi g/\beta_w\lambda)}{(\pi g/\beta_w\lambda)\, I_0(k_p d)}\ ; \qquad L = \frac{p\beta_w\lambda}{2} \qquad (41)$$

The phase velocity β_w of this travelling wave will be chosen to be equal to the particle design velocity β_s . The phase

$$\varphi = \omega t - \frac{\omega z}{\beta_w c} \qquad (42)$$

for a particle of velocity β_s remains approximately constant over one period, and the energy gain both longitudinally and transversely will on the average be the same as in the standing wave case. Therefore we can use this simpler travelling wave field to put into the equations of motion. This method is called smooth approximation.

4. Space charge forces [4),13)]

A modern linear accelerator accelerates bunches which contain on the order of 10^{10} charged particles, which repel each other. To solve the coupled equations of their motion is not possible, even with modern high speed computers. Therefore some assumption about the distribution of the particles inside a bunch has to be made, to simplify the problem. Various approaches to this have been reported in the literature [4),13)-20)].

In individual particle computer programs a bunch is represented by up to a few thousand representative particles, which are traced along the accelerator taking into account the Coulomb forces among them.

Much less time consuming are programs in which a bunch is represented by a three dimensional ellipsoid of uniform charge density all along the accelerator. This assumption leads to simple expressions for the space charge forces, however, it is not self - consistent [13),19)]. Generally, the image forces of the structure walls, the forces between bunches, the scattering of particles within the bunch, and the influence of residiual gas electrons and ions are neglected in these calculations.

The electric field inside such an ellipsoid can be written as [4),21)]

$$E_{\varrho x} = \frac{\varrho}{\varepsilon_0}\left(1-\beta_s^2\right) M_x X\,; \quad E_{\varrho Y} = \frac{\varrho}{\varepsilon_0}\left(1-\beta_s^2\right) M_Y Y\,; \quad E_{\varrho z} = \frac{\varrho}{\varepsilon_0} M_z Z \qquad (43)$$

The distances X,Y,Z from the origin of the ellipsoid and the space charge density ρ are measured in the laboratory system x,y,z. The ellipsoid is moving at the speed β_s along the z-axis, its axes being parallel to the ones of the coordinate system.

$$M_u = \frac{a_x a_y a_z}{2} \int_0^\infty \frac{d\tau}{(a_u^2+\tau)\sqrt{(a_x^2+\tau)(a_y^2+\tau)(a_z^2+\tau)}}\,; \quad u = x,y,z \qquad (44)$$

a_x and a_y are the transverse semiaxes of the ellipsoid; $a_z = b/(\sqrt{1-\beta_s^2})$ is the longitudinal one in the ellipsoid's own system, b the one in the laboratory system.

Generally $M_x + M_y + M_z = 1 \qquad (45)$

If $a_x = a_y$ then: $M_x = M_y = \frac{1 - M_z}{2} \qquad (46)$

$$M_z = \frac{1-\ell^2}{\ell^3}\left(\frac{1}{2}\ln\frac{1+\ell}{1-\ell} - \ell\right);\quad \ell = \sqrt{1-\frac{a_x^2}{a_z^2}}\ ;\ \text{if } a_x < a_z$$

$$M_z = \frac{1+\ell_1^2}{\ell_1^3}\left(\ell_1 - \arctan\ell_1\right);\quad \ell_1 = \sqrt{\frac{a_x^2}{a_z^2}-1}\ ;\ \text{if } a_x > a_z \qquad (47)$$

$$M_z = \frac{1}{3} = M_x = M_y\ ;\qquad \text{if } a_x = a_z$$

If the bunches follow one another at a frequency f, the beam current I is given by

$$I = \frac{\rho\ 4\pi\ a_x a_y b}{3}\ f \qquad (48)$$

In an accelerator with strong focussing by quadrupoles the transverse beam cross section is not circular, so the form factors M_u should be calculated by (44) [18]. To obtain simpler analytic expressions it is a common practice [13),14),15)] to approximate the transverse elliptic cross section by a circular one of radius

$$a = \sqrt{a_x a_y}\ . \qquad (49)$$

The validity of this approximation is checked in appendix 1. Some authors improve it by a correction factor

$$\left\{\frac{2a_{x,y}}{a_x+a_y}\right\}, \qquad (50)$$

so that for the case $a_z \to \infty$ the formulas for an infinite elliptic cylinder are obtained [19),20)]:

$$E_{\varrho x} = \frac{\varrho}{\varepsilon_0}\left(1-\beta_s^2\right)\ \frac{1-M}{2}\left\{\frac{2a_y}{a_x+a_y}\right\}X;\quad E_{\varrho y} = \frac{\varrho}{\varepsilon_0}\left(1-\beta_s^2\right)\frac{1-M}{2}\left\{\frac{2a_x}{a_x+a_y}\right\}Y \qquad (51)$$

$$E_{\varrho z} = \frac{\varrho}{\varepsilon_0}MZ\ ;\qquad M = M_z\left(a_x = a_y = a;\ a_z\right)$$

As the space charge forces are of importance only at small particle velocities, most often the relativistic correction factors are neglected.

5. Focussing forces

Focussing in the transverse direction is generally achieved by strong focussing quadrupole systems. If focussing is in the x-, and defocussing in the y-direction the forces F inside a quadrupole of gradient $B' = \frac{\partial B_x}{\partial y} = \frac{\partial B_y}{\partial x}$ are [22]

$$F_{QP,x} = -qvB'x \; ; \quad F_{QP,y} = qvB'y. \tag{52}$$

The contributions of the Lorentz-force due to transverse velocities have been neglected.

Alternating phase focussing has been suggested as an alternative focussing method for slow particles in high gradient accelerator systems [23),24].

6. Equations of motion [2),3),4]

This chapter recollects the differential equations for both the longitudinal and transverse motion in a linear accelerator. From (1) and (8) one gets for the longitudinal notion:

$$\frac{dW}{dz} = qE_z \tag{53}$$

The contribution of the transverse motion to the change in energy is neglected.

From (1), (3), (7) follows for the radial motion:

$$\beta c \frac{d}{dz}\left(m\gamma\beta c \frac{dr}{dz}\right) = q\left(\vec{E} + \vec{v}_z \times \vec{B}\right)_r \tag{54}$$

z rather than t has been chosen to be the independent variable. Now we consider the influence of the rf field in smooth approximation (3.6). The space charge forces are taken into account by assuming a bunch to be a homogeneously charged ellipsoid (4). Focussing is achieved by quadrupoles (5).

The amplitude of the accelerating wave and the accelerator period is chosen such that there exists a synchronous particle on the accelerator axis which has the speed β_s and a constant phase φ_s relativ to the wave.

The motions of all the other particles are calculated relativ to the synchronous particle. From (42), (1), (2), (3):

$$\frac{d(\varphi-\varphi_s)}{dz} = \omega\left(\frac{dt}{dz}-\frac{dt_s}{dz}\right) = \frac{\omega}{c}\left(\frac{\beta_s-\beta}{\beta\beta_s}\right) \approx -\frac{2\pi(W-W_s)}{\lambda\beta_s^3\gamma_s^3 mc^2} \qquad (55)$$

from (53), (39), (42), (43)

$$\frac{d(W-W_s)}{dz} = q\left\{E_0 T I_0(k_\rho r)\left[\cos\varphi-\cos\varphi_s\right]+\frac{\varrho}{\varepsilon_0}M_z Z\right\} \qquad (56)$$

In (56) it has been assumed that the position of the synchronous particle is identical with the center of the charged ellipsoid. Therefore from (42) for any fixed time t one has:

$$\varphi-\varphi_s = -\frac{2\pi}{\beta_w\lambda}Z \qquad (57)$$

Combining (55), (56), (57) yields the second-order differential equation governing the longitudinal motion:

$$\frac{d}{dz}\left(\beta_s^3\gamma_s^3\frac{d(\varphi-\varphi_s)}{dz}\right)=\frac{q}{mc^2}\left\{-\frac{2\pi}{\lambda}E_0 T I_0(k_\rho r)\left[\cos\varphi-\cos\varphi_s\right]+\frac{\varrho}{\varepsilon_0}M_z\beta_w(\varphi-\varphi_s)\right\} \qquad (58)$$

From (54), (39), (43), (52) we get for the transverse motion:

$$\frac{d}{dz}\left(\beta\gamma\frac{dX}{dz}\right)=\frac{q}{mc^2}\left\{-E_0TI_1(k_pX)\sin\varphi\;\frac{\gamma_w(1-\beta\beta_w)}{\beta}+\frac{\varrho}{\varepsilon_0}\frac{(1-\beta_s^2)}{\beta}M_xX-cB'X\right\}\quad(59)$$

$$\frac{d}{dz}\left(\beta\gamma\frac{dY}{dz}\right)=\frac{q}{mc^2}\left\{-E_0TI_1(k_pY)\sin\varphi\;\frac{\gamma_w(1-\beta\beta_w)}{\beta}+\frac{\varrho}{\varepsilon_0}\frac{(1-\beta_s^2)}{\beta}M_yY+cB'Y\right\}\quad(60)$$

If the change of parameters β_s, γ_s, E_0T, φ_s along the accelerator is sufficiently small, they can be considered to be piecewise constant. Then the equations of motion are solved piecewise. A distinguished discription of this idea is that the acceleration is assumed to be adiabatic.

The equations of motion will be simplified by further approximations in the following chapters. Generally $\beta_w = \beta_s$ will be taken.

7. Longitudinal motion [2),3),4),13)]

7.1 Motion close to the beam axis

In the following we consider only the particle motion close to the beam axis for which

$$I_0(k_p r)\approx 1\quad(61)$$

holds. We introduce:

$$\Delta\varphi=\varphi-\varphi_s\;;\qquad \Delta W=W-W_s\quad(62)$$

$$k_\ell^2=-\frac{q\,2\pi\,E_0T}{mc^2\,\lambda\,\beta_s^3\gamma_s^3}\sin\varphi_s\quad(63)$$

$$\mu_\ell=\frac{q\,\varrho\,M_z}{mc^2\,\varepsilon_0\,\beta_s^2\gamma_s^3\,k_\ell^2}\quad(64)$$

Using (48), the relation $3/(4\pi\varepsilon_0 c) = 90\ \Omega$:

$$\tilde{\mu} = \frac{90\,\Omega\, q\, I\, \lambda}{mc^2 \beta_s^2 \gamma_s^3} \tag{65}$$

one has $$\mu_\ell = \frac{\tilde{\mu}\, M_z}{a_x a_y b\, k_\ell^2} \tag{66}$$

Then (58) can be written in the form

$$\frac{1}{\beta_s^3 \gamma_s^3} \frac{d}{dz}\left(\beta_s^3 \gamma_s^3 \frac{d\Delta\varphi}{dz}\right) = -k_\ell^2 \left[\frac{(\cos\varphi_s - \cos\varphi)}{\Delta\varphi \sin\varphi_s} - \mu_\ell\right] \Delta\varphi \tag{67}$$

μ_ℓ is the ratio of the defocussing space charge force to the restoring force of the rf field. In the following μ_ℓ is assumed to be independent of z, which means that the dimensions of the bunch do not change along the accelerator. Under these assumptions the longitudinal motion is independent of the radial one. Expansion of the trigonometric functions as a function of $\Delta\varphi$ yields:

$$\cos\varphi_s - \cos\varphi \approx \sin\varphi_s \Delta\varphi + \cos\varphi_s \frac{\Delta\varphi^2}{2} - \sin\varphi_s \frac{\Delta\varphi^3}{6} - \cos\varphi_s \frac{\Delta\varphi^4}{24} + \ldots\ldots \tag{68}$$

Then $$\frac{\cos\varphi_s - \cos\varphi}{\Delta\varphi \sin\varphi_s} \approx 1 + \frac{\Delta\varphi}{2\tan\varphi_s} \approx 1 + \frac{\Delta\varphi}{2\varphi_s}, \tag{69}$$

if φ_s is not too large. Using this approximation the differential equation for the longitudinal motion turns out to be:

$$\frac{1}{\beta_s^3 \gamma_s^3} \frac{d}{dz}\left(\beta_s^3 \gamma_s^3 \frac{d\Delta\varphi}{dz}\right) = -k_\ell^2 \left(1 + \frac{\Delta\varphi}{2\varphi_s} - \mu_\ell\right) \Delta\varphi \tag{70}$$

We define:

$$\varphi_{sg} = \varphi_s (1 - \mu_\ell); \qquad k_{\ell g}^2 = k_\ell^2 (1 - \mu_\ell) \tag{71}$$

Then (70) is written as

$$\frac{1}{\beta_s^3 \gamma_s^3} \frac{d}{dz}\left(\beta_s^3 \gamma_s^3 \frac{d\Delta\varphi}{dz}\right) = -k_{\ell s}^2 \left(1+\frac{\Delta\varphi}{2\varphi_{ss}}\right)\Delta\varphi \qquad (72)$$

This has the same form as (70) in the zero space charge limit $\mu_\ell = 0$.

7.2 Acceptance

The particles are performing stable damped oscillations in the $\Delta\varphi$ - ΔW - phase space if $\Delta\varphi$ and ΔW are not too large. The area in this phase space for which the particle motion is stable is called the longitudinal acceptance of the accelerator A_ℓ. The maximum excursions of $\Delta\varphi$ and ΔW can be calculated exactly in the zero space charge limit [2] using equation (67):

$$2\varphi_s \leq \varphi \leq -\varphi_s ; \qquad \varphi_s \leq 0 \qquad (73)$$

$$\Delta W_{max} = \sqrt{\frac{2}{\pi} \lambda q E_0 T mc^2 \beta_s^3 \gamma_s^3 \left(\varphi_s \cos\varphi_s - \sin\varphi_s\right)} \qquad (74)$$

The oscillations in the longitudinal phase space are stable only if $\varphi_s \leq 0$. This means that the synchronous particle reaches the center of the accelerating gap at a moment, when the accelerating field is still rising. Thereby particles ahead of the synchronous one get less acceleration, particles trailing get more acceleration.

Analysing (72) shows that approximately the acceptance in the non-zero space charge case [13] can be obtained from (73), (74) by substituting φ_s by $\varphi_s (1-\mu_\ell)$ As

$$\varphi_s \cos\varphi_s - \sin\varphi_s \approx -\frac{\varphi_s^3}{3} + \frac{\varphi_s^5}{30} \qquad (75)$$

one then has:

$$2\varphi_s(1-\mu_\ell) \leq \varphi \leq -\varphi_s(1-\mu_\ell); \quad \varphi_s \leq 0 \tag{76}$$

$$\Delta W_{max} = \sqrt{-\frac{2\lambda}{3\pi} q E_0 T mc^2 \beta_s^3 \gamma_s^3 \varphi_s^3 (1-\mu_\ell)^3} \tag{77}$$

Equation (76) shows that generally the position of the synchronous particle is not identical with the center of the bunch, although this had been assumed in (56).

The acceptance area A_ℓ in the $\Delta\varphi$ - ΔW - phase space can be approximated by that of an ellipse:

$$A_\ell \approx \pi \frac{3|\varphi_s|(1-\mu_\ell)}{2} \Delta W_{max} \tag{78}$$

The maximum current I_ℓ which can be accelerated in the longitudinal phase space can be estimated in the following manner [4),13)]. Starting from (65), (66), then expressing the length of the bunch b by a width in phase $\Delta\varphi_{max}$ by means of (57),

$$b = \beta_s \lambda \frac{\Delta\varphi_{max}}{2\pi} \tag{79}$$

and taking from (76) that

$$\Delta\varphi_{max} \leq \frac{\tau\, 3|\varphi_s|(1-\mu_\ell)}{2} \tag{80}$$

one has:

$$I_\ell \leq \frac{a_x a_y E_0 T \varphi_s \sin\varphi_s}{60\Omega M_z \lambda} \tau (1-\mu_\ell)\mu_\ell \tag{81}$$

τ is a safety factor, which according to Vlasov [4] should be about 3/4. By assuming this value one excludes phase motions in the extreme nonlinear region. However, Gluckstern in[13] reports that the currents actually observed in linacs, and those calculated numerically by more realistic models are considerably higher than those predicted using $\tau = 1$.

If one approximates M_z by [13]

$$M_z \approx \frac{\sqrt{a_x a_y}}{3b} \quad \text{valid for} \quad 0.8 < \frac{b}{\sqrt{a_x a_y}} < 5 \tag{82}$$

one obtains

$$I_\ell \leq \frac{3\beta_s \sqrt{a_x a_y}\; E_0 T\, \varphi_s^2\, |\sin\varphi_s|\, \tau^2 (1-\mu_\ell)^2 \mu_\ell}{80\pi\Omega} \tag{83}$$

Optimizing I_ℓ as a function of μ_ℓ yields

$$I_\ell \leq \frac{\tau^2 \beta_s \sqrt{a_x a_y}\; E_0 T\, \varphi_s^2\, |\sin\varphi_s|}{180\pi\Omega} \;;\; \mu_\ell = \frac{1}{3} \tag{84}$$

7.3 Liouville's theorem

The equations (55), (56), (57), (62) can be written in the form of canonical equations with a Hamiltonion

$$H = -\frac{\pi}{\lambda \beta_s^3 \gamma_s^3 mc^2} (\Delta W)^2 - q E_0 T I_0(k_p \tau)(\sin\varphi - \varphi\cos\varphi_s) + \frac{\varrho M_z \beta_w \lambda}{\varepsilon_0 4\pi} (\Delta\varphi)^2 \tag{85}$$

$$\frac{d(\Delta W)}{dz} = -\frac{\partial H}{\partial(\Delta\varphi)} \;; \qquad \frac{d(\Delta\varphi)}{dz} = \frac{\partial H}{\partial(\Delta W)} \tag{86}$$

Therefore Liouville's theorem applies to the motion in the $\Delta\varphi$-ΔW-plane also, if the space charge forces are approximated in the manner of chapter 4. This theorem states among other that the phase volume $\Delta\varphi\ \Delta W$ (for the radial direction $\Delta r\ \Delta r'$) is a constant of motion, if coupling between longitudinal and transverse motions is neglected.

7.4 Phase oscillations of small amplitude

For small deviations from the synchronous phase equation (72) can be further simplified (see (1), (2), (53), (39), (42)):

$$\frac{1}{\beta_s^3\gamma_s^3}\frac{d}{dz}\left(\beta_s^3\gamma_s^3\frac{d\Delta\varphi}{dz}\right) = \frac{d^2\Delta\varphi}{dz^2} + \frac{qE_0T\cos\varphi_s}{mc^2}\frac{3}{\beta\beta_s\gamma_s}\frac{d\Delta\varphi}{dz} = -k_{\ell s}^2\,\Delta\varphi \qquad (87)$$

The acceleration can be considered as adiabatic if

$$\left|\frac{\dfrac{qE_0T\cos\varphi_s}{mc^2}\ \dfrac{3}{\beta\beta_s\gamma_s}\ \dfrac{d\Delta\varphi}{dz}}{k_{\ell s}^2\,\Delta\varphi}\right| \ll 1 \qquad (88)$$

We take $\beta_s \approx \beta$ and call $\Delta(\Delta\varphi)$ the change of $\Delta\varphi$ over a length of $\beta_s\lambda$. Then the condition (88) can be written as:

$$\left|\frac{3\gamma_s^2}{2\pi\tan\varphi_s\,(1-\mu_\ell)}\ \frac{\Delta(\Delta\varphi)}{\Delta\varphi}\right| \ll 1 \qquad (89)$$

For large particle energy ($\gamma_s >> 1$) there are no longer phase oscillations, as the particle velocity does not depend any more on its energy. We therefore consider only the case $\gamma_s \approx 1$. Generally $\varphi_s \approx -30^\circ$, $\mu_\ell \leq 0.5$, then

$$\frac{\Delta(\Delta\varphi)}{\Delta\varphi} \ll 1 \qquad (90)$$

is the condition for adiabaticity.

Under these assumptions the equations of motion in the $\Delta\varphi$ - ΔW phase space are (see (87), (56), (57), (61), (55), (64), (71), (62)) :

$$\frac{d^2\Delta\varphi}{dz^2} + k_{\ell s}^2 \Delta\varphi = 0 \qquad (91)$$

$$\frac{d^2\Delta W}{dz^2} + k_{\ell s}^2 \Delta W = 0 \qquad (92)$$

$$\frac{d\Delta W}{dz} = \beta_s^3 \gamma_s^3 mc^2 \frac{\lambda}{2\pi} k_{\ell s}^2 \Delta\varphi \qquad (93)$$

$$\Delta W = -\beta_s^3 \gamma_s^3 mc^2 \frac{\lambda}{2\pi} \frac{d\Delta\varphi}{dz}$$

The oscillations are stable if $k_{\ell\rho}^2 > 0$, which is the case only if $\varphi_s < 0$ and $\mu_\ell < 1$.

If we take as solution of (91):

$$\Delta\varphi = \phi \cos k_{\ell s} z \qquad (94)$$

then the solution of (93) is:

$$\Delta W = \sqrt{-q E_o T \sin\varphi_s \beta_s^3 \gamma_s^3 mc^2 \frac{\lambda}{2\pi} (1-\mu_\ell)}\ \phi \sin k_{\ell s} z \qquad (95)$$

As the parameters like β_s, φ_s and E_oT will change along the accelerator the amplitude of the oscillations will change too. One can relate the amplitudes $\Delta\varphi_1$ and ΔW_1 at a point 1 in the linac with those at a point 2 by making use of Liouville's theorem (see 7.3):

$$\Delta\varphi_1 \, \Delta W_1 = \Delta\varphi_2 \, \Delta W_2 \tag{96}$$

and assuming an adiabatic change of parameters:

$$\Delta W_i = \sqrt{-q E_{o_1} T_1 \sin\varphi_{s_i} \beta_{s_i}^3 \gamma_{s_i}^3 mc^2 \frac{\lambda}{2\pi} (1-\mu_{\ell_i})} \, \Delta\varphi_i \,, \quad i = 1,2 \tag{97}$$

Then $$\frac{\Delta\varphi_2}{\Delta\varphi_1} = \frac{\Delta W_1}{\Delta W_2} = \left[\frac{E_{o_1} T_1 \sin\varphi_{s_1} \beta_{s_1}^3 \gamma_{s_1}^3 (1-\mu_{\ell_1})}{E_{o_2} T_2 \sin\varphi_{s_2} \beta_{s_2}^3 \gamma_{s_2}^3 (1-\mu_{\ell_2})} \right]^{\frac{1}{4}} \tag{98}$$

With increasing particle velocity the oscillations of the phase are damped, whereas the absolute spread in energy increases. The behavior of phase oscillations of large amplitudes is generally studied only numerically.

8. Transverse motion close to the beam axis

We shall write down only the formulas for motion in the x-direction. The one in the y-direction can be obtained by substituting x with y, and y with x. Like for the longitudinal motion the rf field close to the beam axis is expanded into a Taylor series and only the first term of this expansion is kept:

$$I_1(k_p x) \approx \frac{k_p x}{2} \tag{99}$$

Using this and $\beta_w = \beta_s \approx \beta$, (59) is simplified to

$$\frac{d}{dz}\left(\beta_s \gamma_s \frac{dx}{dz}\right) = \frac{q}{mc^2} \left\{ \frac{-\pi E_o T \sin\varphi}{\lambda \beta_s^2 \gamma_s^2} + \frac{\varrho \, M_x}{\varepsilon_o \beta_s \gamma_s^2} - cB' \right\} x \tag{100}$$

One defines

$$k_{t,rf}^2 = -\frac{q}{mc^2}\,\frac{\pi E_0 T \sin\varphi}{\lambda \beta_s^3 \gamma_s^3} = \frac{k_e^2 \sin\varphi}{2 \sin\varphi_s} \qquad \text{(see (63))} \tag{101}$$

$$k_{t,q}^2 = \frac{q}{mc^2}\,\frac{cB'}{\beta_s \gamma_s} = \frac{qB'}{m\gamma_s v_s} \tag{102}$$

$$k_t^2 = k_{t,q}^2 - k_{t,rf}^2 \tag{103}$$

$$\mu_t = \frac{q}{mc^2}\,\frac{\varrho M_x}{\varepsilon_0 \beta_s^2 \gamma_s^3 k_t^2} = \frac{\tilde{\mu} M_x}{a_x a_y b k_t^2} \tag{104}$$

$$k_{t\varrho}^2 = k_t^2 (1 - \mu_t) \tag{105}$$

With these definitions (100) can be written as

$$\frac{1}{\beta_s \gamma_s}\,\frac{d}{dz}\left(\beta_s \gamma_s \frac{dX}{dz}\right) = -k_t^2 (1 - \mu_t) X = -k_{t\varrho}^2 X \tag{106}$$

In evaluating this equation one should keep in mind that many of the variables on which $k_{t\varrho}^2$ depends are themselves dependent on z: B' changes sign going from a focussing to a defocussing quadrupole, being zero in between; for the effect of the rf field we have used the smooth approximation (see chapter 3.6); φ is the phase of the individual particle whose transverse motion is described by (106) and its variation with z is given by the phase oscillations (67); a_x and a_y very due to the strong focussing, and the variation of b depends on the low of phase damping (e.q. (98)); further β_s and γ_s change because the particles are accelerated; $E_0 T$ may also change along the accelerator.

9. Beam dynamics for periodic structures

9.1 Properties of Hill's differential equation [4),25),26),27)]

Now we recollect some results of the theory on periodic structures. We start with Hill's differential equation

$$\frac{d^2\tau}{dz^2} + k^2(z)\tau = 0 \tag{107}$$

where k(z) is a periodic function with a period ℓ.

The general solution of (107) can be written as

$$\tau = C\sqrt{\beta_\tau(z)}\cos\left[\psi(z) + \delta\right] \tag{108}$$

C and δ are constants fixed by the initial conditions, say at $z=z_o$. The betatron function $\beta_r(z)$ has the same periodicity as k(z), and is a solution of

$$\frac{d^2}{dz^2}\sqrt{\beta_\tau} - \frac{1}{(\sqrt{\beta_\tau})^3} + k^2(z)\sqrt{\beta_\tau} = 0 \tag{109}$$

$\sqrt{\beta_r}$ determines the amplitudes of the solutions of (107).

The phase function $\psi(z)$ is obtained from β_r by

$$\psi(z) = \int_{z_o}^{z} \frac{dz}{\beta_\tau} \tag{110}$$

Of great importance is the change of the phase over one period, which is called μ:

$$\mu = \int_{z_o}^{z+\ell} \frac{dz}{\beta_\tau} = \psi(z_o + \ell) \tag{111}$$

We turn now to the question of acceptance and emittance. Call "a" the maximum value which r(z) is allowed to take. As an example, in

the transverse phase space "a" will be the maximum radius which the beam is allowed. Be β_{max} the maximum value of $\beta_r(z)$. Solutions (108) in which r can actually reach the value of "a" can then be written as

$$r = \frac{a}{\sqrt{\beta_{max}}} \sqrt{\beta_r} \cos(\psi + \delta) \tag{112}$$

The acceptance A is defined as an area in the r-r'-phase space depending on "a": for any pair of initial conditions (r_o, r_o') at $z=z_o$ which are lying inside this acceptance area the maximum value of r(z) will at most be "a". The shape of the acceptance is an ellipse, we call its semi-axes Δr and $\Delta r'$. Its value is

$$A = \pi \Delta r \, \Delta r' = \pi(a)\left(\frac{a}{\beta_{max}}\right) = \frac{\pi a^2}{\beta_{max}} \tag{113}$$

The area in r-r'-phase space which is actually occupied by particles is called emittance E. Generally one wants to have that E is smaller than A. Now we want to write down a differential equation for the envelope, that is for the maximum value of r as a function of z, which we call r_m.

From (112) we have

$$r_m(z) = \frac{a}{\sqrt{\beta_{max}}} \sqrt{\beta_r(z)} \tag{114}$$

We choose the emittance equal to the acceptance (E=A) and can then write (109) as an envelope equation:

$$\frac{d^2 r_m}{dz^2} - \frac{(E/\pi)^2}{r_m^3} + k^2(z) r_m = 0 \tag{115}$$

The interpretation of this equation is the following: if the beam has the emittance E, than its envelope $r_m(z)$ can be derived from this envelope equation.

Often the smooth approximation is used to study the behaviour of the envelope. This is achieved by first calculating μ, e. g. by means of the matrix formalism (see 9.3). Next one defines a wave number k of the oscillation, which is constant over the whole period and gives the same μ as the complicated function k(z):

from (107), (108) follows that if k^2 = const., then also β_r = const; then from (109):

$$\beta_r = \pm \frac{1}{k} \qquad k = \text{const.} \tag{116}$$

and from (111): $$k = \frac{\mu}{\ell} = \text{const} \; ; \quad A = \frac{\pi a^2 \mu}{\ell} \tag{117}$$

9.2 Equations of the beam envelope [20)]

The motion in the transverse phase space is described by a linear differential equation (106), if the parameters β_s and γ_s change adiabatically. Similarily a linear differential equation was derived for the motions of small amplitude in the longitudinal phase space (91), (92). Important properties of these motions can be evaluated, if one assumes in addition that the coefficients $k^2_{\ell\rho}$ and $k^2_{t\rho}$ are periodic as a function of z. Then the results of the theory on periodic structures can be applied to the motion of particles in a linear accelerator. We take as a period (see Fig.2 on page 34, (32))

$$\ell = 2NL = N\, p \beta_s \lambda \tag{118}$$

As an example, for an Alvarez structure with N=1 we have p=2, so that one period contains two drift tubes: one of them with a quadrupole focussing in the x-direction, the other one defocussing.

From (79), (91) and (115) we get the envelope equation for the longitudinal motion for small amplitudes:

$$\frac{d^2}{dz^2} b - \frac{(E_\ell/\pi)^2}{b^3} + k_{\ell s}^2(z)\, b = 0 \qquad (119)$$

E_ℓ is the longitudinal emittance in the Z-Z' - phase space (see (43)). 2 b is the length of a bunch (see (44)).

The relation between E_ℓ and the emittance $\pi\Delta\varphi\Delta W$ measured in the $\Delta\varphi$ - ΔW-phase space is given by (see (55), (79))

$$\pi\Delta\varphi\,\Delta W = \frac{2\pi\beta_s\gamma_s^3}{\lambda} mc^2 E_\ell \qquad (120)$$

From (106) and (115) we get the envelope equation for the transverse motion:

$$\frac{d^2}{dz^2} a_x - \frac{(E_t/\pi)^2}{a_x^3} + k_{ts}^2(z)\, a_x = 0 \qquad (121)$$

E_z is the transverse emittance in the X-X'-phase space (see (43)). $2a_x$ is the diameter of the bunch measured in the x-direction (see (44)).

The envelope equations (119) and (121) are coupled, as both $k_{\ell\rho}^2$ and $k_{t\rho}^2$ depend on b, a_x and a_y. Their solution has been studied in the literature [13),15),20)].

9.3 Properties of matrix transformations [25)-28)]

How can one obtain the betatron function $\beta_r(z)$, and thereby also μ, the phase shift of r(z) over one period, and the acceptance A? One possibility is to solve (109). Another method is furnished if one relates the values of r and r' at any z to their values at z+ℓ by means of the matrix formalism. For stable oscillations of r(z) this transformation is given by

$$\begin{pmatrix} r(z+\ell) \\ r'(z+\ell) \end{pmatrix} = \begin{pmatrix} \cos\mu + \alpha(z)\sin\mu & \beta_r(z)\sin\mu \\ -\frac{1+\alpha^2(z)}{\beta_r(z)}\sin\mu & \cos\mu - \alpha(z)\sin\mu \end{pmatrix} \begin{pmatrix} r(z) \\ r'(z) \end{pmatrix} \tag{122}$$

The oscillations of r(z) are stable, if the trace of the transfer matrix for one period is smaller than two:

$$|\cos\mu| \leq 1 \tag{123}$$

α is related to β_r by

$$\alpha = -\frac{\beta_r'}{2} \tag{124}$$

The transfer matrix (122) - and therefore also $\beta_r(z)$ - can be calculated as a function of z by a product of relatively simple matrices, if $k^2(z)$ can be approximated by a function which is piecewise constant. If for example $k^2(z)=\pm k^2 = \text{const}$ from z_o to z_o+L, then the transfer matrix from z_o to z_o+L [22] for a focussing section is:

$$\begin{pmatrix} \cos\Theta & \frac{\sin\Theta}{k} \\ -k\sin\Theta & \cos\Theta \end{pmatrix}; \qquad k^2 > 0 \tag{125}$$

with $$\Theta = kL; \tag{126}$$

for a defocussing section:

$$\begin{pmatrix} \cosh\Theta & \frac{\sinh\Theta}{k} \\ k\sinh\Theta & \cosh\Theta \end{pmatrix}; \qquad -k^2 < 0 \tag{127}$$

and for a drift space:

$$\begin{pmatrix} 1 & L \\ 0 & 1 \end{pmatrix}; \qquad k^2 = 0 \tag{128}$$

We also quote the transfer matrix of a thin lens [22]:

$$\begin{pmatrix} 1 & 0 \\ -\frac{1}{F} & 1 \end{pmatrix} \tag{129}$$

F is the focal distance of the lens, being positive for a focussing and negative for a defocussing one.

If the ensemble of particles to be traced can be represented in phase space by an ellipse the envelope of the particles can be traced rather simple. Be M the transfer matrix for one structure element of the type (125) to (129). Further the equation of the ellipse be

$$\gamma r^2 + 2\alpha r r' + \beta r'^2 = \frac{E}{\pi} \qquad (129\ a)$$

with $$\beta\gamma - \alpha^2 = 1$$

Then the ellipse transformation through the element M is obtained from

$$\begin{pmatrix} \beta(z) & -\alpha(z) \\ -\alpha(z) & \gamma(z) \end{pmatrix} = M \begin{pmatrix} \beta(z_0) & -\alpha(z_0) \\ -\alpha(z_0) & \gamma(z_0) \end{pmatrix} M^T \qquad (129\ b)$$

with M^T being the transposed matrix belonging to M [34].

The main parameters characterizing the motion of r(z) are μ and the maximum and minimum value of the betatron function, β_{max} and β_{min}. As will be shown now, these parameters can be obtained relatively easy, if the periodic structure posesses a symmetry plane. Suppose a periodic structure which is symmetric about z=0:

$$k^2(z+\ell) = k^2(z) \quad \text{and} \quad k^2(-z) = k^2(z) \qquad (130)$$

Then $$k^2\left(\frac{\ell}{2}+z\right) = k^2\left(-\frac{\ell}{2}-z\right) = k^2\left(\frac{\ell}{2}-z\right) \qquad (131)$$

the structure is also **symmetric** about $z = \frac{\ell}{2}$.

We divide the length ℓ in 2n intervalls, such that $k^2(z)$ is approximately constant in each intervall. Then because of (131) the transfer matrix M for the period from z = 0 to z = ℓ can be written as

$$M = M_1 M_2 \ldots\ldots M_n \cdot M_n \ldots\ldots M_2 M_1$$

$$= M'_h \cdot M_h \qquad (132)$$

Each M_i will either have the form (125) or (127), and therefore

$$M_{i,11} = M_{i,22} \qquad (133)$$

Let A and B be matrices with

$$A_{11} = A_{22} \quad \text{and} \quad B_{11} = B_{22} \qquad (134)$$

$$\text{then also} \quad (ABA)_{11} = (ABA)_{22} \qquad (135)$$

$$\text{From this follows that} \quad M_{11} = M_{22} \qquad (136)$$

Comparing this result with (122) gives

$$\alpha(0) = 0 \qquad (137)$$

$$\text{Then from (124)} \quad \beta'_r(0) = 0. \qquad (138)$$

Thus $\beta_r(z)$ has the same symmetry properties as $k^2(z)$.

For the radial motion often symmetry planes will be located at the center of focussing or defocussing quadrupoles. As $\beta_r' = 0$ at these locations, the maximum amplitude of the radial motion will occur at the center of a focussing quadrupole, whereas the minimum amplitude at the center of a defocussing one. For a symmetric periodic structure all the information necessary is already cointained in the transformation matrix M_h for half a period. Especially M_h' can be obtained from M_h by the relation

$$M_{h'} = \begin{pmatrix} M'_{h_{11}} & M'_{h_{12}} \\ M'_{h_{21}} & M'_{h_{22}} \end{pmatrix} = \begin{pmatrix} M_{h_{22}} & M_{h_{12}} \\ M_{h_{21}} & M_{h_{11}} \end{pmatrix} \qquad (139)$$

which can be proven as follows:

For n = 1 the relation (139) is correct, as $M_h' = M_1 = M_h$. Suppose we had proven (139) for some arbitrary number n. Then because of (133) one has for n+1:

$$M_h'(n+1) = M_h'(n)\, M_{n+1} = \begin{pmatrix} M_h(n)_{22} & M_h(n)_{12} \\ M_h(n)_{21} & M_h(n)_{11} \end{pmatrix} \begin{pmatrix} M_{n+1,11} & M_{n+1,12} \\ M_{n+1,21} & M_{n+1,11} \end{pmatrix} \qquad (140)$$

$$M_h(n+1) = M_{n+1}\, M_h(n) = \begin{pmatrix} M_{n+1,11} & M_{n+1,12} \\ M_{n+1,21} & M_{n+1,11} \end{pmatrix} \begin{pmatrix} M_h(n)_{11} & M_h(n)_{12} \\ M_h(n)_{21} & M_h(n)_{22} \end{pmatrix} \qquad (141)$$

Evaluating these equations shows that (139) is also true for the number n+1, and therefore for any value of n.

Then the transfer matrix for one period, starting at the symmetry plane at z = 0 is - using (122), (132), (138), and (139) - :

$$M = \begin{pmatrix} \cos\mu & \beta_{max} \sin\mu \\ -\frac{\sin\mu}{\beta_{max}} & \cos\mu \end{pmatrix} = M_h' M_h \qquad (142)$$

In (142) we assumed that z = 0 is the center of a focussing quadrupole.

It follows that - because of det $M_i = 1$, see (125) and (127) - :

$$\cos\mu = M_{h11} M_{h22} + M_{h12} M_{h21} = 2 M_{h11} M_{h22} - 1 \qquad (143)$$

$$\beta_{max}^2 = - \frac{M_{h12} M_{h22}}{M_{h21} M_{h11}}$$

Suppose now that at $z = \ell/2$ there is the center of a defocussing quadrupole and the betatron function at that point is β_{min}. Then calculating the transfer matrix for one period, starting at $z = \ell/2$ results in:

$$\begin{pmatrix} \cos\mu & \beta_{min} \sin\mu \\ -\frac{\sin\mu}{\beta_{min}} & \cos\mu \end{pmatrix} = M_h M_h' \qquad (144)$$

from which follows:

$$\beta_{min}^2 = - \frac{M_{h12} M_{h11}}{M_{h21} M_{h22}} \qquad (145)$$

Therefore the modulation ratio of the beam is given by

$$\psi = \frac{r_{max}}{r_{min}} = \sqrt{\frac{\beta_{max}}{\beta_{min}}} = \sqrt{\frac{M_{h22}}{M_{h11}}} \qquad (146)$$

9.4 Estimation of transverse acceptance [27), 28)]

In this chapter we consider a periodic sequence of focussing (F) and defocussing (D) quadrupoles, and of rf gaps (0) (as sketched in Fig. 2 for a N = 1 grouping of quadrupoles).The integer N is the number of quadrupoles of the same polarity in successive drift tubes. N = 2 would correspond to a FOFODODO lattice. **Each drift tube contains one quadrupole. One has to keep in mind that this is difficult to realize in a Wideroe type structure (p = 1 or p = 3) [33)].**

Now we apply the methods developped in 9.3. However, instead of using the smooth approximation for the defocussing effect of the rf field - as one could do by using (103) - we follow the common practice of the literature, and use the thin lens approximation (see ref. 22) on page 367). The defocussing effect of the space charge will be treated as like.

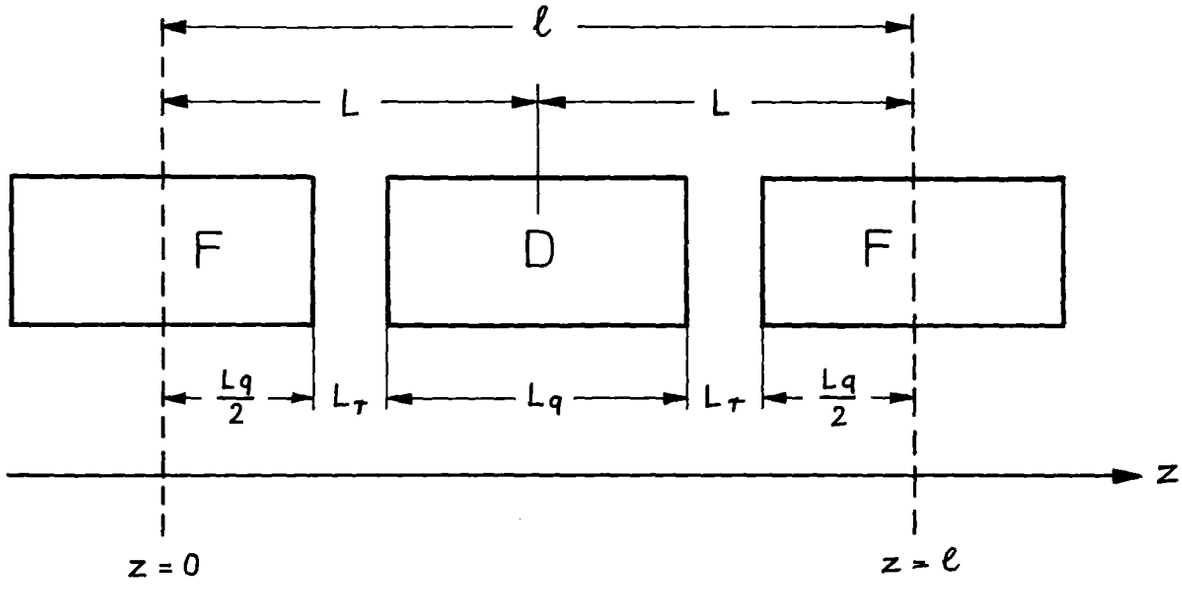

Fig. 2: FODO lattice , l = 2NL ; $L = \frac{p\beta_s\lambda}{2}$

The transfer matrix of a defocussing lens of the length L can be written as [22)]

$$M_\tau = \begin{pmatrix} 1 & S \\ 0 & 1 \end{pmatrix} \begin{pmatrix} 1 & 0 \\ -\frac{1}{f_d} & 1 \end{pmatrix} \begin{pmatrix} 1 & S \\ 0 & 1 \end{pmatrix} \qquad (147)$$

$$-\frac{1}{f_d} = +k \sinh(kL) \approx k^2 L \left(1 + \frac{(kL)^2}{6}\right) \geq 0 \qquad (148)$$

$$s = \frac{\cosh(kL) - 1}{k \sinh(kL)} - \frac{L_q}{2} \approx \frac{L_r}{2}\left(1 - \frac{(kL)^2}{12}\right) \qquad (149)$$

The term $-L_q/2$ appears in s, because the quadrupoles are treated separately. We take k^2 from (100), (101) and define

$$\Theta_r^2 = -\frac{q}{mc^2} \frac{\pi E_0 T \sin\varphi L^2}{\lambda \beta_s^3 \gamma_s^3} = k_{t,rf}^2 L^2 \qquad (150)$$

$$\Theta_\varrho^2 = \frac{q}{mc^2} \frac{\varrho M_x L^2}{\varepsilon_0 \beta_s^2 \gamma_s^3} = 90\Omega \frac{q}{mc^2} \frac{I M_x \lambda L^2}{a_x a_y b \beta^2 \gamma^3} = \frac{\tilde{\mu} M_x L^2}{a_x a_y b} \qquad (151)$$

(see (48), (65))

$$\Delta = -\left(\Theta_r^2 + \Theta_\varrho^2\right) \equiv -(kL)^2 \qquad (152)$$

In the literature Δ characterizes the defocussing effect of the rf field only, whereas here also the space charge part is included. Generally one will have $\varphi < 0$ and therefore $\Theta_r^2 > 0$, but $\Delta < 0$. In this approximation Δ is assumed to be independent of z, which particularly means that for φ, a_x, a_y and b we shall take values which are averaged over one period. By doing this the motion in the x-direction is decoupled from those in the y-and z-directions.

Rewriting:

$$-\frac{1}{f_d} \approx -\frac{\Delta}{L}\left(1 - \frac{\Delta^2}{6}\right) \qquad (153)$$

$$s \approx \frac{L_r}{2}\left(1 + \frac{\Delta^2}{12}\right) \qquad (154)$$

For about $|\Delta| < 0.5$ the following thin lens approximation for M_r is justified [26]:

$$M_\tau \approx \begin{pmatrix} 1 & \frac{L_\tau}{2} \\ 0 & 1 \end{pmatrix} \begin{pmatrix} 1 & 0 \\ -\frac{\Delta}{L} & 1 \end{pmatrix} \begin{pmatrix} 1 & \frac{L_\tau}{2} \\ 0 & 1 \end{pmatrix} \tag{155}$$

Be further

$$\Theta_0 = k_q L\,; \quad \Lambda = \frac{L_q}{L}\,; \quad L_\tau = (1-\Lambda)L\,; \quad 2NL = \ell \tag{156}$$

with $k_q = k_{t,q}$ from (102).

Using Taylor series for the trigonometric and hyperbolic functions one arrives at the following approximate formulas [27), 28)] for the transfer properties of the whole period from z = 0 to z = ℓ:

$$\cos\mu_N \approx 1 - \left[\frac{N^2(N^2+2-2\Lambda)}{6}\right]\Lambda^2\Theta_0^4 - 2N^2\Delta \tag{157}$$

$$\gamma_N = \frac{\beta_{max,N}}{L} \approx \frac{2N\left[1+\left\{\frac{N^2+1-\Lambda}{N^2}\right\}\frac{\Lambda}{4}\Theta_0^2 - \frac{\Delta}{12}\left\{\frac{8N^2+1}{8N^2-2}\right\}\right]}{\sin\mu_N} \tag{158}$$

$$\psi_N = \sqrt{\frac{\beta_{max,N}}{\beta_{min,N}}} \approx \frac{1+\left\{\frac{N^2+1-\Lambda}{N^2}\right\}\frac{\Lambda}{4}\Theta_0^2 - \frac{\Delta}{2}N^2}{\cos(\mu_N/2)}\,; \quad \begin{Bmatrix} N = \text{odd} \\ N = \text{even} \end{Bmatrix} \tag{159}$$

Note that (158) in [27)] contains an error. Explicitely for the cases N=1 and N=2 the results are collected in Table (160) and also in Fig. 3 - 6.

The x-axis of the acceptance ellipse is a, whereas the x'-axis is a/β_{max}, as our first quadrupole is focussing in the x-direction [26]. One operates at the center of the stability region if cos $\mu_N \sim 0$. About for this value of cos μ_N the acceptance in the x-direction will be maximum. The imput beam has to be matched to the acceptances in the x- and y- direction to fully make use of the acceptance (162) in both directions. Therefore at the first quadrupole of the linac the beam should have a focus in the defocussing direction of that quadrupole, whereas in the focussing direction of it the beam will assume its maximum extension.

The lower border of the stability region is reached for $\cos\mu = 1$, whereas for cos $\mu < -1$ overfocussing takes place. From (160) the following trends can be analyzed:

the larger N is, the lower the quadrupole gradient has to be to obtain stability of the x - x' - motion; however, the larger N is the lower is the acceptance; the modulation ratio of the beam cross section, Ψ_N, gets larger with increasing N, therefore space charge problems will be minimized for N = 1; the quadrupole gradient necessary to operate in the center of the stability region is proportional to L^{-2}; however the acceptance scales as L^{-1}.

To conclude we point out once more that it has been assumed in (160) that each drift tube contains a quadrupole. The formulas could be applied also to the case of only every other drift tube containing a quadrupole, as has been realized in a Wideroe type of accelerator (p = 1, 3; N=1) [33]. The variables ℓ, L and Λ would have to be changed and two rf gaps would have to be represented by one thin lens. However, the condition $|\Delta| < 0.5$ (153), (154) will then no longer be fullfilled for high beam current. This case would be treated better by applying (122) with computer methods, which on the other hand means to dispense with handy formulas to study functional dependences of the varions parameters.

Table (160):

	N = 1	N = 2
$\cos \mu_N$	$1 - \left(\frac{1}{2} - \frac{\Lambda}{3}\right) \Lambda^2 \Theta_0^4 - 2\Delta$	$1 - \left(4 - \frac{4}{3}\Lambda\right) \Lambda^2 \Theta_0^4 - 8\Delta$
Θ_0^2	$\left[\frac{1 - \cos \mu_1 - 2\Delta}{\Lambda^2 \left(\frac{1}{2} - \frac{\Lambda}{3}\right)}\right]^{\frac{1}{2}}$	$\left[\frac{1 - \cos \mu_2 - 8\Delta}{\Lambda^2 \left(4 - \frac{4}{3}\Lambda\right)}\right]^{\frac{1}{2}}$
$\beta_{max,N}$	$\frac{2L\left[1 + \left(1 - \frac{\Lambda}{2}\right)\frac{\Lambda \Theta_0^2}{2} - \frac{3\Delta}{4}\right]}{\sin \mu_1}$	$\frac{4L\left[1 + \Lambda \Theta_0^2 - \frac{5}{2}\Delta\right]}{\sin \mu_2}$
ψ_N	$\frac{1 + \left(1 - \frac{\Lambda}{2}\right)\frac{\Lambda \Theta_0^2}{2} - \frac{\Delta}{2}}{\cos\left(\mu_1/2\right)}$	$\frac{1 + \Lambda \Theta_0^2 - 2\Delta}{\cos\left(\mu_2/2\right)}$

Having determined Θ_0^2, the quadrupole gradient will we obtained from (see (102), (156)):

$$B' = \frac{mc \gamma_s \beta_s \Theta_0^2}{q L^2} \tag{161}$$

and the acceptance in the x-plane is (see (113)):

$$A_{x,N} = \frac{\pi a^2}{\beta_{max,N}} \tag{162}$$

fig. 3 : (160)

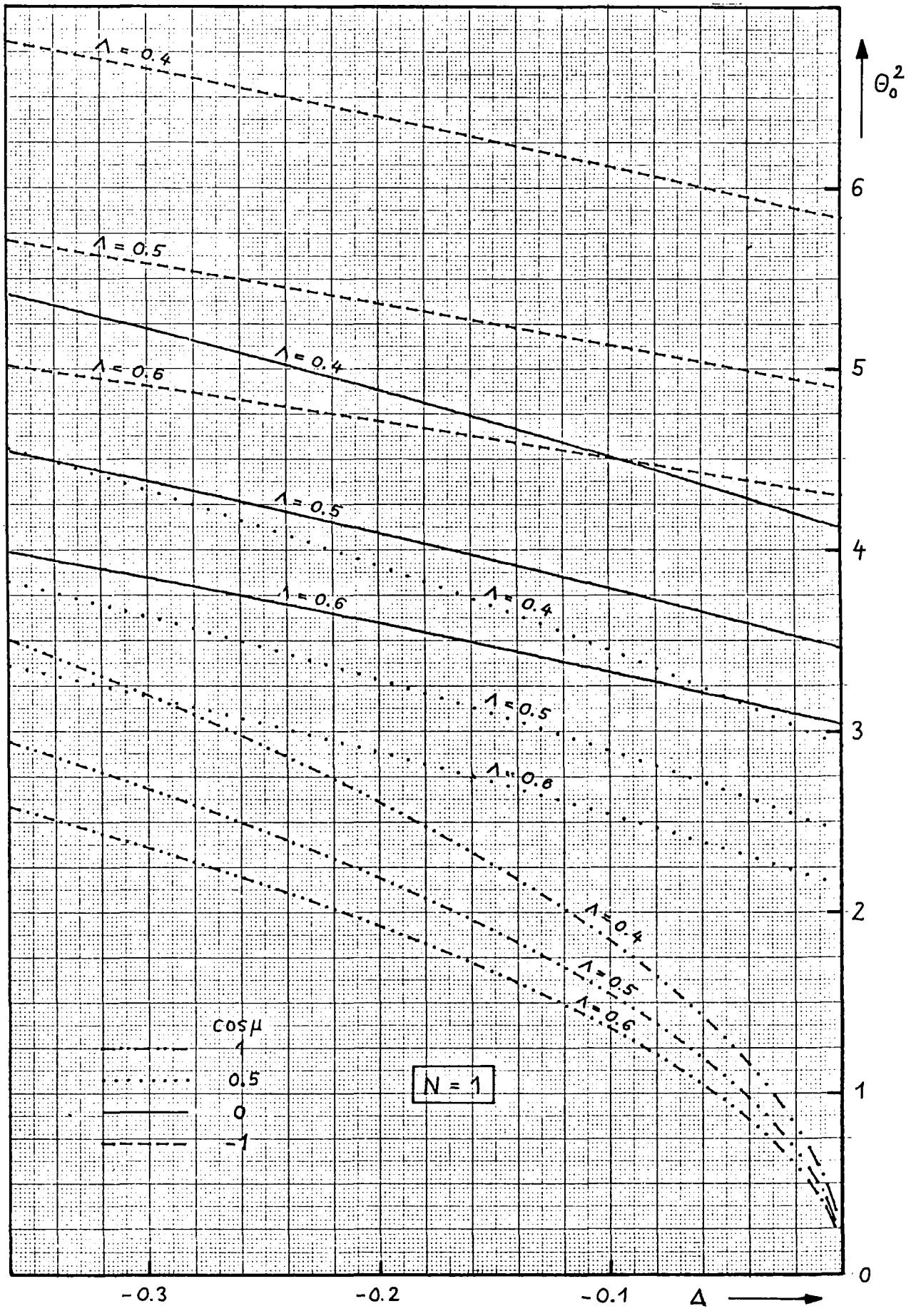
Λ = 0.4
Λ = 0.5
Λ = 0.6
Λ = 0.4
Λ = 0.5
Λ = 0.6
Λ = 0.4
Λ = 0.5
Λ = 0.6
Λ = 0.4
Λ = 0.5
Λ = 0.6
cosμ
1
0.5
0
-1
N = 1
Θ_0^2
6
5
4
3
2
1
0
-0.3
-0.2
-0.1
Δ

fig 4 : (160)

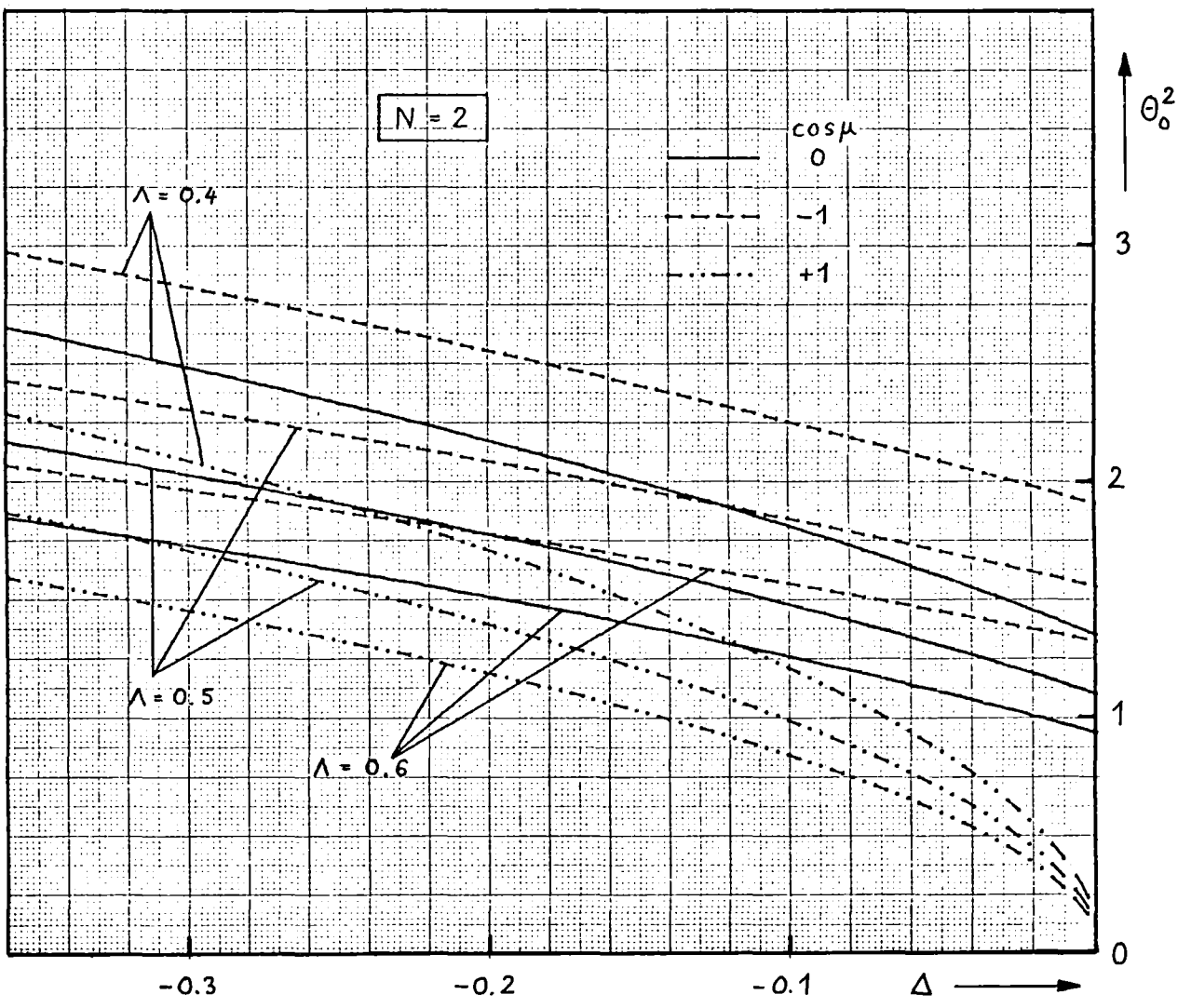

fig. 5 : (160)

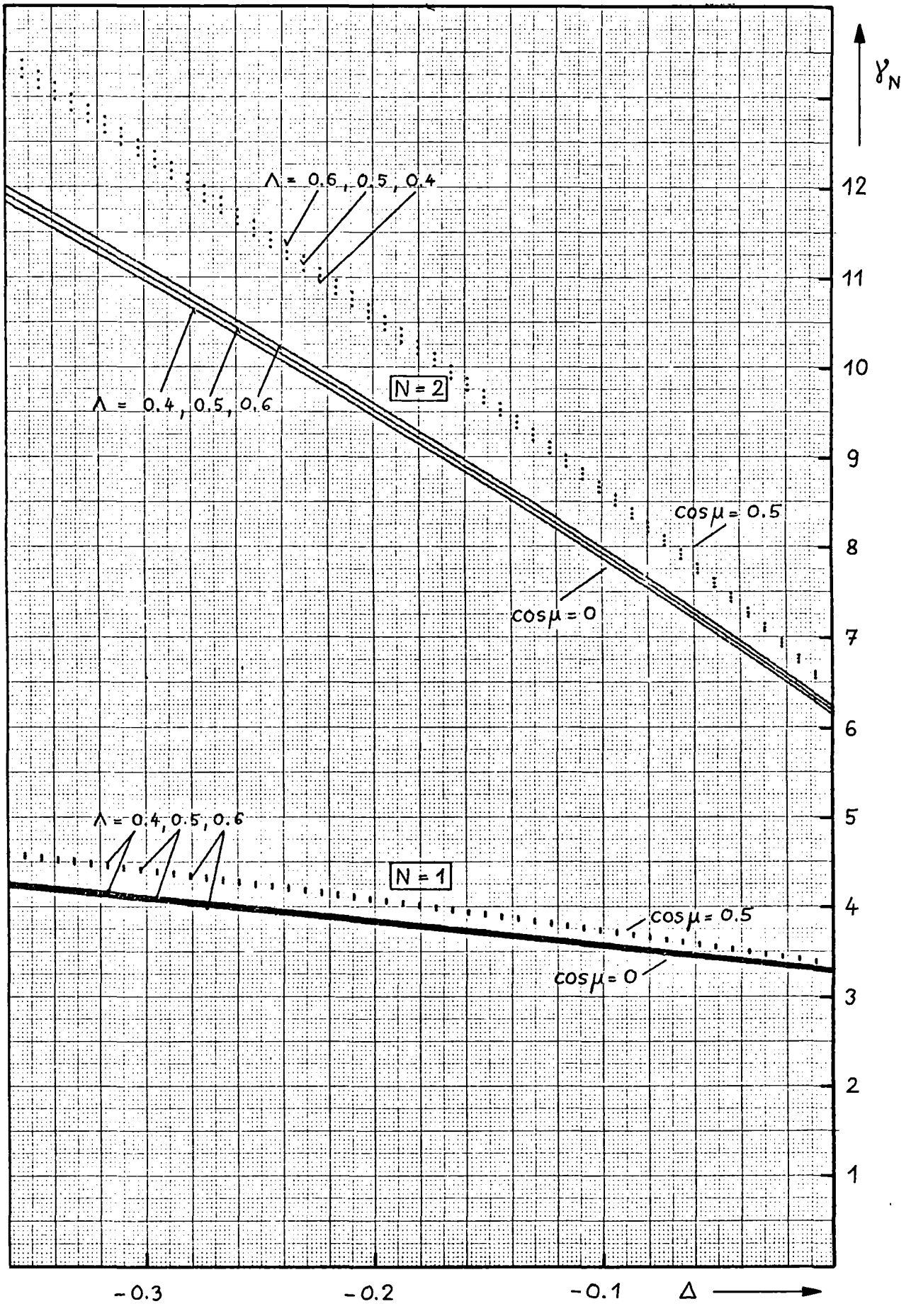
γ_N
12
11
10
9
8
7
6
5
4
3
2
1
$\Lambda = 0.6, 0.5, 0.4$
$\Lambda = 0.4, 0.5, 0.6$
N = 2
$\cos\mu = 0.5$
$\cos\mu = 0$
$\Lambda = 0.4, 0.5, 0.6$
N = 1
$\cos\mu = 0.5$
$\cos\mu = 0$
-0.3
-0.2
-0.1
Δ

fig. 6 : (160)

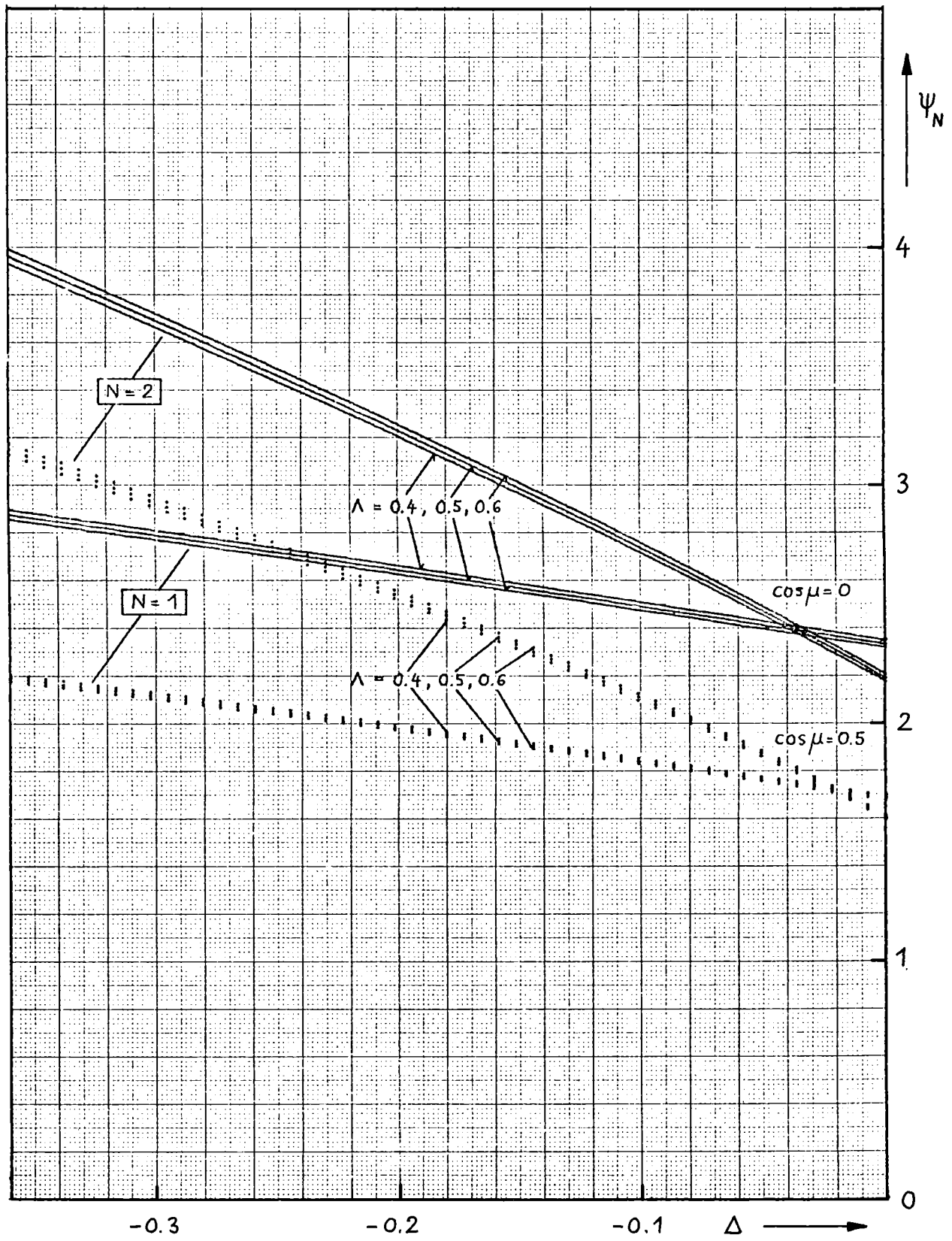

10. Choice of linac parameters

10.1 The main parameters

First of all the choice of linac parameters is dictated by the demands of the users. These are:

1. kind of particles to be accelerated:	m and q
2. beam current	I
3. final energy	

Second, the properties of the injection system have a large influence on the linac parameters:

1. exit energy	β and γ
2. longitudinal emittance	E_ℓ
3. transverse emittance	E_t

However, the parameters of the injection system may also be affected by properties of the linac, especially by its acceptances.

Once the kind of particles to be accelerated and the beam current is specified by the users, the main parameters of a linac are:

1. type of accelerating structure and mode of operation (e. g. 0 - or π-mode)	
2. rf frequency	f or λ
3. injection energy	β and γ
4. accelerating field and fill factor	$E_o T, \Lambda$
5. phase of synchronous particle	φ_s
6. maximum beam radius allowed	a

Some criteria for the optimization of these parameters are:

1. high reliability of linac operation
2. low cost of construction
3. low cost of operation

These criteria cannot be related to the linac parameters in a well defined manner, and the optimization will have to be guided by experience and intuition.

A criterion to describe the efficiency of the linac to transform the rf power into beam energy is the shunt impedance:

$$Z_{eff} = \frac{E_{eff}^2 L}{P_s} \quad , \qquad E_{eff} = E_o T \cos \varphi_s \tag{163}$$

P_s is the rf power which is dissipated in the walls of the accelerator structure of length L. A review on structures and on their shunt impedances can be found in [7].

An upper limit on the amplitude E_o of the electric field is given by the onset of sparking in the accelerating gap [29),30)], or by problems in cooling the accelerator structure.

10.2 On designing a high current deuteron linac

10.21 Bunch dimensions

Now we shall leave the general treatment and turn to the problem of designing a deuteron accelerator, which has as high a current as possible and a final energy of about 40 MeV. This results in the demand to optimize the acceptances in the longitudinal and transverse phase space, A_ℓ and A_t, which have to be larger than the emittances of the injection system. A_ℓ and A_t depend on the main parameters of the linac, as described in the previous chapters 7.2 and 9.4.

A_t is the larger the larger "a" is. However, upper limits on "a" are set by the required efficiency of acceleration and by strong focussing requirements. Increasing "a" - and therefore also the drift tube radius d - lowers the transit time factor T; increasing d results in a higher magnetic field B_{max} at the pole tip of the quadrupoles. B_{max} should not be larger than about 1 Tesla, due to the saturation property of iron magnetization. Also, with increasing "a" the coupling between the longitudinal and transverse motions gets larger resulting in a reduction of acceptances.

Therefore, and to reduce the number of independent linac parameters, we require for the first tank of the linac: **(each drift tube containing a quadrupole):**

1) from (39), (40), (41):

$$d \leq \frac{\beta\lambda}{2\pi} ; \qquad \beta \approx \beta_s ; \qquad \gamma \approx 1 \tag{164}$$

which corresponds to

$$k_p d \leq 1 ; \qquad I_0 (k_p d) \leq 1.266 \tag{165}$$

Further one allows for some clearance between beam and drift tube [16], which we assume to be 25% of d, then

$$a = \sigma \cdot \frac{\beta\lambda}{2\pi} ; \quad I_0 (k_p a) \leq 1.15 ; \quad \sigma \leq 0.75 \tag{166}$$

2) from (32) and (161)

$$d \leq \frac{\pi q B_{max}}{2 mc} \cdot \frac{p^2 \lambda}{\Theta_0^2} \cdot \frac{\beta\lambda}{2\pi} ; \quad B_{max} \leq 1 \text{ Tesla} \tag{167}$$

that is for deuterons: $$d \leq \frac{p^2}{4\Theta_0^2} \cdot \frac{\lambda}{\text{meter}} \cdot \frac{\beta\lambda}{2\pi} \tag{168}$$

The aperture will not be limited by the achievable quadrupole field if:

for deuterons: $$\frac{\lambda}{\text{meter}} \geq \frac{4\Theta_0^2}{p^2} \tag{169}$$

Θ_0^2 can be taken from Fig. 3 and 4, we estimate:

$$\Theta_0^2 \leq 5 \quad \text{for } N=1, \quad \Theta_0^2 \leq 2.5 \quad \text{for } N=2 \qquad \text{if } \mu_N = 90^\circ \tag{170}$$

Then the aperture will not be limited by the achievable quadrupole field, if λ is larger than indicated in (171); λ = 3 m corresponds to f = 100 MHz.

for deuterons:

λ/meter $\geq$	p = 1	p = 2	p = 3	p = 4
N = 1	20	5	2.2	1.25
N = 2	10	2.5	1.1	0.63

(171)

For the new CERN p-linac N=1, p=2, λ=1.5 m, $\mu_N = 39^\circ$ were chosen, whereas λ=2.5 would have been indicated by (164), (167) for $\mu_N = 90^\circ$.

3) In order to be able to give an estimate of the space charge problem, we will now also specify the bunch length 2b; and refer to the study of the longitudinal acceptance in chapter 7.2. Taking τ=1 and expecting μ_ℓ to be of the order of 1/3 we get from (79), (80):

$$\Delta\varphi_{max} = |\varphi_s| \quad ; \quad b = |\varphi_s| \cdot \frac{\beta\lambda}{2\pi} \tag{172}$$

Typically φ_s will be of the order of -0.6, corresponding to -35°. The shape of the bunch will be close to that of a sphere.

10.2.2 Longitudinal acceptance

As in 9.4 we assume that the focussing lattice of the linac starts in the center of a quadrupole focussing in the x-direction. Then the flutter factor due to strong focussing is

$$\psi_N = \left.\frac{a_x}{a_y}\right|_{z=o} = \frac{a}{a_y} \tag{173}$$

According to [20] ψ_1 is space charge independent. However, our result in Fig. 6 together with (151), (152) is, that ψ_N does increase with increasing I, if one wants to operate in the center of the stability region (cos μ = o) for all currents. We assume that the average bunch diameter is independent of z:

$$\sqrt{a_x(z)\, a_y(z)} \approx \frac{a}{\sqrt{\psi_N}} = \frac{\sigma \beta \lambda}{2\pi \sqrt{\psi_N}} \tag{174}$$

Further, approximating the longitudinal form factor M_z by (82), using (166) and (172) the longitudinal space charge parameter (66) is:

$$\mu_\ell = - \frac{120 \pi^2 \Omega \sqrt{\psi_N}}{\sigma \varphi_s^2 \sin\varphi_s E_o T} \cdot \frac{I}{\beta^2 \lambda} \tag{175}$$

For a typical data get of $\psi_N = 2.8$, $\sigma = 0.75$, $\varphi_s = -40^o$, $E_oT = 1MV/m$ we get

$$\mu_\ell = 8.4 \times 10^{-3} \frac{I/A}{\beta^2 \lambda/m} \tag{176}$$

In (84) we found that the current will be maximum for $\mu_\ell = 1/3$; therefore the longidudinal phase space can accept at most a current of

$$I_\ell = \frac{\sigma \varphi_s^2 \sin|\varphi_s| E_o T}{360 \pi^2 \Omega \sqrt{\psi_N}} \cdot \beta^2 \lambda \equiv 39.5 \frac{\beta^2 \lambda}{m} \tag{177}$$

(177) is tabulated below for some typical values of β and λ.

From (76) and (77), taking $\mu_\ell = 1/3$, the longitudinal acceptance is for the data set given in table (177)

$$\Delta\varphi_{max} = |\varphi_s| = 40^o \equiv 0.7 \tag{178}$$

$$\Delta W_{max} = \frac{4}{q} \sqrt{-\frac{\lambda}{\pi} q E_o T mc^2 \beta^3 \gamma^3 \varphi_s^3} = 6.3\,MeV \sqrt{\beta^3 \lambda/m} \tag{179}$$

for: ⟶	ψ_N = 2.8 ;	σ = 0.75 ;	φ_s = -40° ;	E_oT = 1 MV/m
I_ℓ /A ≥	λ = 11.1 m (f = 27 MHz)	λ = 5.56 m (f = 54 MHz)	λ = 2.78 m (f = 108 MHz)	λ = 1.48 m (f = 202 MHz)
β = 0.0193 (d, 350 keV)	0.16	0.08	0.04	0.02
β = 0.0231 (d, 500 keV)	0.23	0.12	0.06	0.03
β = 0.0283 (d, 750 keV)	0.35	0.17	0.09	0.05
β = 0.04 (p, 750 keV)	0.70	0.35	0.17	0.11 A CERN new linac E_oT = 1.2 MV/m φ_s = - 35° ψ_1 = 1.6

The CERN new 50 MeV linac for protons operates at 202.5 MHz with an injection energy of 750 keV (β = 0.04) and E_oT = 1.2 MV/m at injection. The maximum current to be accelerated is 150 mA [9]. From (177) we would have expected that in this case for currents above 110 mA some particles would get lost from the longitudinal phase space. In a proton accelerator some particle loss can be tolerated, as the activation problems are not as severe as with deuterons. For a deuteron accelerator more accurate calculations than the ones presented above, and may be also experiments on existing linacs are necessary in order to predict the particle loss for currents higher than indicated by (177).

10.2.3 Transverse acceptance

According to (32), (158), (162), (166) the transverse acceptance is

$$A_t = \pi \cdot \frac{\sigma^2}{2\pi^2 \gamma_N} \cdot \frac{\beta\lambda}{P} \qquad (180)$$

We assume to operate at the center of the stability region ($\cos\mu = 0$) for all currents [14], recollect that then the frequency should not be larger than indicated by (171). For a N = 1 quadrupole grouping γ_N depends only slightly on the defocussing rf and space charge forces $\Delta < 0$, as can be seen from Fig. 5 and (152):

$$\gamma_1 \approx 3.3 - 2.7\Delta \quad \text{for } \cos\mu = 0 \tag{181}$$

if (171), then: $$A_t\,(N=1) = \pi \cdot \frac{8.6\cdot 10^{-3}}{1-0.81\Delta} \cdot \frac{\beta\lambda}{p}\,;\ \sigma = 0.75 \tag{182}$$

For N = 2 γ_2 depends more strongly on Δ, and therefore also $A_t(N = 2)$. A good approximation is:

$$\gamma_2 \approx 6.2 - 16\Delta \quad \text{for } \cos\mu = 0, \tag{183}$$

if (171), then: $$A_t\,(N=2) = \pi \cdot \frac{4.6\cdot 10^{-3}}{1-2.6\Delta} \cdot \frac{\beta\lambda}{p}\,;\ \sigma = 0.75 \tag{184}$$

The transverse space charge parameters can be written as follows: from (45), (82), (172), (174) and $M_x \approx M_y$:

$$M_x \approx \frac{1}{2}\left(1 - \frac{\sigma}{3\,|\varphi_s|\,\sqrt{\psi_N}}\right) \tag{185}$$

from (41), (151), (172), (174):

$$\theta_\varrho^2 = \frac{90\,\Omega\,\pi^3\,q\,\psi_N\left(1 - \frac{\sigma}{3|\varphi_s|\sqrt{\psi_N}}\right)}{mc^2\,\sigma^2\,|\varphi_s|} \cdot \frac{p^2 I}{\beta^3} \tag{186}$$

from (104), (151): $$\mu_t = \frac{\theta_\varrho^2}{k_t^2 L^2} \tag{187}$$

in smooth approximation from (103), (104), (105), (117), (156):

$$\mu_t = \frac{\Theta_s^2}{\left(\frac{\mu_N}{2N}\right)^2 + \Theta_s^2} \; ; \qquad k_{t_s} = \frac{\mu_N}{\ell} = \frac{\mu_N}{2NL} \tag{188}$$

Note that μ_N^2 will finally become negative, if B' is kept constant and I is increased.

Again for a typical data set like

$$\psi_N = 2.8 \, , \quad \sigma = 0.75 \, , \quad \varphi_s = -40^\circ \, , \quad \mu_N \approx \pi/2 \tag{189}$$

one has for deuterons:

$$M_x = 0.39 \tag{190}$$

$$\Theta_s^2 = 8.3 \cdot 10^{-6} \, \frac{p^2 I/A}{\beta^3}$$

$$\mu_t = \frac{I/A}{I/A + 7.4 \cdot 10^4 \beta^3/(pN)^2}$$

Let us again check these estimates by comparing with the parameters of the CERN new 50 MeV p-linac:

β=0.04, p=2, N=1, $E_o T \approx 1.2$ MV/m, $\varphi_s \approx -35^\circ$, λ=1.48 m, I=0.15 A, $\mu_N = 39^\circ$

Then from (150) we get for $\varphi = \varphi_s$: $\Theta_r^2 = 0.086$

With $\sigma = 0.75$, $\psi_1 = 1.6$ and (174): $\sqrt{a_x a_y} = 5.7 \times 10^{-3}$ m;

from (172): $b = 5.8 \times 10^{-3}$ m

from (185): $M_x = 0.34$

from (186): $\theta_S^2 = 0.088$

from (152): $\Delta = -0.17$

from (160), (182), scaling $A_t \sim \sigma^2 \sin\mu_N$

$$A_t = \pi \cdot 250 \text{ mm}\cdot\text{mrad}$$

According to [14] A_t(CERN linac) = π 300 mm mrad at 150 mA and $\mu_N = 39^\circ$. Thus the agreement between our estimates of acceptances and the more accurate CERN calculations is reasonable.

10.2.4 Electric peak fields and drift tube geometry

We reduce the number of free parameters further: from (177) follows that the accelerating field should be as large as possible for a high current accelerator. We assume that cooling problems can be solved and take as a limit for E_o the conservative Kilpatrick criterium [29),30)]. A good approximation for the criterium is

$$\frac{E_p}{\text{MV/m}} = 9.23 \left(\frac{5.56 \text{ m}}{\lambda}\right)^{1/3} \qquad \text{for } 1.5 \text{ m} \leq \lambda \leq 12 \text{ m}$$

$$\text{if } \frac{E_p \lambda^2}{g} \leq 1.4 \times 10^4 \text{ MV} \tag{191}$$

E_p is the peak electric surface field and g is the gap distance.

If $\frac{E_p \lambda^2}{g} > 1.4 \times 10^4$ MV we approximate (see ref. 29 for notation)

$$W = V(1-e^{-1.1\ V/V^*}) \tag{192}$$

and obtain a transcendental equation for E_p which we solve numerically for given values of g and λ:

$$E_p^3 g \left[1 - \exp\left(\frac{-9.33\cdot 10^{-11} E_p \lambda^2}{g \ \text{Volt}}\right)\right] \exp\left(\frac{-1.7\cdot 10^7 \text{Volt}}{E_p \ \text{meter}}\right) = 1.8\cdot 10^{18} \frac{\text{Volt}^3}{\text{meter}^2} \quad (193)$$

E_p can be related to E_o by (see (26))

$$E_o = \frac{g}{L} E_z(z, r=d) \approx \frac{g E_p}{1.3\ L} \quad (194)$$

The factor 1.3 is introduced empirically to account for the field enhancement at the drift tube.

From transit time factor considerations generally

$$g \approx \frac{\beta\lambda}{4.5} \quad (195)$$

is taken at injection.

From (36), (164) and (193) we estimate the transit time factor to be

$$T \approx \frac{\sin\frac{\pi}{4.5}}{\frac{\pi}{4.5}\cdot I_o(1)} = 0.73 \quad (196)$$

Then with (32), (192), (193), (194) we get

$$E_o T \approx \frac{E_p T}{2.93 p} \approx \frac{2.3}{p}\left(\frac{5.56\ m}{\lambda}\right)^{1/3} \frac{MV}{m} \quad (197)$$

The effective accelerating field is

$$E_{eff} = E_o T \cos\varphi_s \quad (198)$$

The fill factor Λ is approximimated with (32), (195) to be

$$\Lambda \approx \frac{L - g - 0.012\ m}{L} = 1 - \frac{0.44}{p} - \frac{0.024\ m}{p\beta\lambda} \qquad (199)$$

We assumed 0.012 m space for the drift tube housing.

We take the inner radius of the quadrupole d_q to be

$$d_q = d + 0.002\ m = \frac{\beta\lambda}{2\pi} + 0.002\ m \qquad (200)$$

Generally $L_q > d_q$ will hold, so that the quadrupole field is not dominated by end effects.

11. A computer program to aid in linac design

Again we concentrate on designing a high current deuteron linac. From the discussion above follows that the injection energy into the linac and the rf wavelength should be as large as possible to get large acceptances and small space charge problems. From technical considerations just the opposite is desired: the dc preaccelerator for large currents is the less problematic the lower the terminal voltage is, 750 keV seems to be the upper limit for an open air cascade; Alvarez structures of 50 MHz operation frequency have already a diameter of about 4 m, so that an even lower frequency seems not to be reasonable for this type of structure, whereas a Wideroe accelerator of 27 MHz is still a possible option.

The choice of frequency and injection energy will also be influenced by the beam emittance of the injection system; for the smaller the emittance for a given current is, the larger frequency or injection energy can be.

These complex considerations cannot be incorporated into the formalism presented in the previous chapters. We therefore choose to write a computer program, which has among other the frequency and injection energy as free parameters. This program will now be described.

The input parameters of the program are:

particle mass	m
particle velocity	β
rf wavelength	λ
typ of rf mode	p
synchronous phase	φ_s
particle phase	φ
quadrupole configuration	N
betatron phase advance/quadrupole period	$\mu_N(I=0)$
stay clear factor	σ

The program calculates as a function of beam current I the following quantities (see appendix 2 for the description of the program):

		see
current allowed in longitudinal phase space	I_ℓ	(84)
phase acceptance	$\Delta\varphi_{max}$	(80)
energy acceptance	ΔW_{max}	(77)
normalized transverse acceptance	$\pi\beta A_t$	(180)
longitudinal space charge parameter	μ_ℓ	(66)
transverse space charge parameter	μ_t	(188)
bunch length	2b	(172)
average bunch radius	$\sqrt{a_x a_y}$	(174)
betatron phase advance/quadrupole period	$\mu_N(I)$	
magnetic field at bore radius of quadrupole	B_{max}	(200),(161)
magnetic field at bore radius of quadrupole if $\mu_N(I) = \mu_N(I=0) = \text{const}$	B_{max}	(161),(200)
effective accelerating field	E_{eff}	(197)

In order to obtain these quantities at a current I the beam cross section modulation ratio at that current $\psi_N(I)$ has to be known. However $\psi_N(I)$ depends on the defocussing space charge force parameter θ_ς^2, which again depends on $\psi_N(I)$ (see (151), (152), (159), (174)). In the program I is increased in steps of ΔI, and ΔI is taken sufficiently small such that $\theta_\varsigma^2(I-\Delta I)$ can be used to calculated $\psi_N(I)$, which in turn is needed to obtain $\theta_\varsigma^2(I)$.

As I_ℓ depends on $\psi_N(I)$ and $\psi_N(I)$ is not constant, also I_ℓ depends on I.

$\mu_N(I)$ is kept constant by the program as long as $B_{max} \leq 1$ T. For $B_{max} > 1$ T $\mu_N(I)$ is decreased such that now $B_{max}(I) = 1$ T = const.

The following formulas are used in the program:

d = (164), a = (166), d_q = (200), g = (195), L = (41), Λ = (199), γ = (1), E_p = (191), (193), E_o = (194), T = (196), Θ_o^2 = (160), ψ_N = (160), γ_N = (160), Θ_r^2 = (150), $a_x a_y$ = (174), Θ_s^2 = (151), Δ = (152), M_z = (47), M_x = (46).

A program list can be found in the appendix. In order to check the results of the program it was applied to the design of the new CERN 50 MeV linac. The results are shown in figs. 31 to 36. They agree reasonably well with those given in [9), 14)]

at I = 0.15 A	CERN data	this report
I_ℓ(A)	0.15	0.105
$\Delta\varphi_{max}$ (^{o})	35	35
ΔW_{max} (keV)	33	28
$A_t\beta/\pi$ (cm mrad)	1.2 x σ^2 = 0.68	0.67
B' (T/m)	93	83
E_{eff} (MV/m)	1	1.02
E_p (MV/m)	10	14

A main discrepancy occurred in the value of E_p, which we calculated according to Kilpatrick's criterium. The lower value of E_p = 10 MV/m (also taken in our program to obtain figs.31, 32, 33) was chosen by the CERN group, in order to obtain sligthly lower quadrupole gradients and to be with regard to the electric peak fields at the very conservative side especially also avoiding problems by field emission [31)]. The results for E_p = 14 MV/m are shown in fig. 34, 35, 36.

12. Parameters of a high current deuteron linac

Next we calculated various deuteron accelerators (figs. 7 to 30). The current which can be accelerated in the longitudinal phase space increases as $\varphi_s^2 \sin\varphi_s$ (177), the rate of acceleration decreases as $\cos\varphi_s$ (198), the transverse space charge problems decrease as φ_s^{-1} (186), whereas the rf defocussing effect scales as $\sin\varphi$ (150). Therefore, a reasonable choice for φ_s seems to be -40°, which we kept constant for all cases computed.

Further we choose to operate at the center of the transverse stability region $\mu_N = 90^\circ$ for all currents in order to reduce the loss of particles from the transverse phase space due to coupling of longitudinal and radial motion. A lower value of μ_N results in smaller quadrupole gradients, smaller modulation of the beam cross section but also smaller width of the stability region. More detailed studies are necessary to find the optimum value of μ_N, and of course also of all the other parameters.

An analysis of fig. 7 to 30 is summarized in table (201).
To compare the varions options we require that the normalized transverse acceptance A_t of the linac should be 1π cm mrad. I_{max} is the maximum current which then can be accelerated. However, the dependence of I_{max} on A_t and A_ℓ is not always very strong. Therefore the figures should be consulted as well.

Our conclusion is, that there are two options for a high current deuteron linac. First, an Alvarez type linac, operating at about 54 MHz (λ = 5.56 m) with an injection energy of at least 500 keV (β = 0.0231), but much preferable 750 keV (β = 0.0283), having 200 mA as maximum current. Second, a Wideroe type linac, operating at about 27 MHz (λ = 11.1 m) with an injection energy of at least 350 keV (I_{max} = 100 mA), but also preferable higher injection energies: at 500 keV we get I_{max} = 0.1 A, and at 750 keV I_{max} = 0.4 A. The results about the Alvarez option agree reasonably well with those quoted in the literature [15), 16)]. The Wideroe option has the disadvantage that it cannot accelerate the deuterons much beyond 10 MeV (β = 0.1) because the shuntimpedance of the structure gets too low. Therefore a second type of linac , probably an Alvarez type operating at 54 MHz, is necessary to accelerate the

deuterons further. This increases the complexity of the system and also may cause acceptance mismatches between the two structures.

Further,the Wideroe structures considered here contain a quadrupole in each drift tube, which may turn out to be too complicated to realize in hardware[33]. If quadrupoles can be incorporated only into every other drift tube, the required gradients will increase, the beam cross section modulation will increase and the acceptances will decrease. For this case the approximations of chapter 9.4 are no longer valid.

Instead of the Wideroe type structure an IH - type structure could also be considered, in which one quadrupole in each drift tube is possible.

A more detailed analysis of the problem is necessary, which will be presented in another report.

Table (201): Maximum beam current of various deuteron accelerator configurations

β (E_{kin}/keV)	λ/m (f/MHz)	p	N	limitation in current due to	I_{max}/A	fig.
0.0193	11.1	1	1	B_{max}	-	7
		1	2	B_{max}, A_t, Wideroe design?	0.1	8
		2	1;2	Alvarez diameter to large	-	9
(350)	(27)	$\geq$3	1;2	μ_ℓ, A_t	-	
0.0231	11.1	1	1	B_{max}	-	10
		1	2	B_{max}, Wideroe design?	0.2	11
		2	1;2	Alvarez diameter to large	-	12
(500)	(27)	3	1	μ_ℓ, A_t, Wideroe design?	0.05	
		3	2	μ_ℓ, A_t	-	
		4	1;2	μ_ℓ, A_t	-	
0.0283	11.1	1	1	B_{max}, Wideroe design?	-	13
		1	2	Wideroe design?	0.4	14
(750)	(27)	2	1;2	Alvarez diameter too large	-	15
		$\geq$2	1;2	p = 1 is a better choice	-	
0.0193	5.56	1	1;2	B_{max}	-	16,17,
(350)	(54)	$\geq$2	1;2	μ_ℓ, A_t	-	18
0.0231	5.56	1	1;2	B_{max}	-	19
		2	1	A_t, μ_ℓ	0.05	20
(500)	(54)	2	2	A_t, μ_ℓ	-	21
		$\geq$3	1;2	A_t, μ_ℓ	-	
0.0283	5.56	1	1;2	B_{max}	-	22
(750)	(54)	2	1	A_ℓ; not strong dependent	0.2	23
		2	2	A_t	-	24
		$\geq$3	1;2	A_t	-	
0.0231	2.78	$\geq$1	1;2	A_z, μ_ℓ, B_{max}	-	25,26,
(500)	(108)					27
0.0283	2.78	1	1;2	B_{max}	-	28
(750)	(108)	2	1	B_{max}, A_t	-	29
		2	2	A_t	-	30
		$\geq$3	1;2	A_t, μ_ℓ, A_ℓ	-	

fig. 7

BETA = 0.0193 ; LAMBDA = 11.10 METER ; SIGMA = 0.75 ; MASS = 2

MUE(I=0) = 90 DEGREE ; PHI-S = -40 DEGREE ; PHI = -40 DEGREE

EPEAK = 7.6 MVOLT/METER

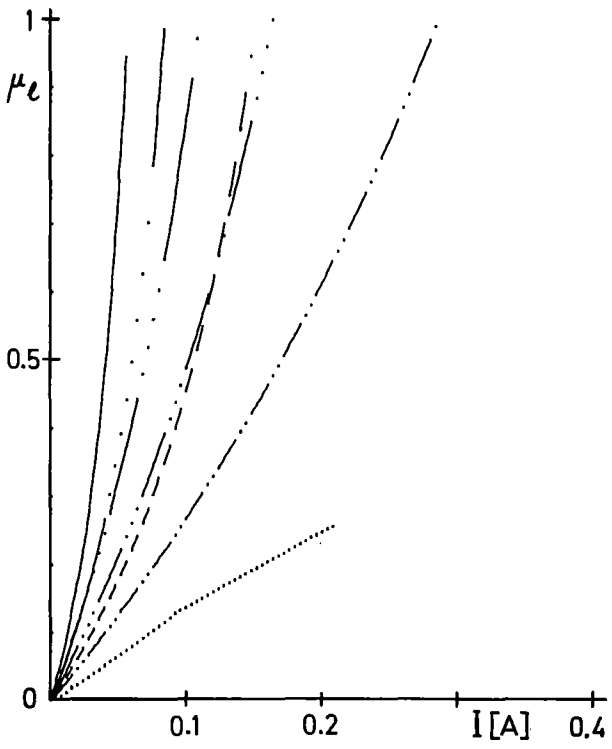

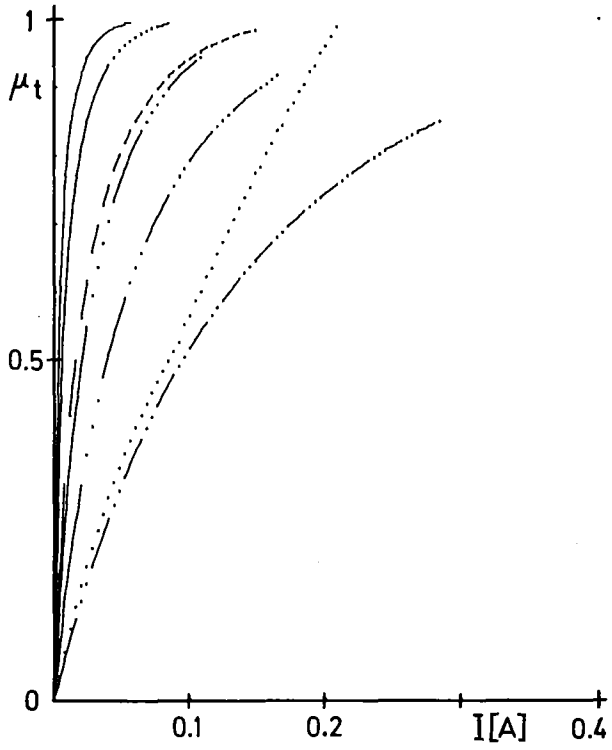

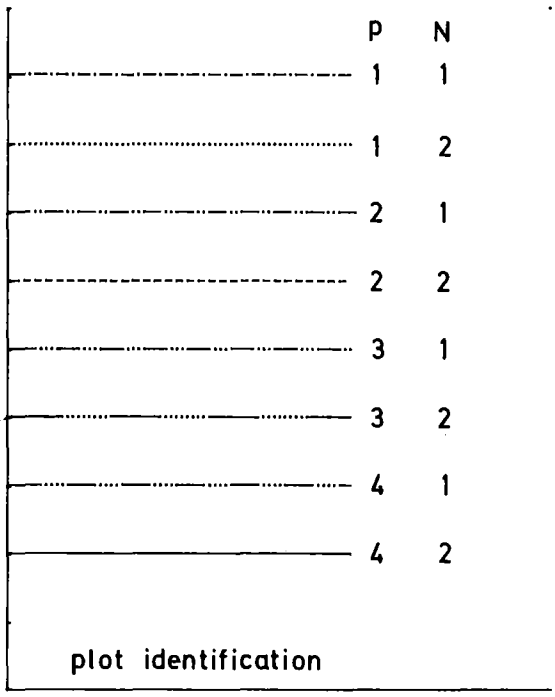

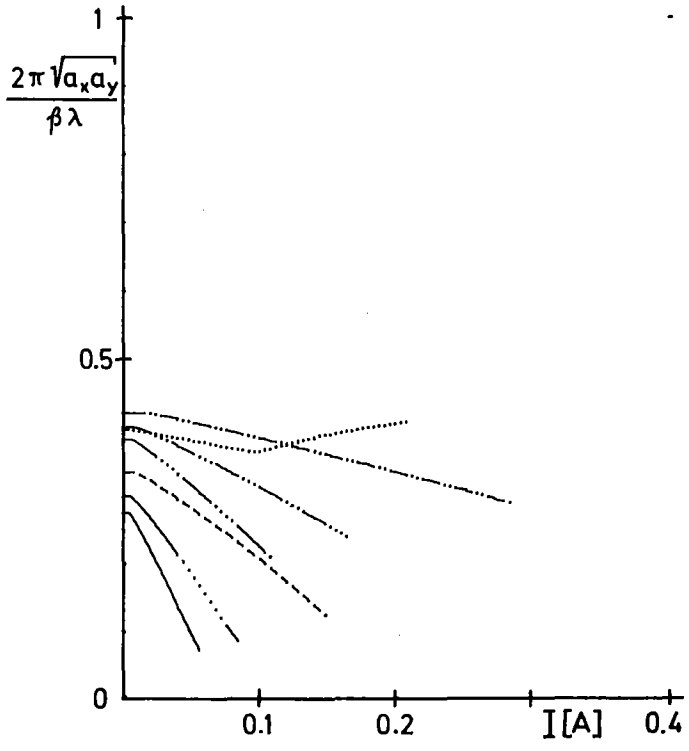

fig. 8

BETA = 0.0193 ; LAMBDA = 11.10 METER ; SIGMA = 0.75 ; MASS = 2

MUE(I=0) = 90 DEGREE ; PHI-S = -40 DEGREE ; PHI = -40 DEGREE

EPEAK = 7.6 MVOLT/METER

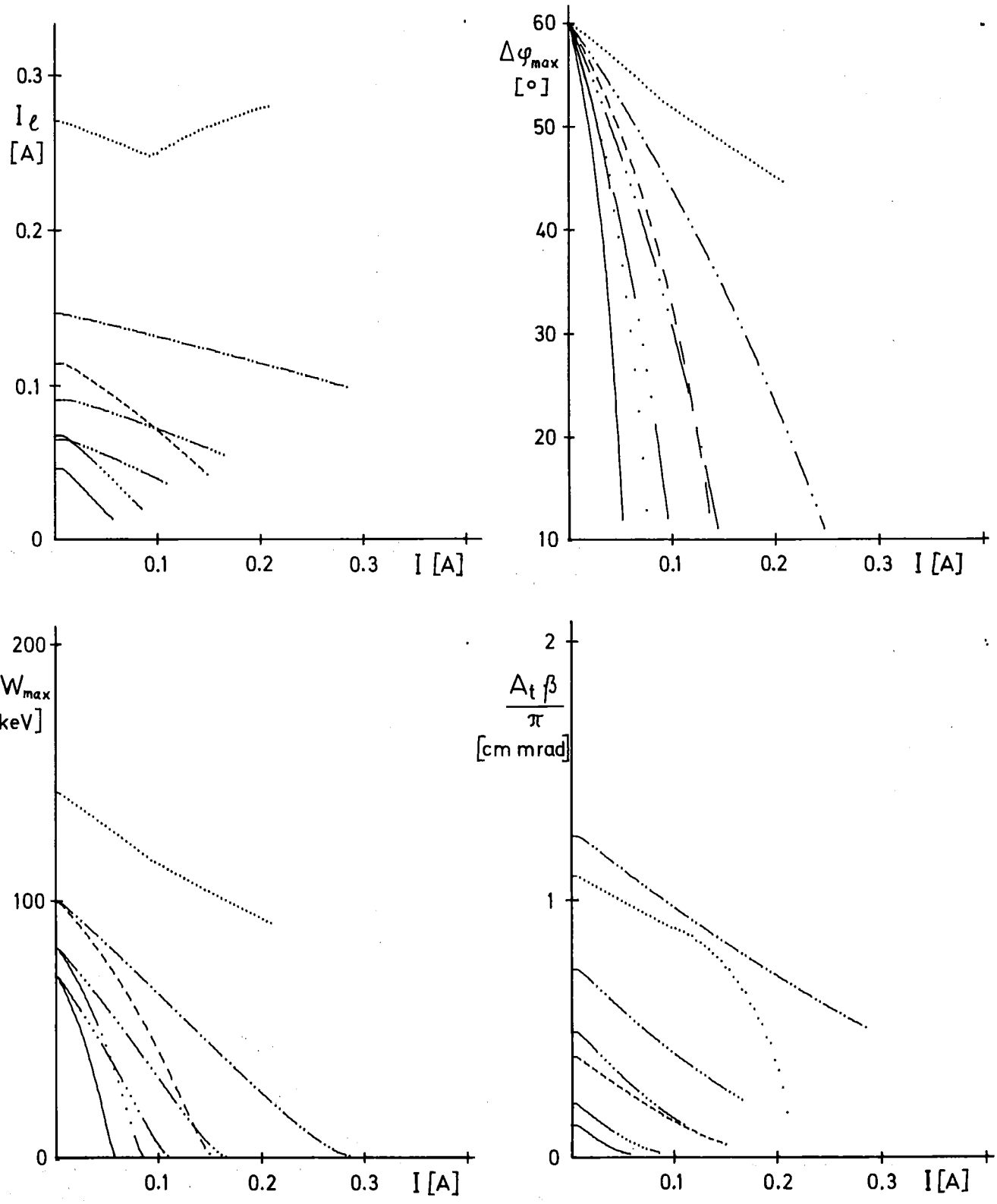

fig. 9

BETA = 0.0193 ; LAMBDA = 11.10 METER ; SIGMA = 0.75 ; MASS = 2

MUE(I=0) = 90 DEGREE ; PHI-S = -40 DEGREE ; PHI = -40 DEGREE

EPEAK = 7.6 MVOLT/METER

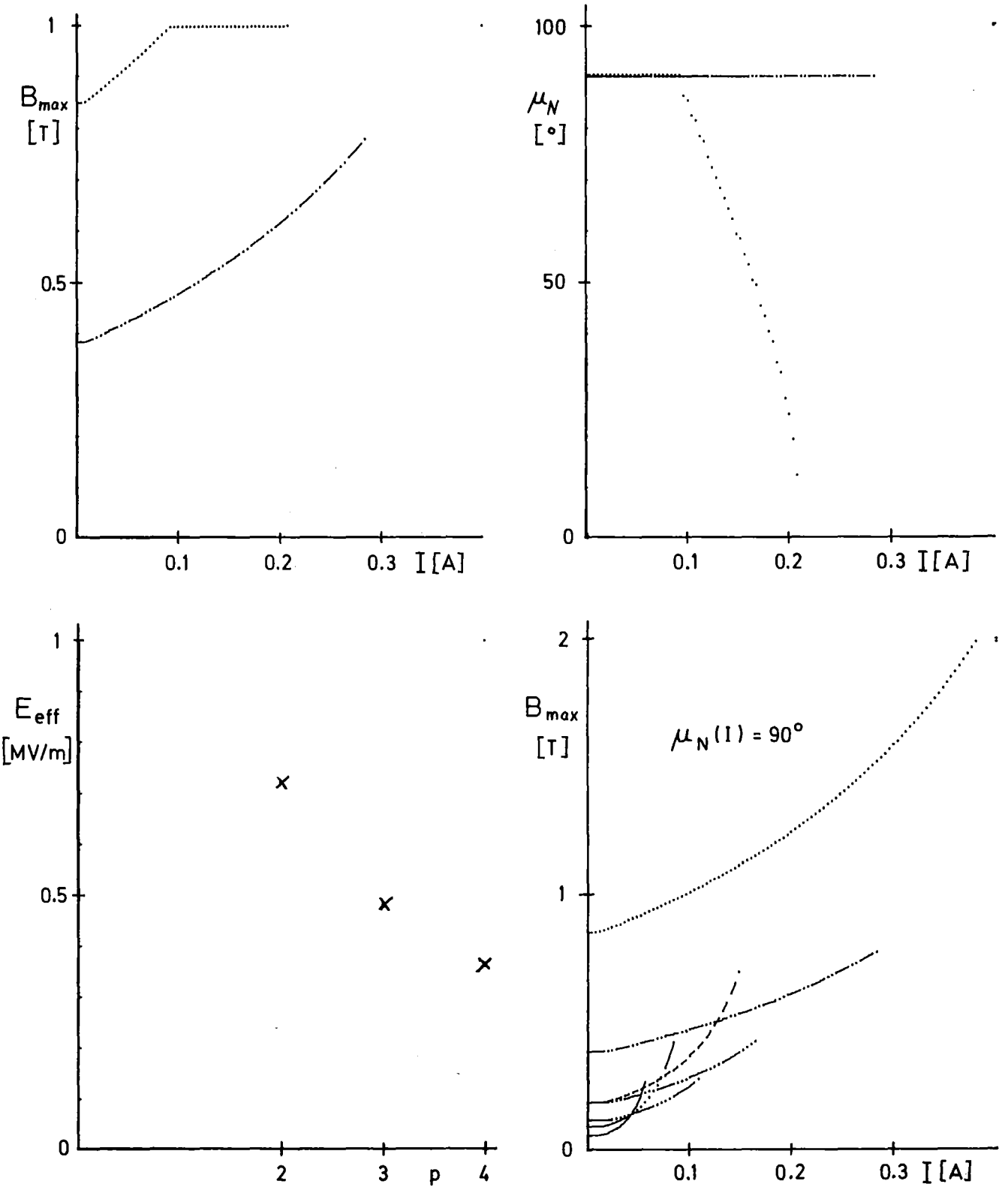

fig. 10

BETA = 0.0231 ; LAMBDA = 11.10 METER ; SIGMA = 0.75 ; MASS = 2

MUE(I=0) = 90 DEGREE ; PHI-S = -40 DEGREE ; PHI = -40 DEGREE

EPEAK = 7.4 MVOLT/METER

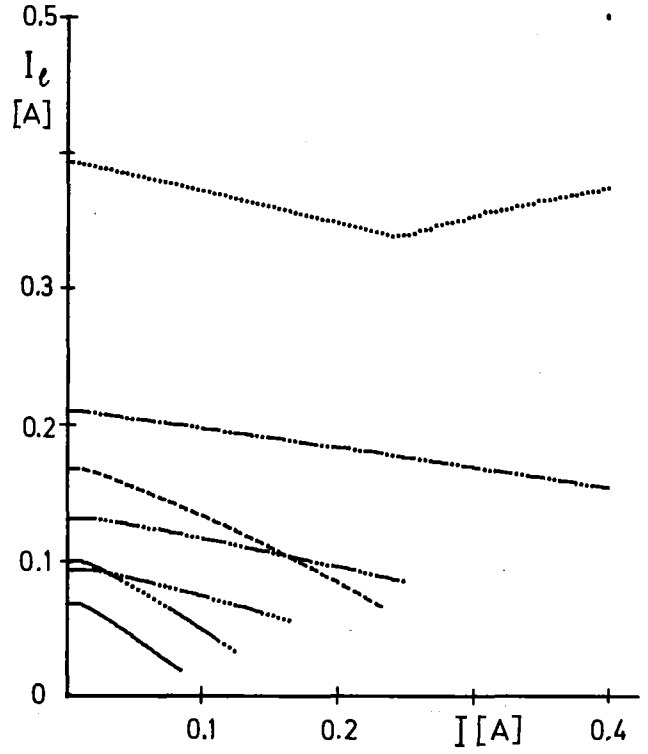

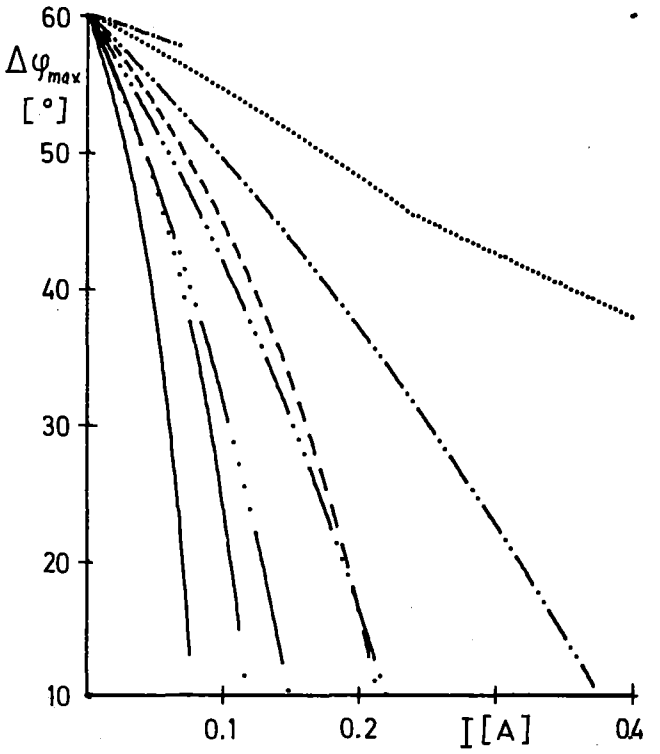

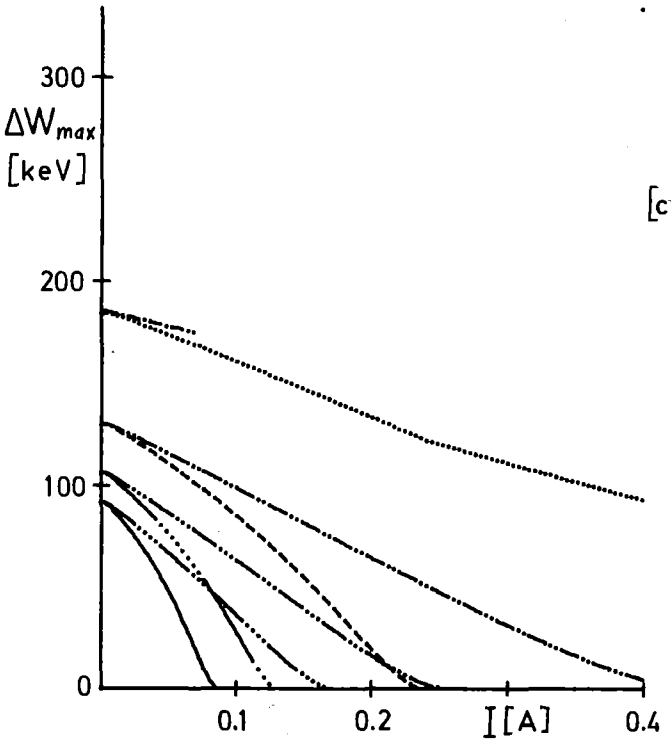

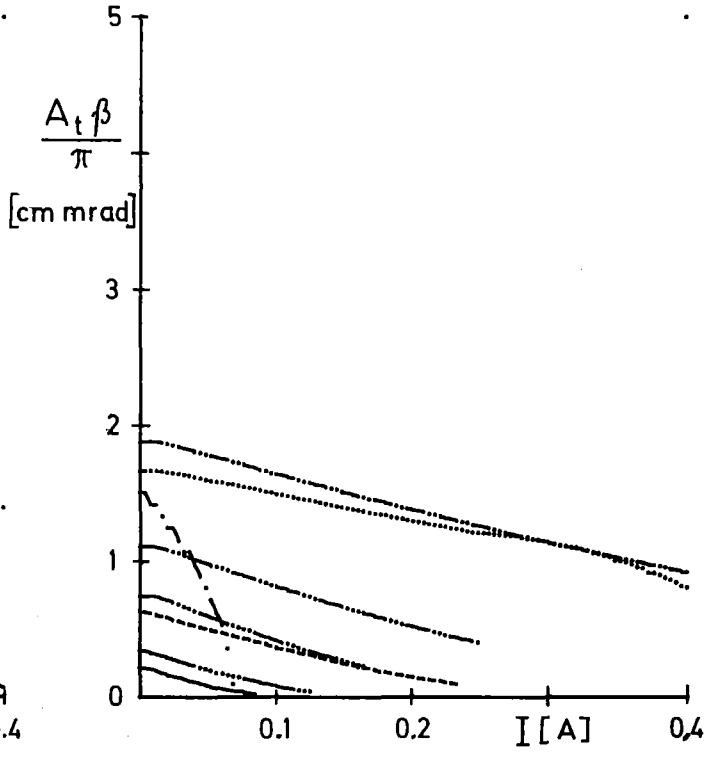

fig. 11

BETA = 0.0231 ; LAMBDA = 11.10 METER ; SIGMA = 0.75 ; MASS = 2

MUE(I=0) = 90 DEGREE ; PHI-S = -40 DEGREE ; PHI = -40 DEGREE

EPEAK = 7.4 MVOLT/METER

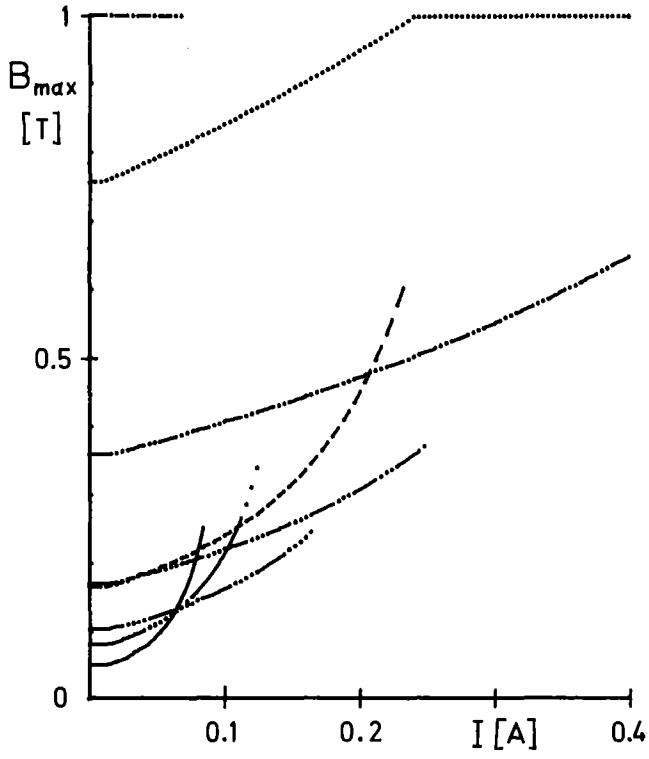

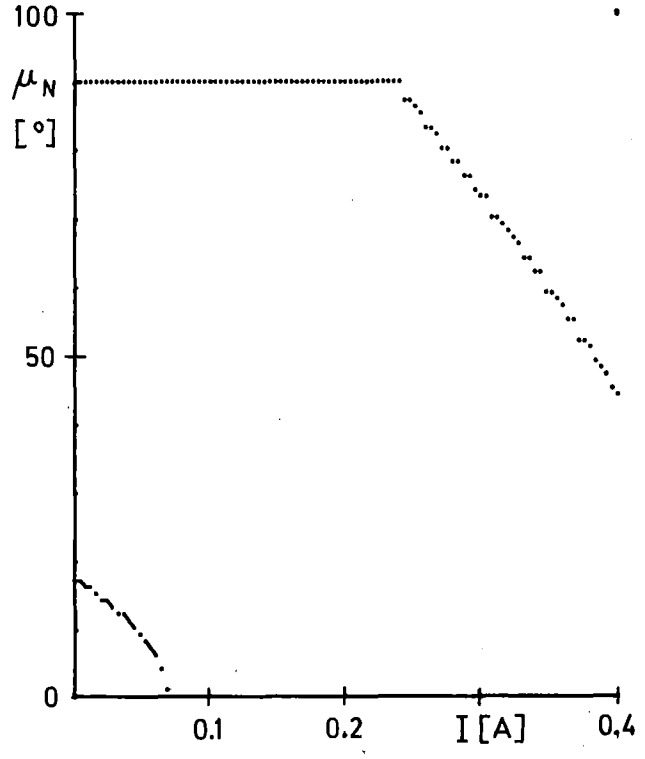

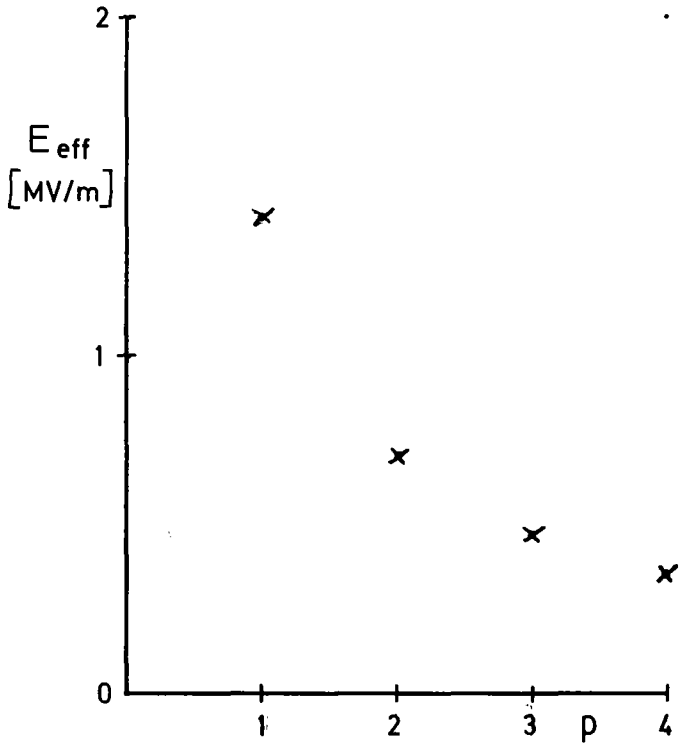

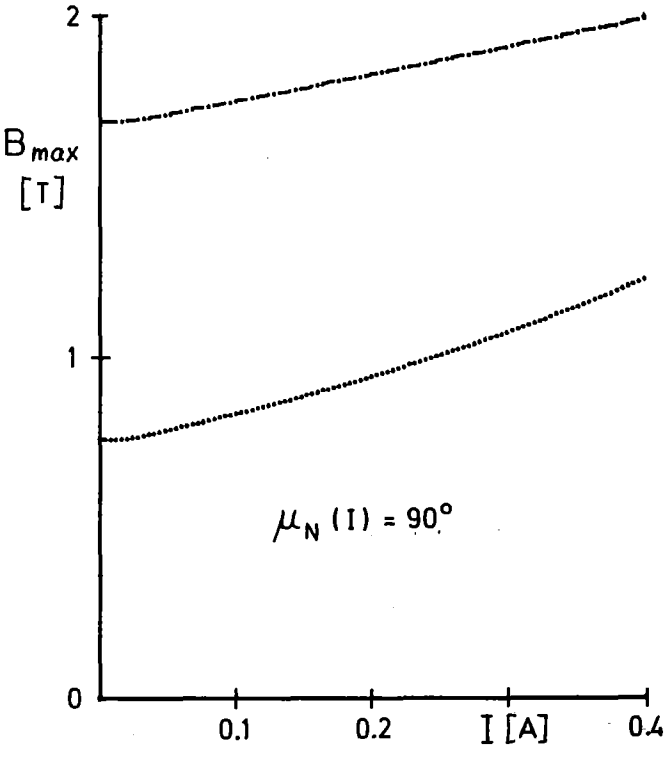

fig. 12

BETA = 0.0231 ; LAMBDA = 11.10 METER ; SIGMA = 0.75 ; MASS = 2

MUE(I=0) = 90 DEGREE ; PHI-S = -40 DEGREE ; PHI = -40 DEGREE

EPEAK = 7.4 MVOLT/METER

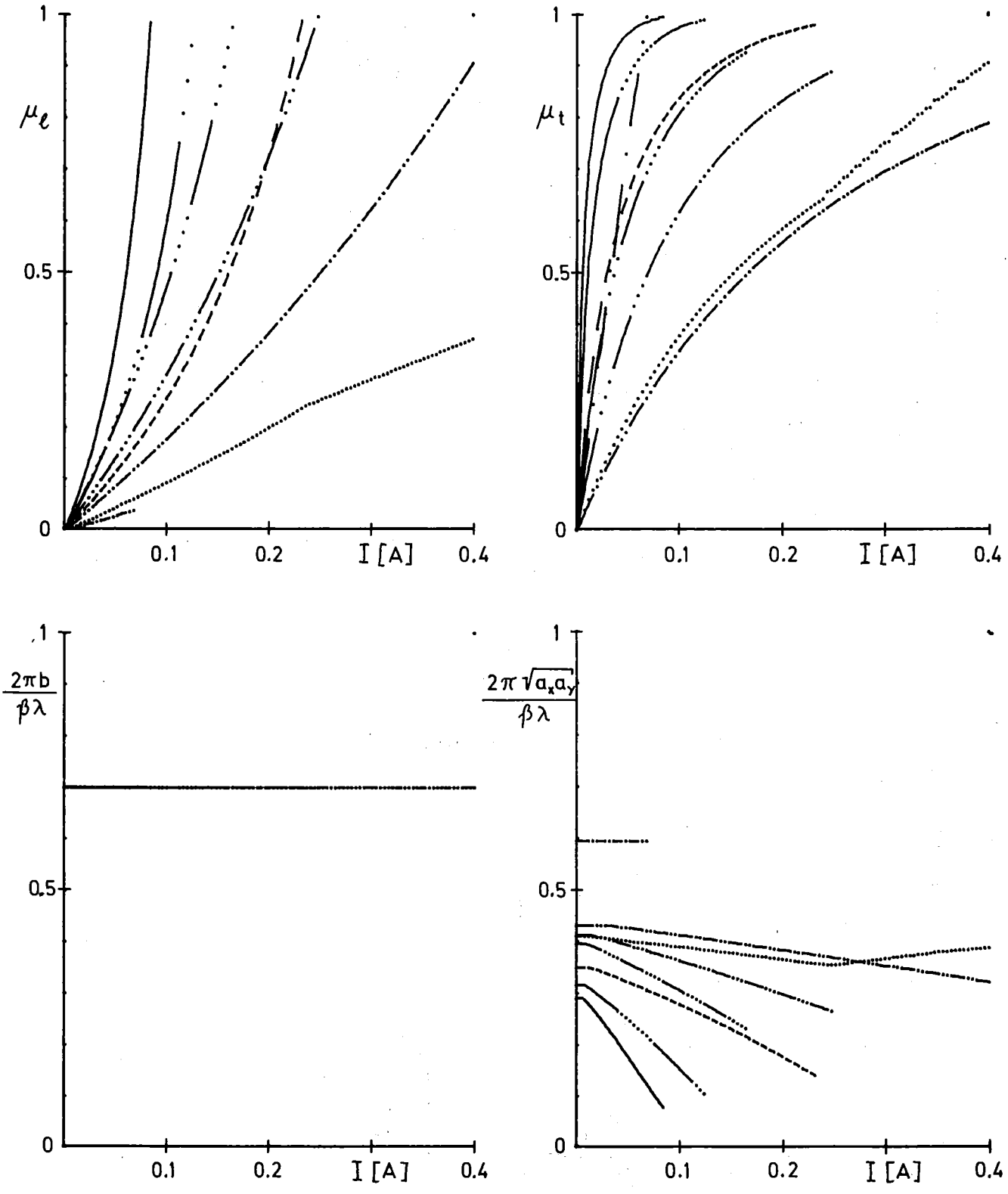

fig. 13

BETA = 0.0283 ; LAMBDA = 11.10 METER ; SIGMA = 0.75 ; MASS = 2

MUE(I=0) = 90 DEGREE ; PHI-S = -40 DEGREE ; PHI = -40 DEGREE

EPEAK = 7.3 MVOLT/METER

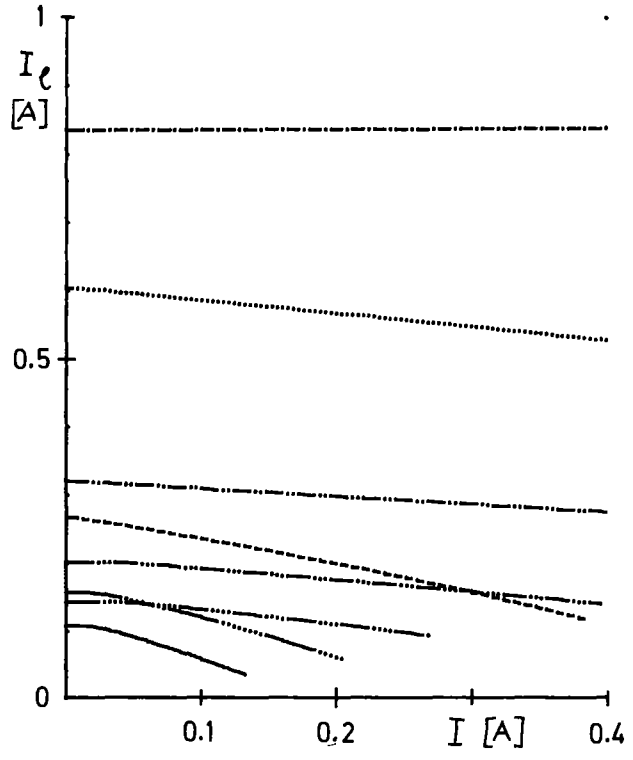

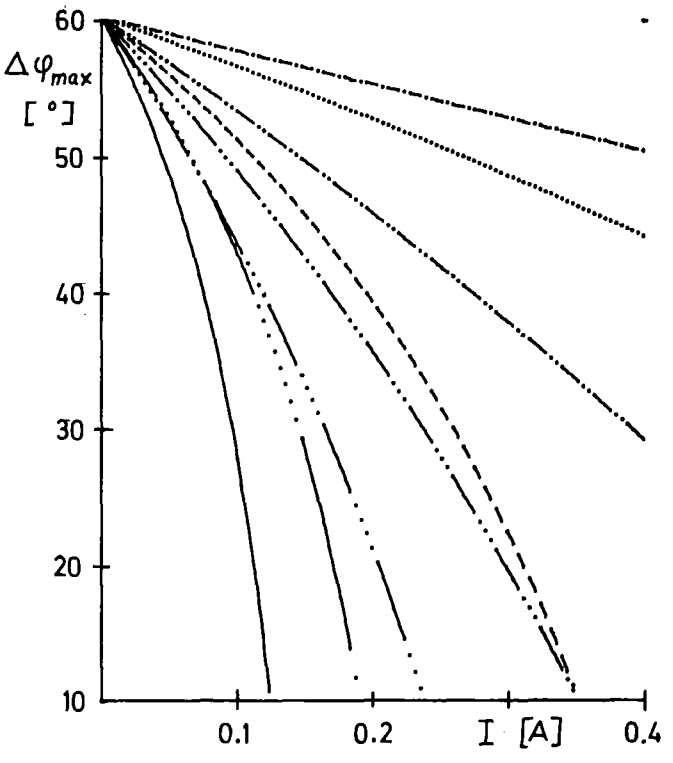

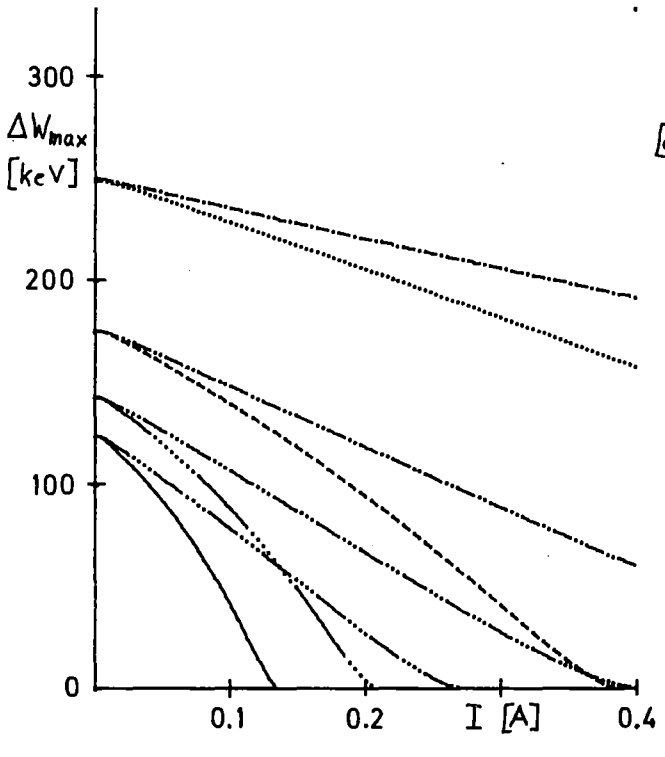

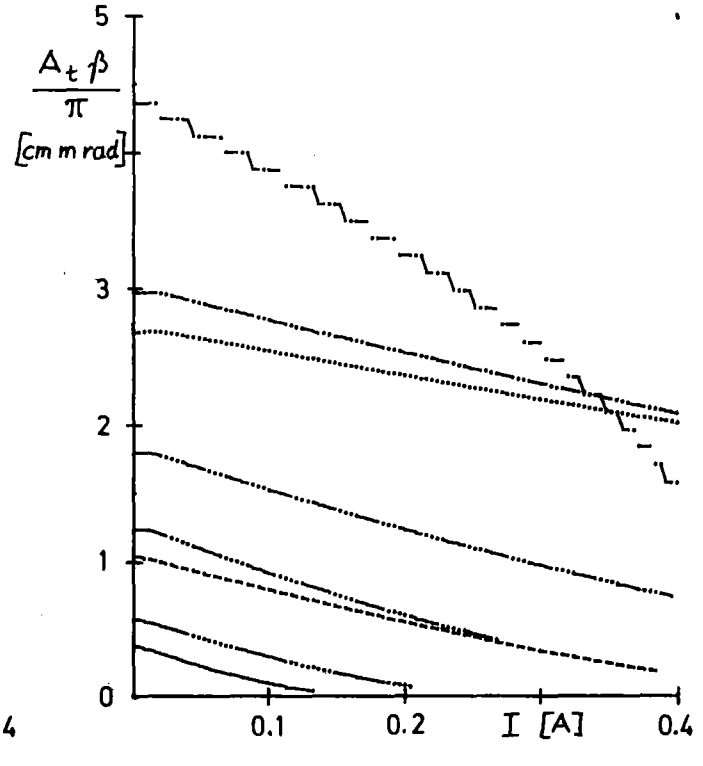

fig. 14

BETA = 0.0283 ; LAMBDA = 11.10 METER ; SIGMA = 0.75 ; MASS = 2

MUE(I=0) = 90 DEGREE ; PHI-S = -40 DEGREE ; PHI = -40 DEGREE

EPEAK = 7.3 MVOLT/METER

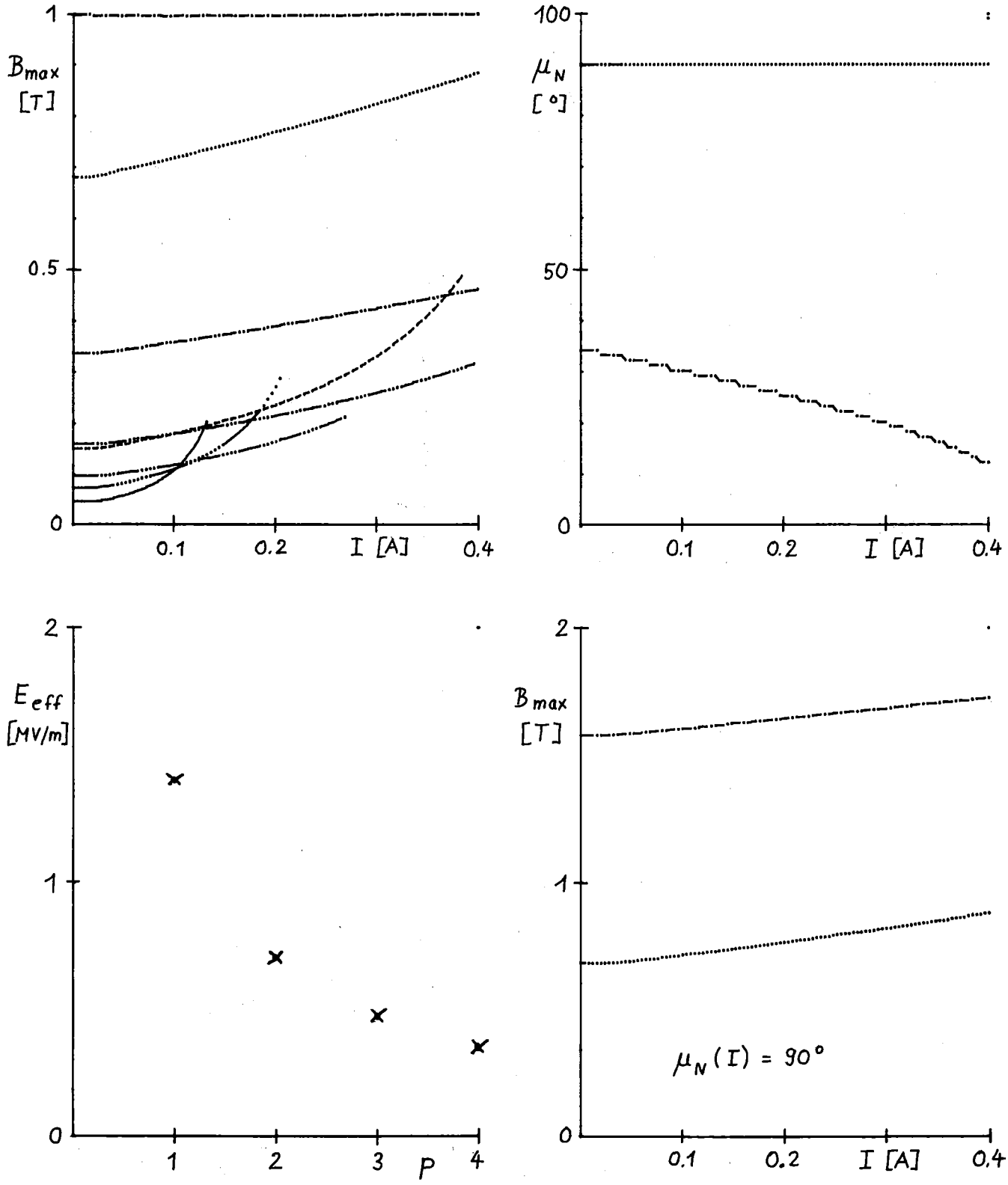

fig. 15

BETA = 0.0283 ; LAMBDA = 11.10 METER ; SIGMA = 0.75 ; MASS = 2

MUE(I=0) = 90 DEGREE ; PHI-S = -40 DEGREE ; PHI = -40 DEGREE

EPEAK = 7.3 MVOLT/METER

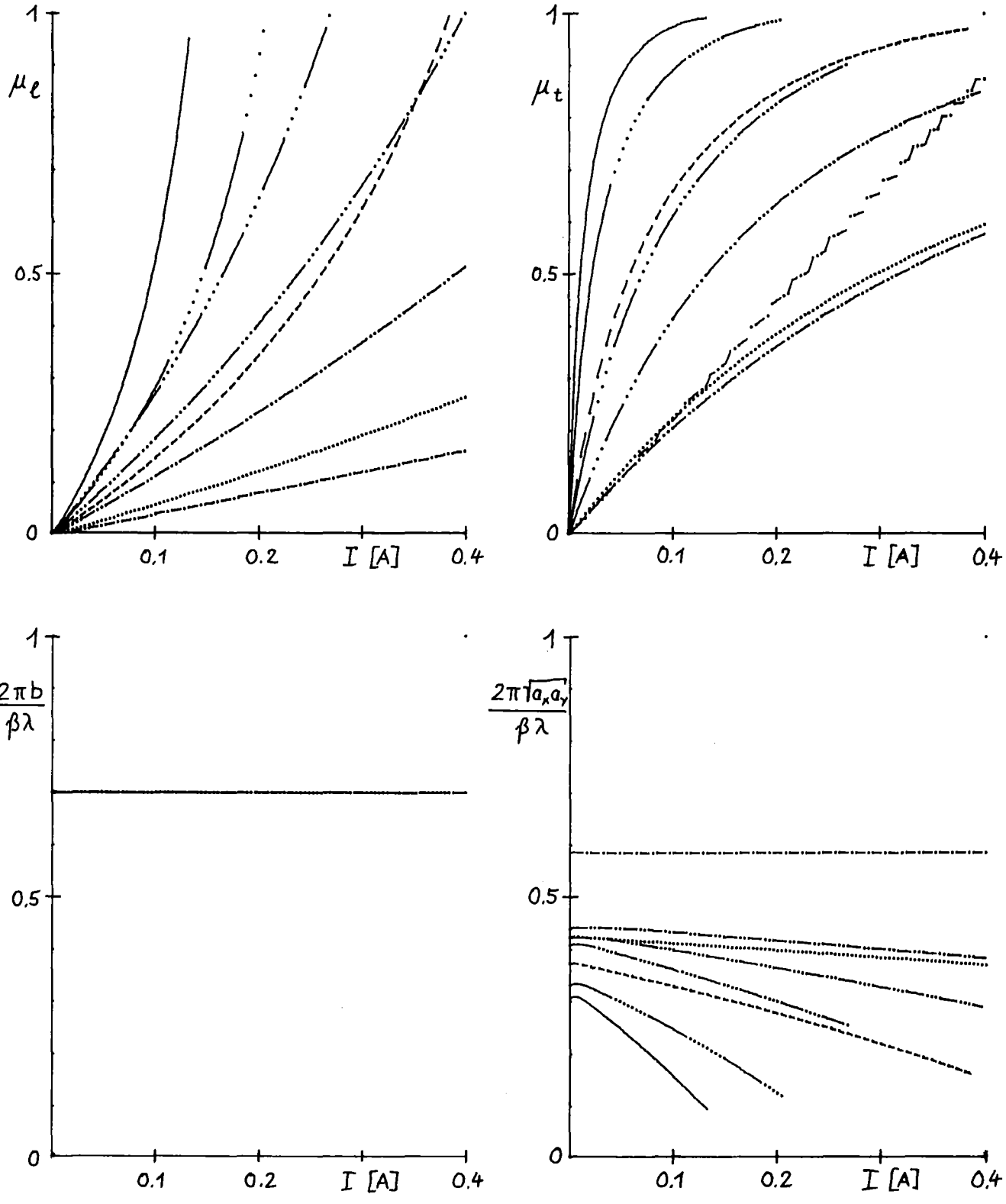

fig. 16

BETA = 0.0193 ; LAMBDA = 5.56 METER ; SIGMA = 0.75 ; MASS = 2

MUE(I=0) = 90 DEGREE ; PHI-S = -40 DEGREE ; PHI = -40 DEGREE

EPEAK = 9.2 MVOLT/METER

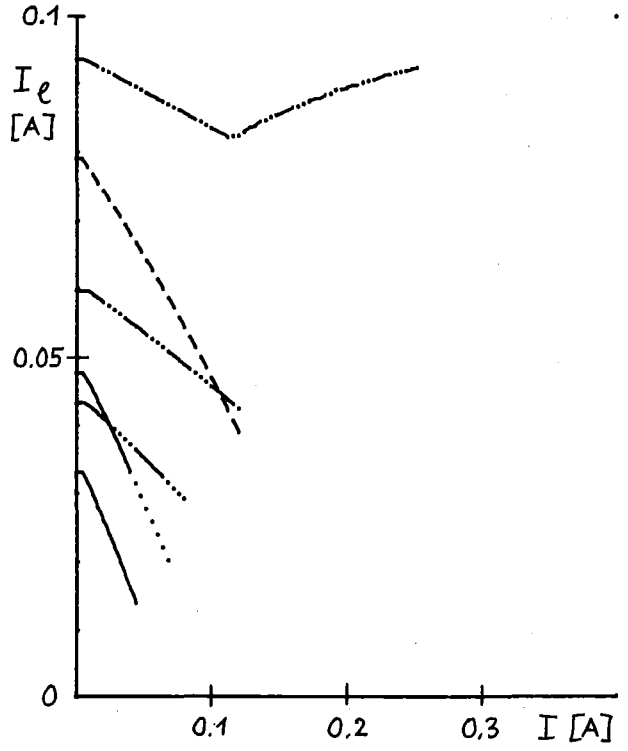

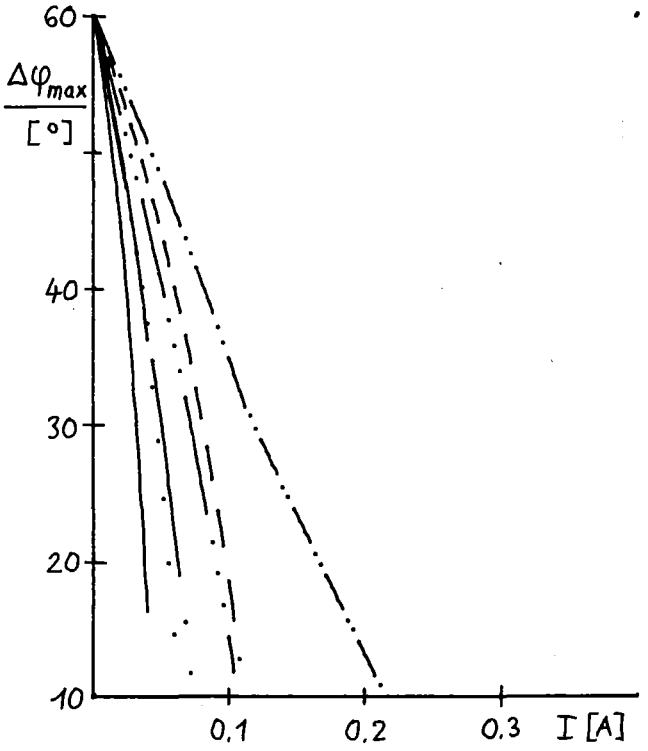

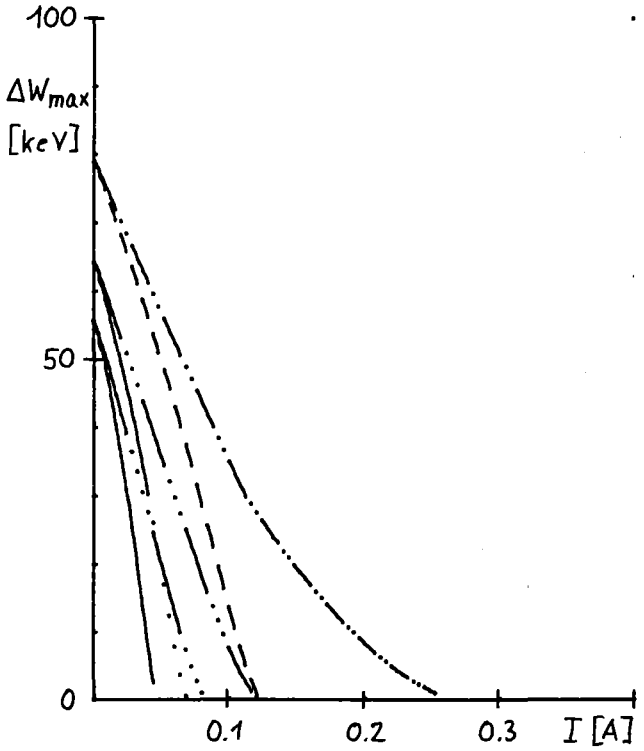

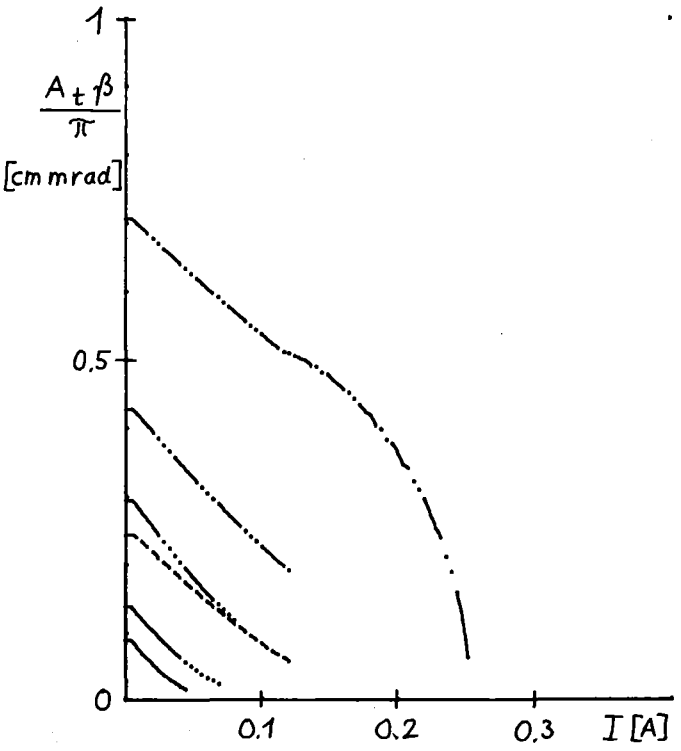

fig. 17

BETA = 0.0193 ; LAMBDA = 5.56 METER ; SIGMA = 0.75 ; MASS = 2

MUE(I=0) = 90 DEGREE ; PHI-S = -40 DEGREE ; PHI = -40 DEGREE

EPEAK = 9.2 MVOLT/METER

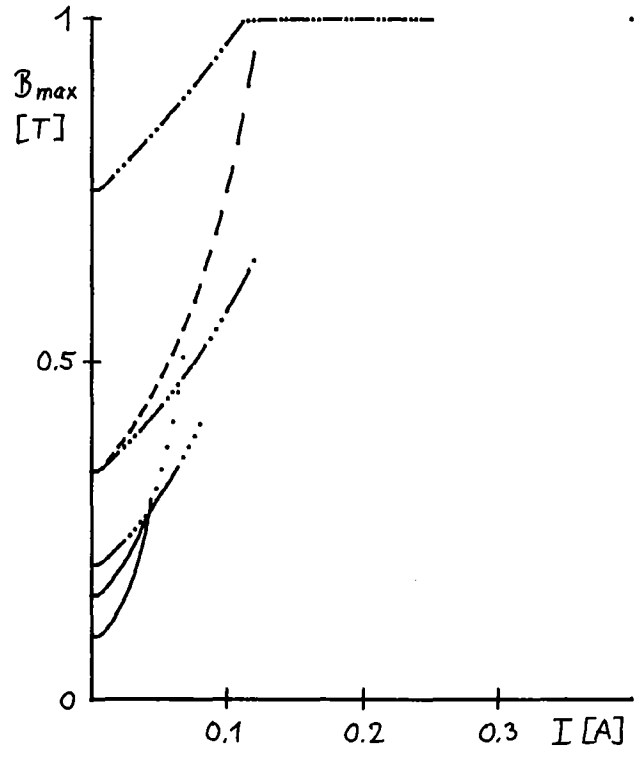

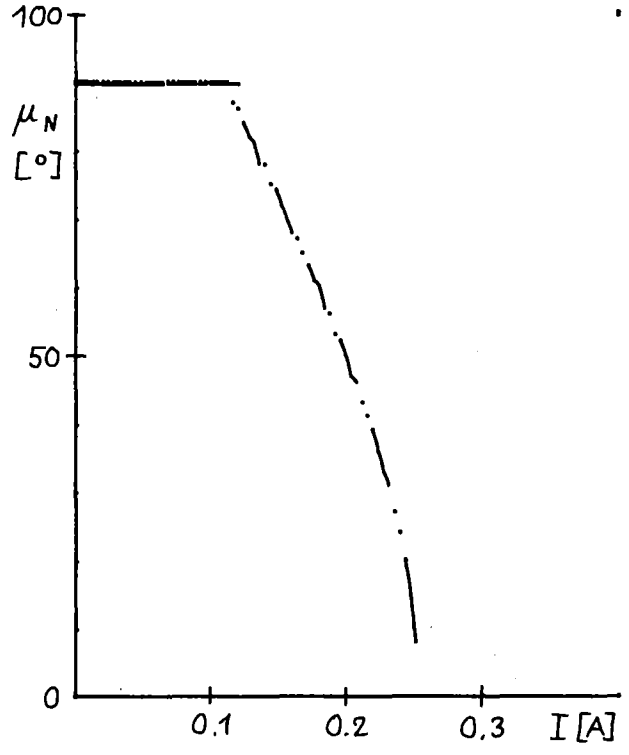

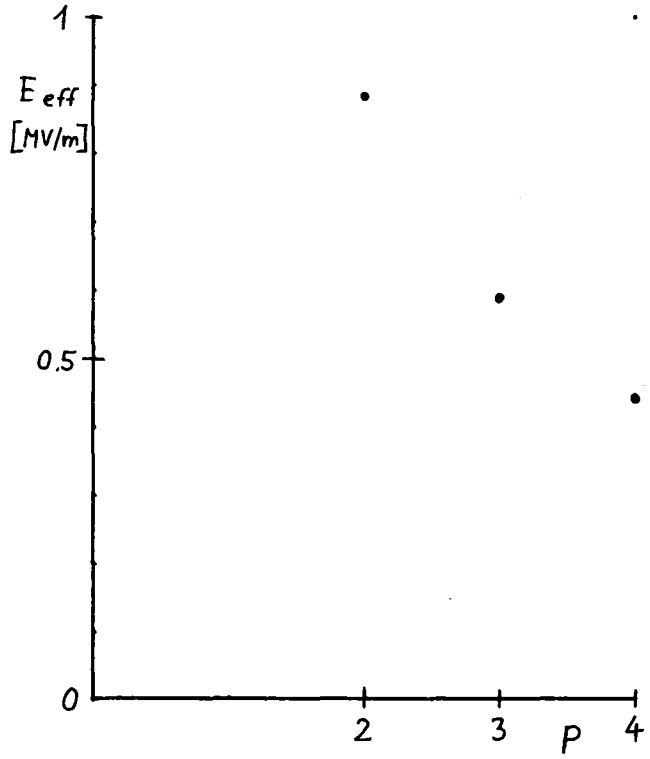

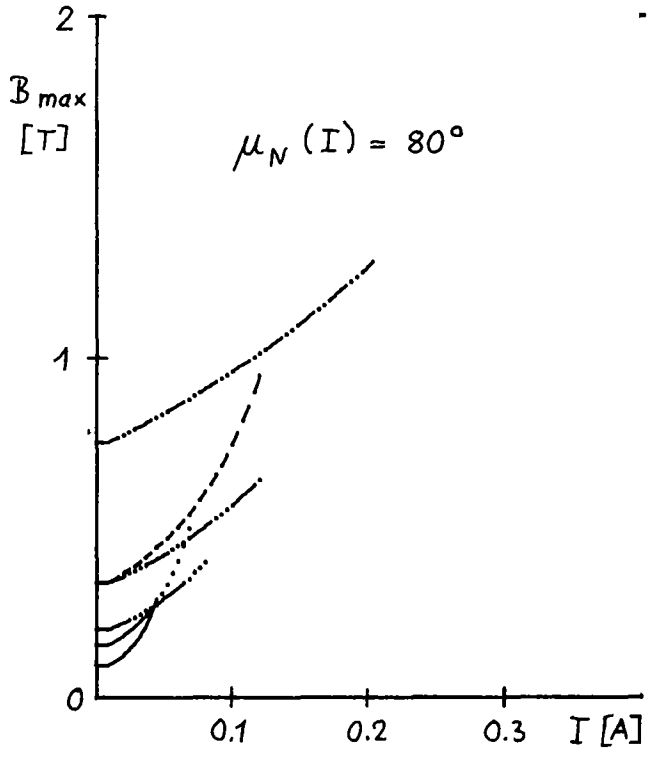

fig. 18

BETA = 0.0193 ; LAMBDA = 5.56 METER ; SIGMA = 0.75 ; MASS = 2

MUE(I=0) = 90 DEGREE ; PHI-S = -40 DEGREE ; PHI = -40 DEGREE

EPEAK = 9.2 MVOLT/METER

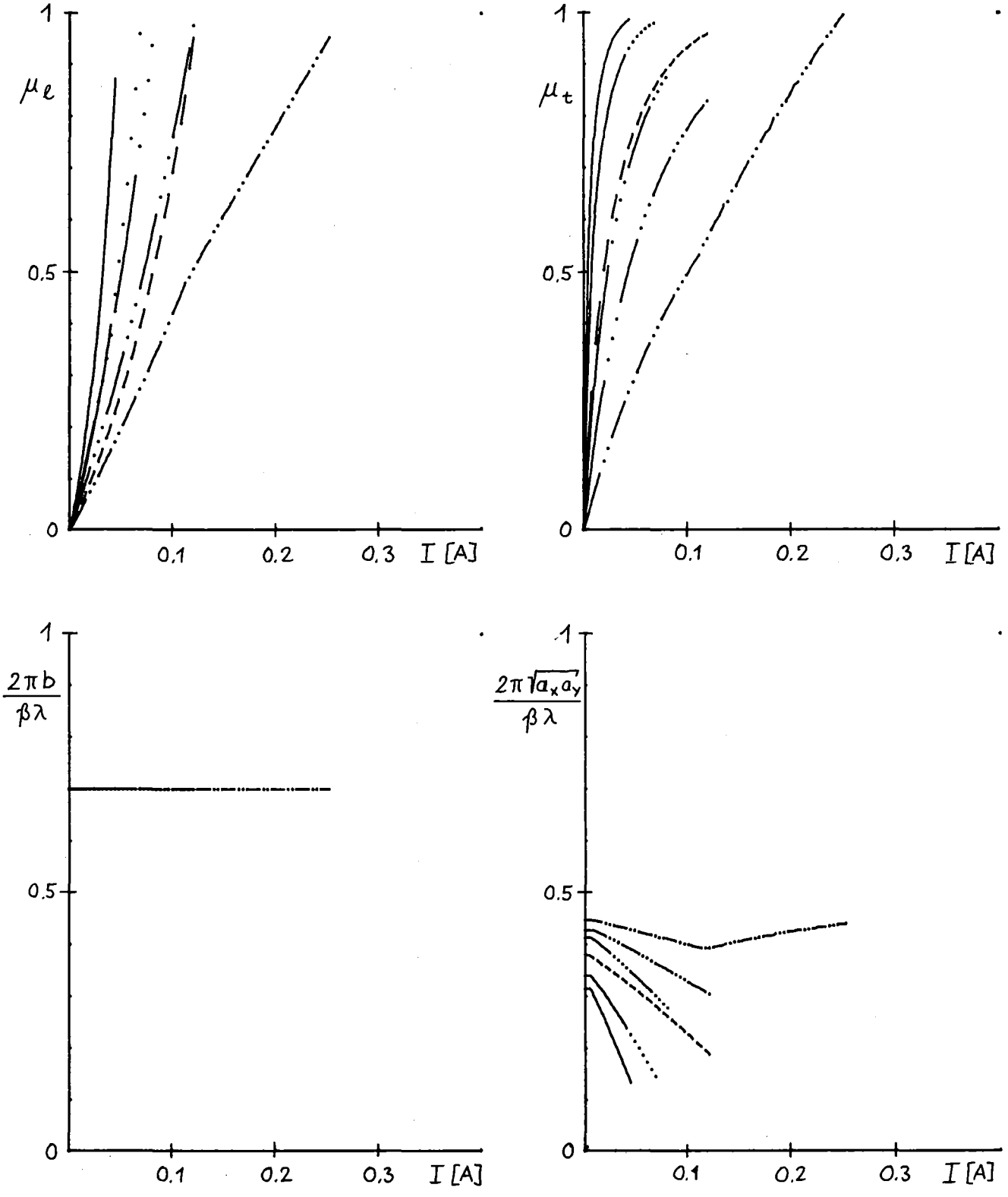

fig. 19

BETA = 0.0231 ; LAMBDA = 5.56 METER ; SIGMA = 0.75 ; MASS = 2

MUE(I=0) = 90 DEGREE ; PHI-S = -40 DEGREE ; PHI = -40 DEGREE

EPEAK = 9.2 MVOLT/METER

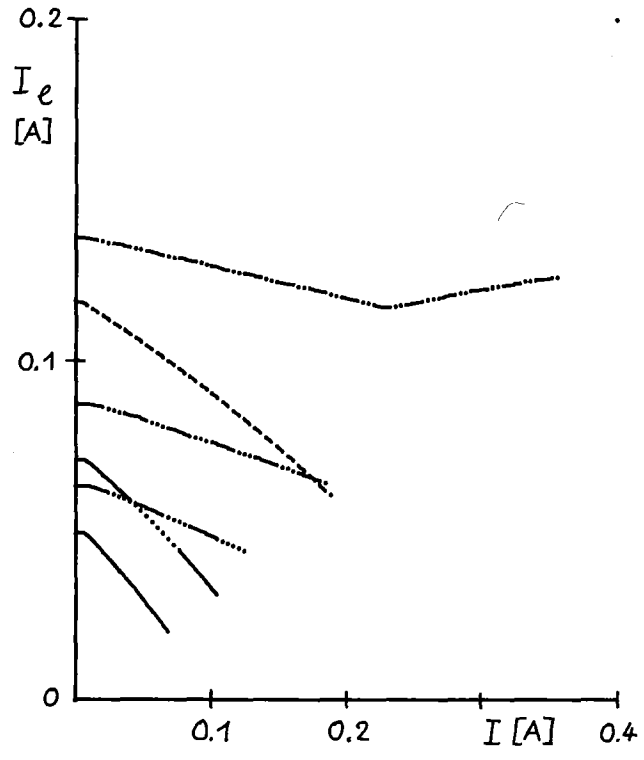

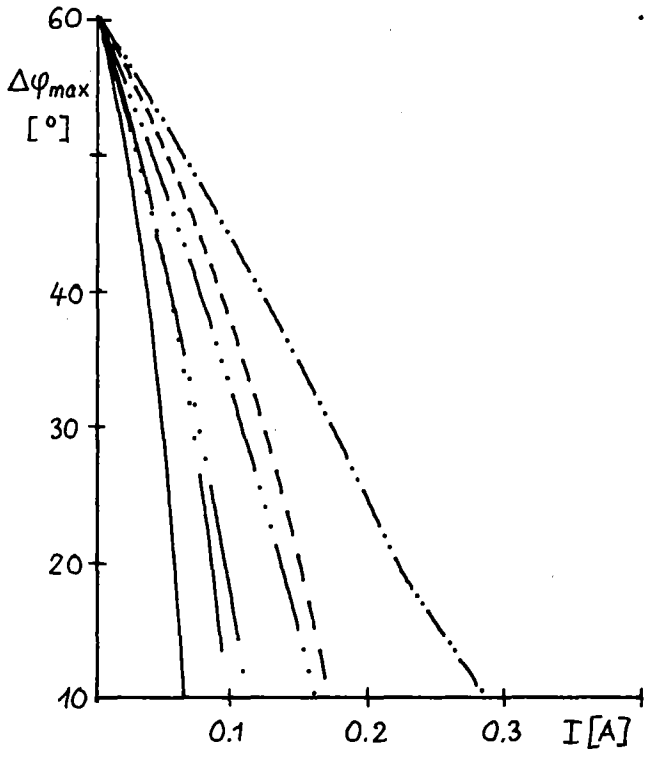

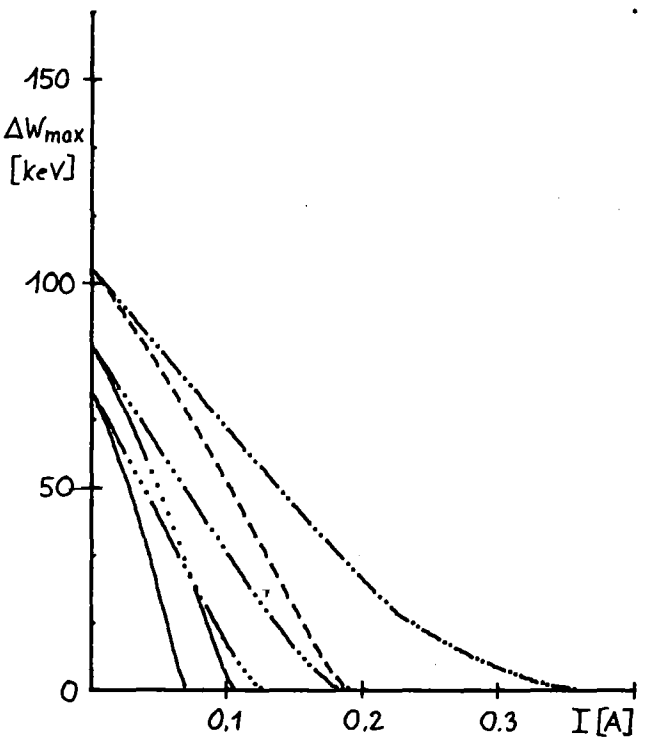

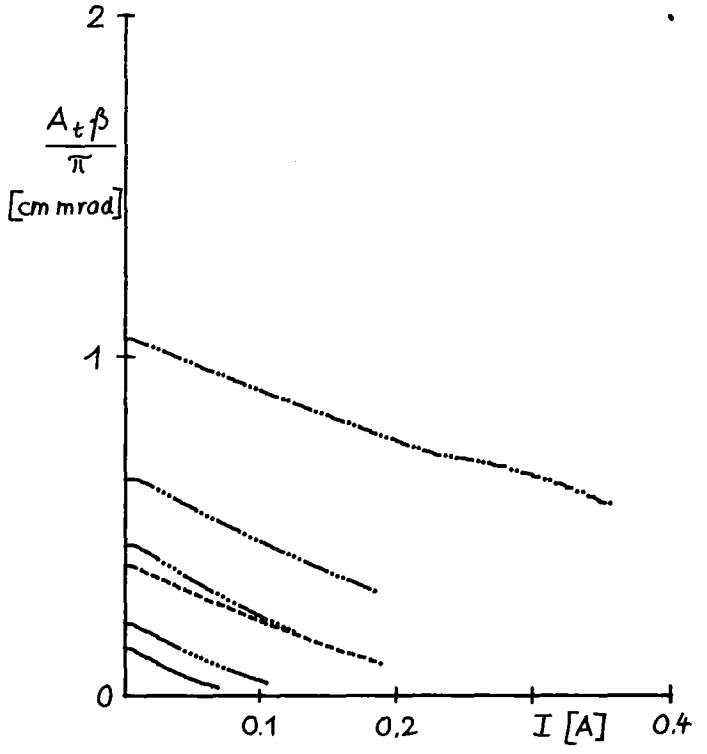

fig. 20

BETA = 0.0231 ; LAMBDA = 5.56 METER ; SIGMA = 0.75 ; MASS = 2

MUE(I=0) = 90 DEGREE ; PHI-S = -40 DEGREE ; PHI = -40 DEGREE

EPEAK = 9.2 MVOLT/METER

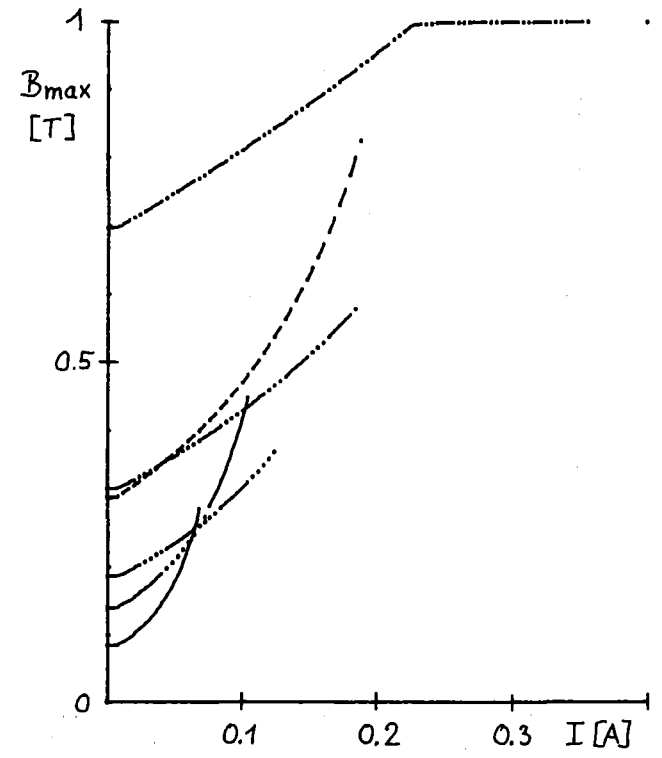

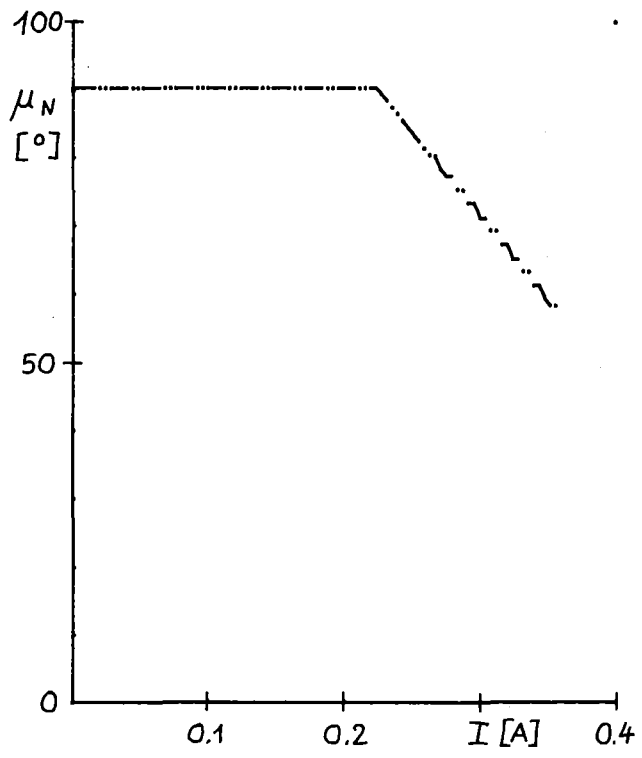

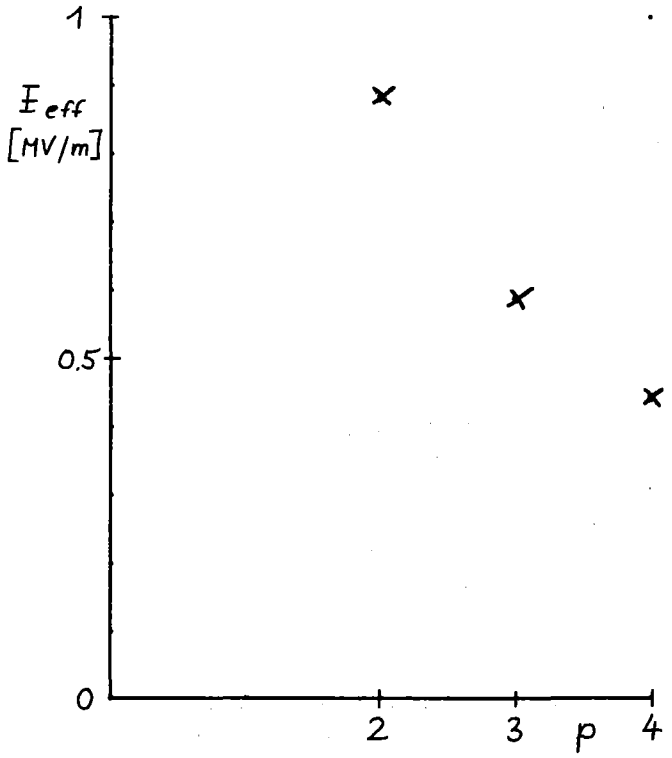

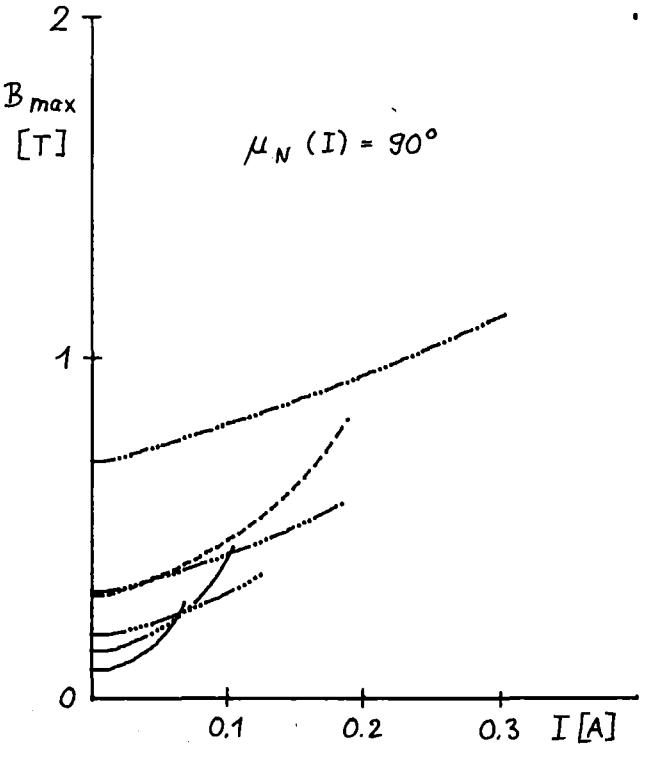

fig. 21

BETA = 0.0231 ; LAMBDA = 5.56 METER ; SIGMA = 0.75 ; MASS = 2

MUE(I=0) = 90 DEGREE ; PHI-S = -40 DEGREE ; PHI = -40 DEGREE

EPEAK = 9.2 MVOLT/METER

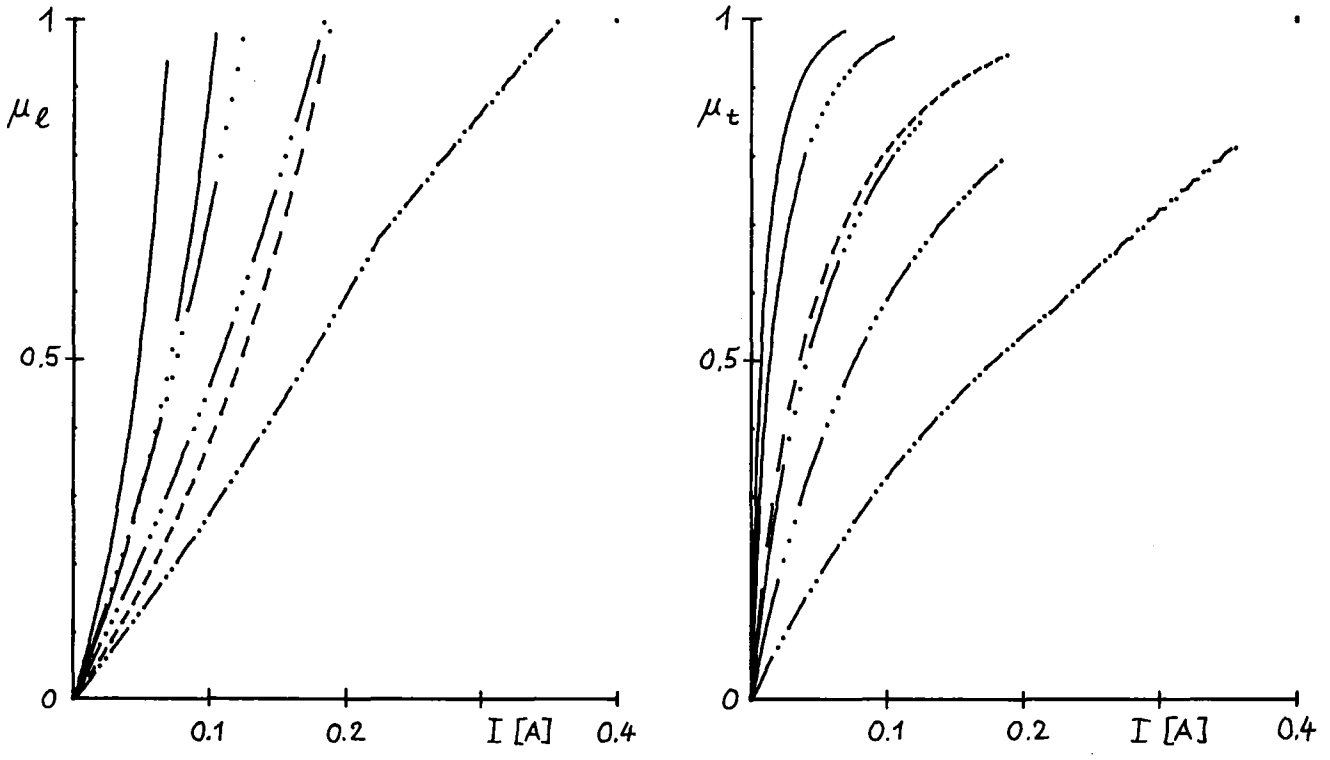

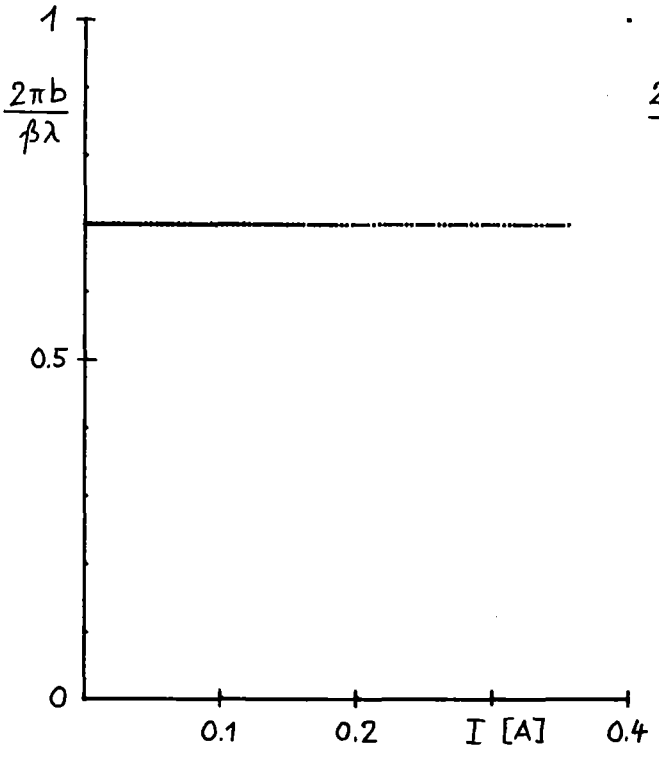

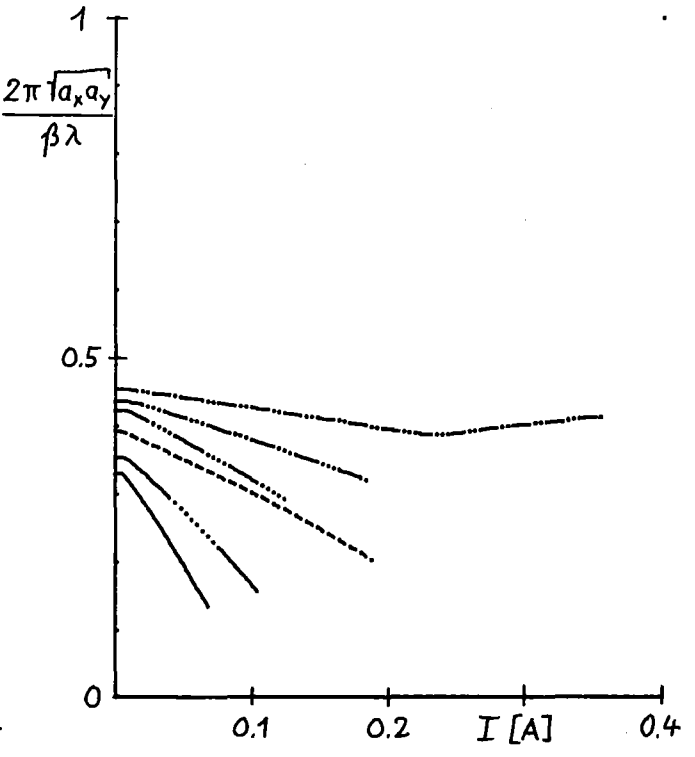

fig. 22

BETA = 0.0283 ; LAMBDA = 5.56 METER ; SIGMA = 0.75 ; MASS = 2

MUE(I=0) = 90 DEGREE ; PHI-S = -40 DEGREE ; PHI = -40 DEGREE

EPEAK = 9.2 MVOLT/METER

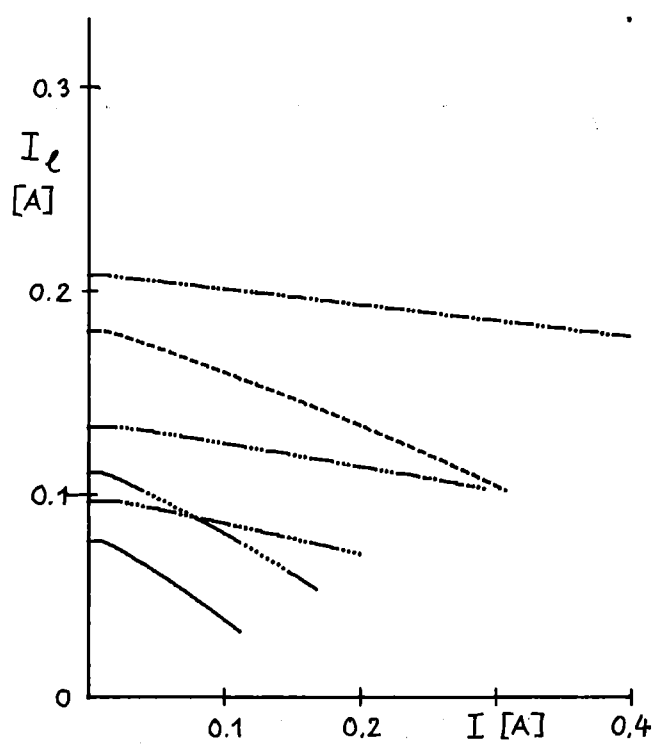

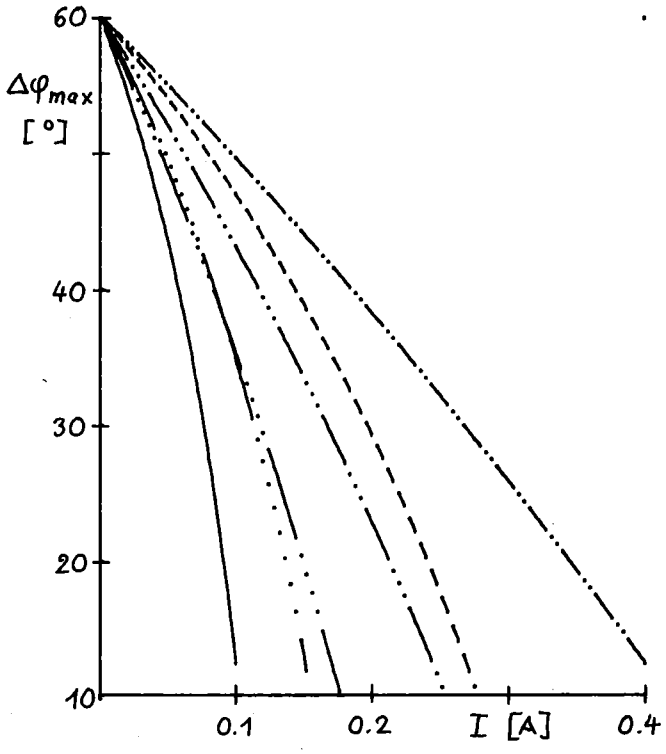

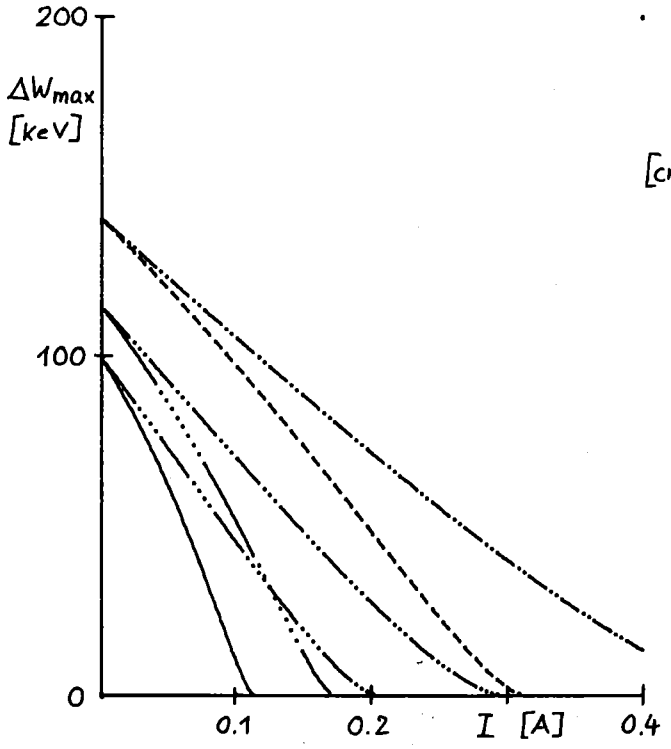

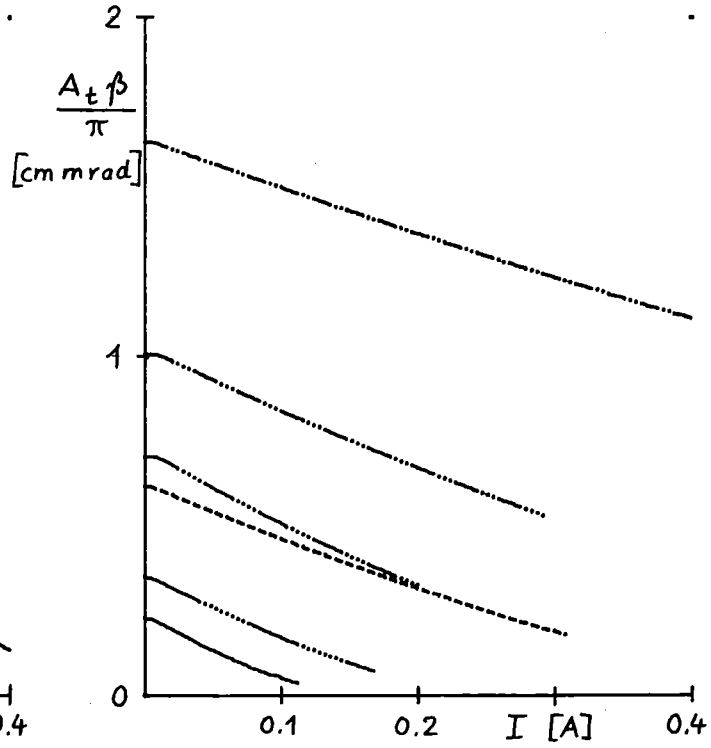

fig. 23

BETA = 0.0283 ; LAMBDA = 5.56 METER ; SIGMA = 0.75 ; MASS = 2

MUE(I=0) = 90 DEGREE ; PHI-S = -40 DEGREE ; PHI = -40 DEGREE

EPEAK = 9.2 MVOLT/METER

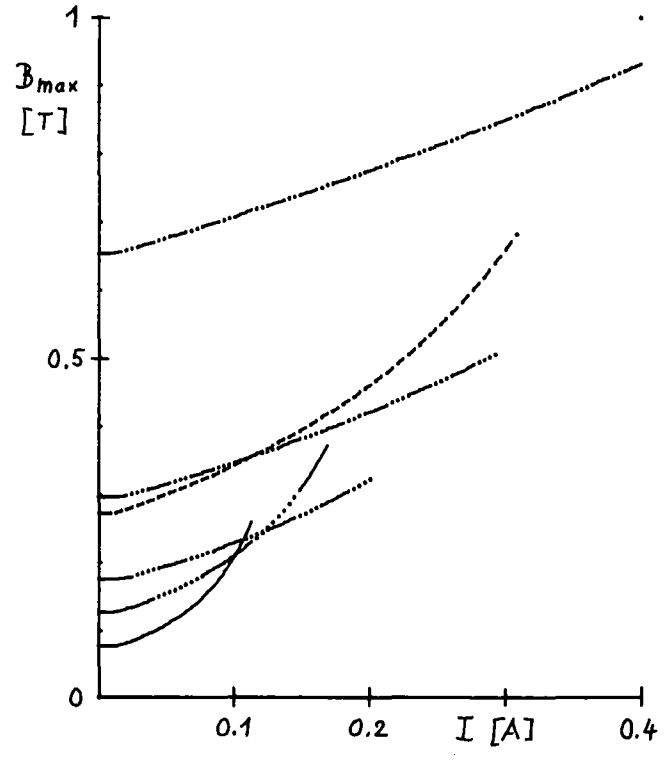

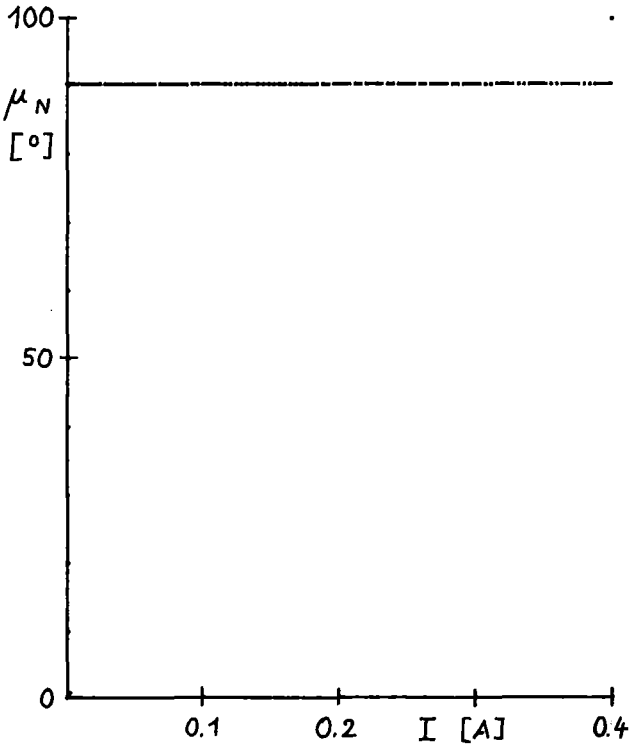

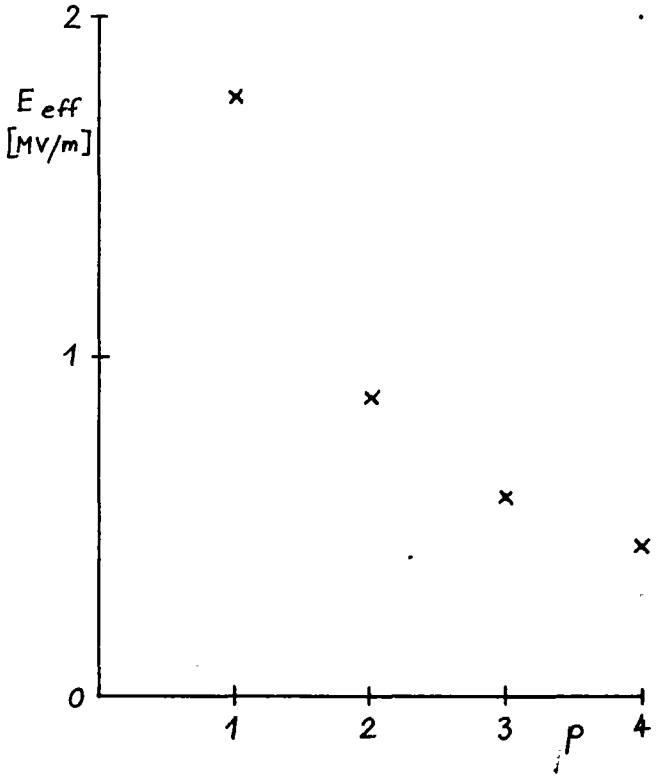

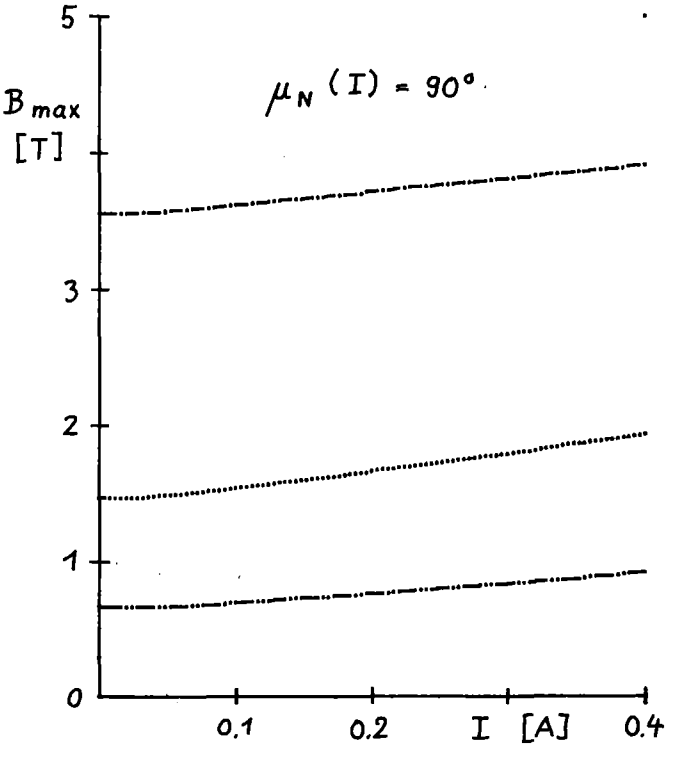

fig. 24

BETA = 0.0283 ; LAMBDA = 5.56 METER ; SIGMA = 0.75 ; MASS = 2

MUE(I=0) = 90 DEGREE ; PHI-S = -40 DEGREE ; PHI = -40 DEGREE

EPEAK = 9.2 MVOLT/METER

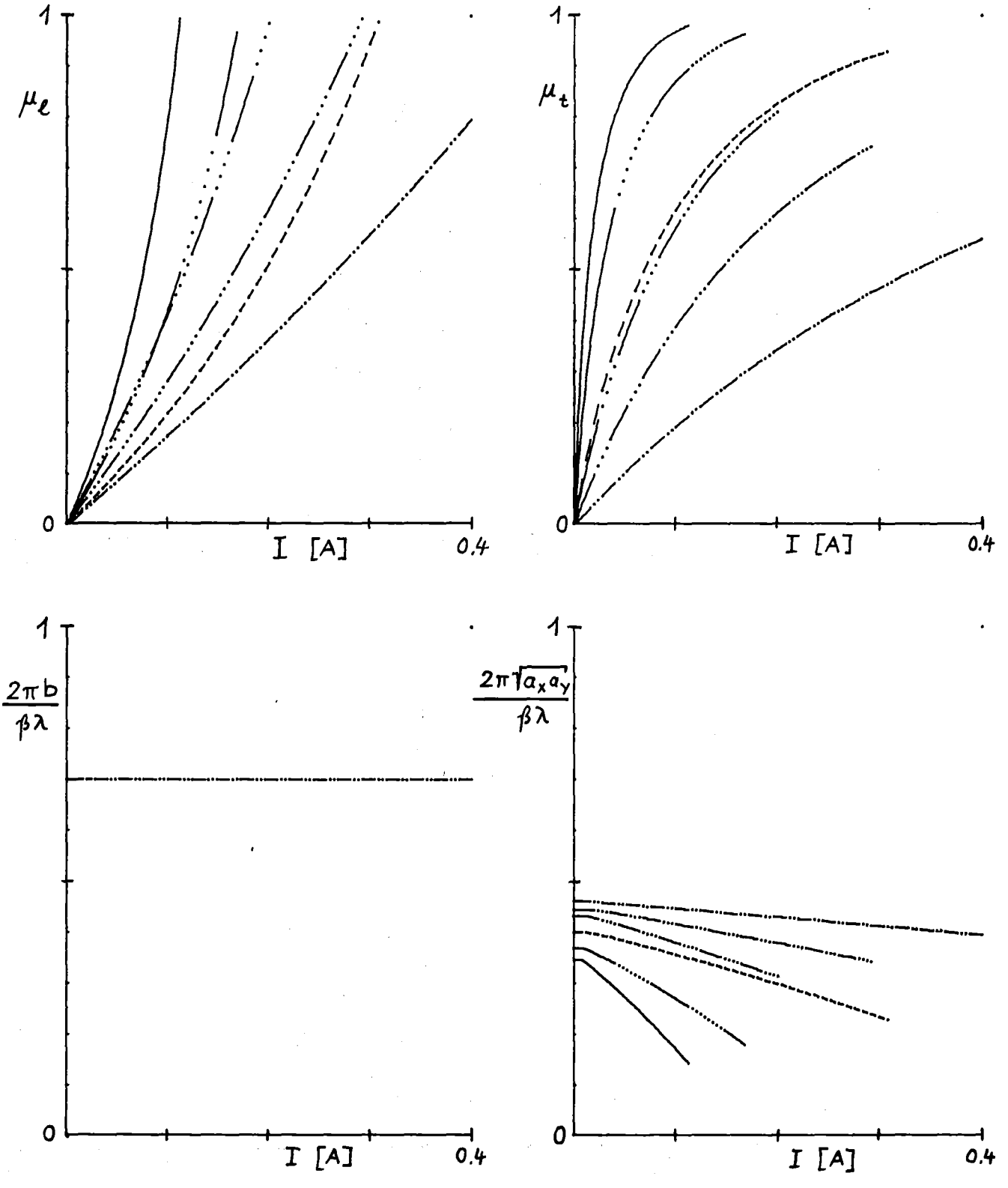

fig. 25

BETA = 0.0231 ; LAMBDA = 2.78 METER ; SIGMA = 0.75 ; MASS = 2

MUE(I=0) = 90 DEGREE ; PHI-S = -40 DEGREE ; PHI = -40 DEGREE

EPEAK = 11.6 MVOLT/METER

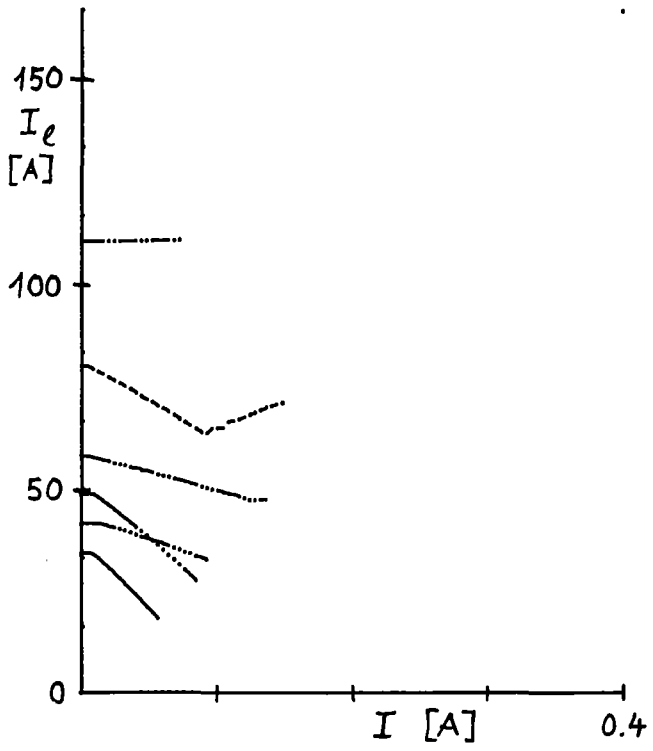

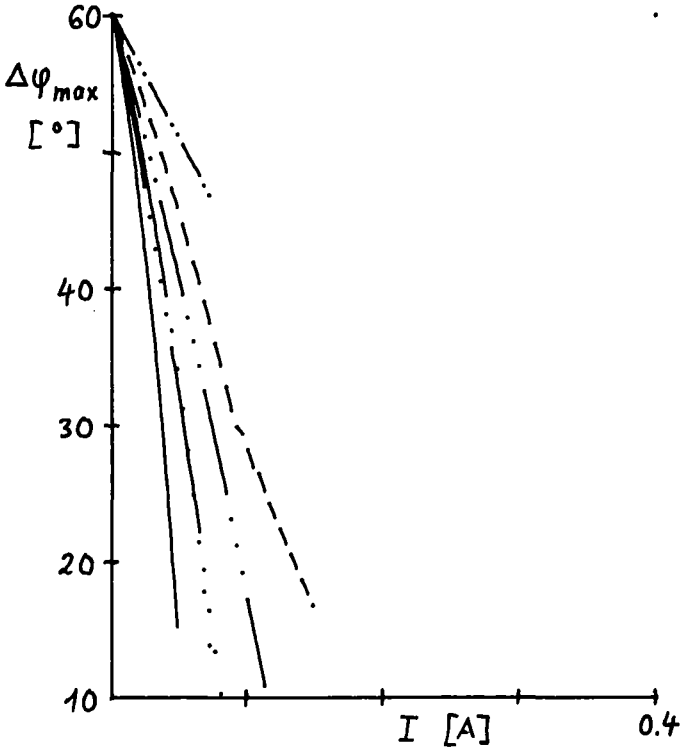

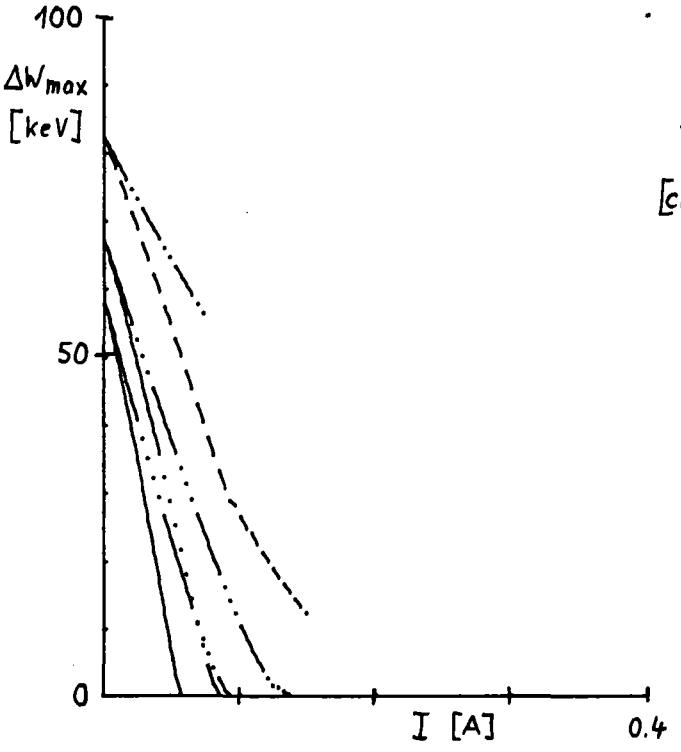

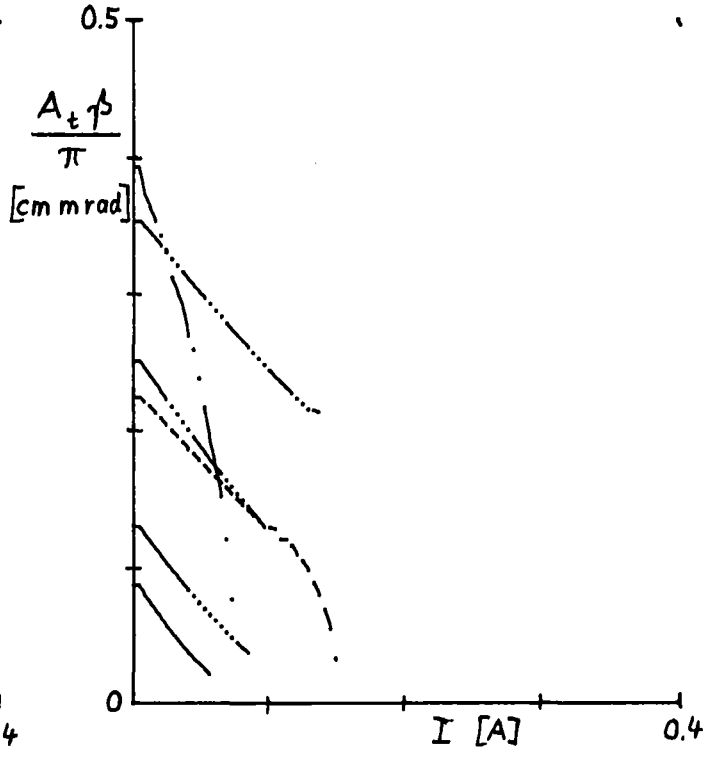

fig. 26

BETA = 0.0231 ; LAMBDA = 2.78 METER ; SIGMA = 0.75 ; MASS = 2

MUE(I=0) = 90 DEGREE ; PHI-S = -40 DEGREE ; PHI = -40 DEGREE

EPEAK = 11.6 MVOLT/METER

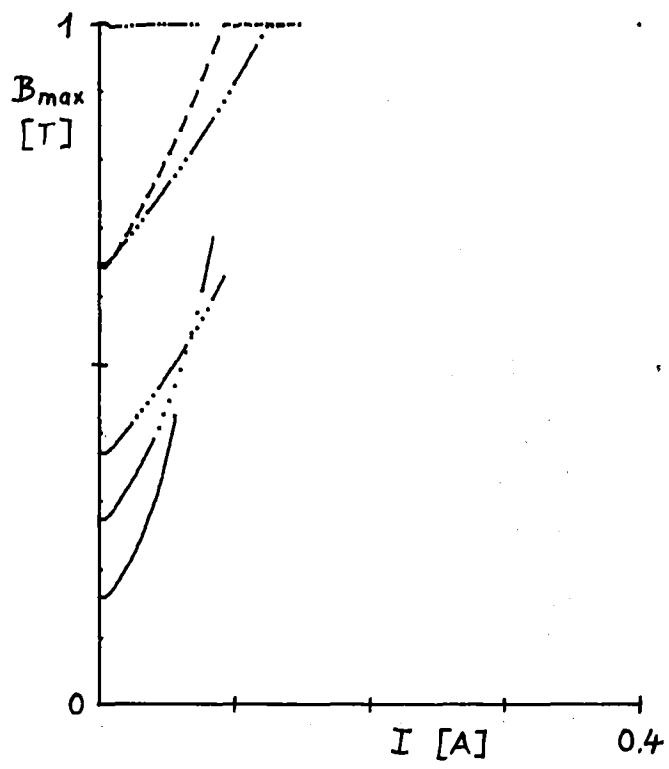

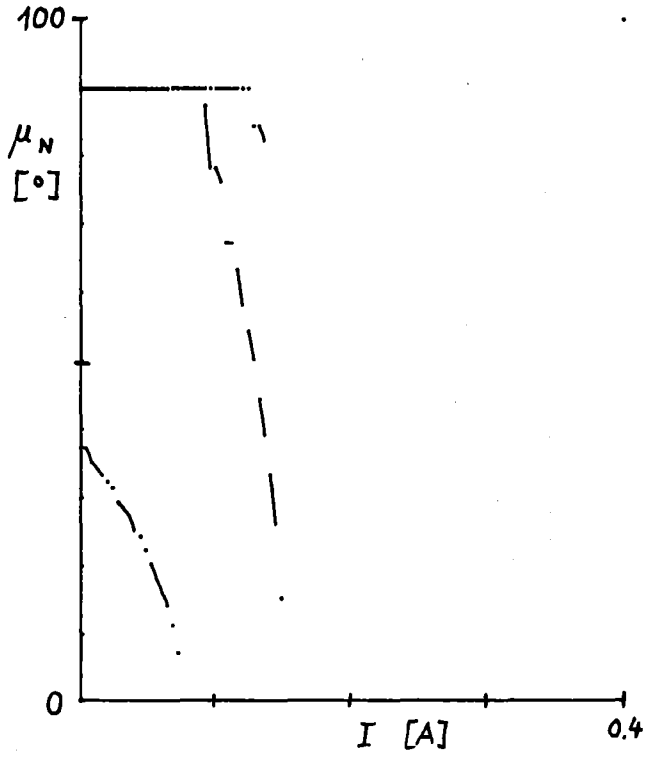

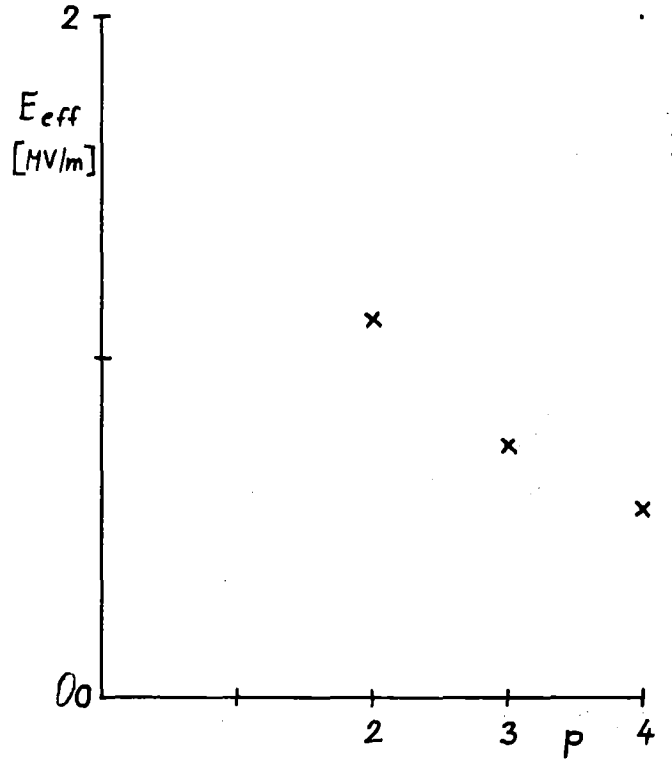

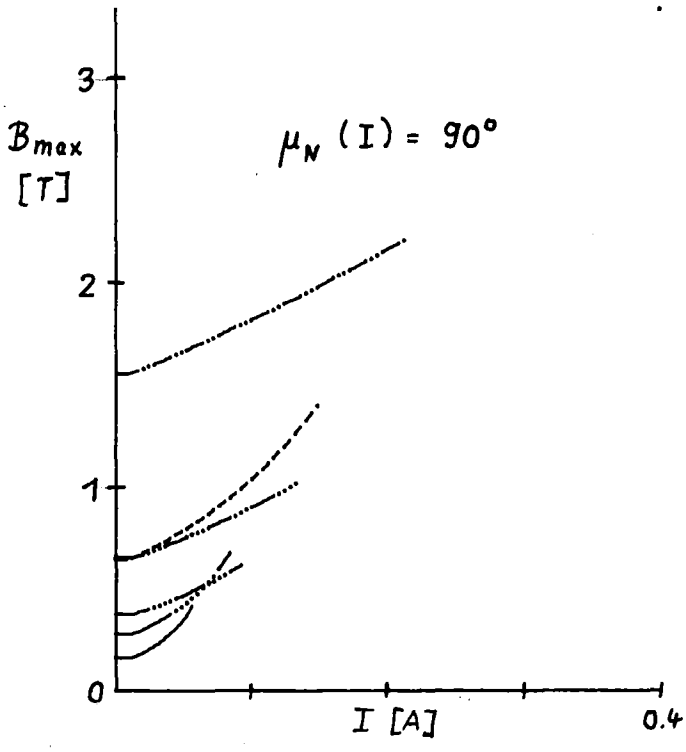

fig. 27

BETA = 0.0231 ; LAMBDA = 2.78 METER ; SIGMA = 0.75 ; MASS = 2

MUE(I=0) = 90 DEGREE ; PHI-S = -40 DEGREE ; PHI = -40 DEGREE

EPEAK = 11.6 MVOLT/METER

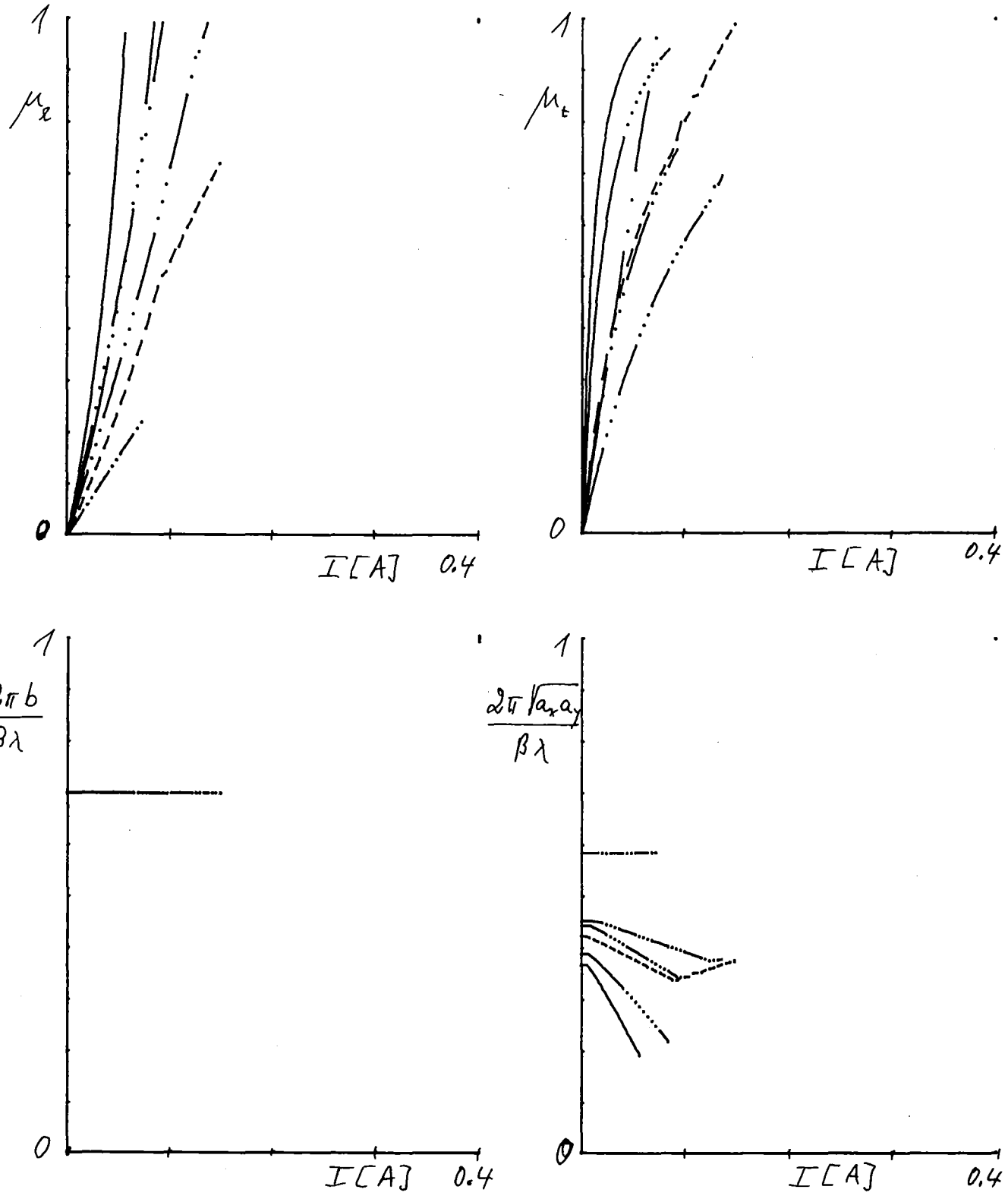

fig. 28

BETA = 0.0283 ; LAMBDA = 2.78 METER ; SIGMA = 0.75 ; MASS = 2

MUE(I=0) = 90 DEGREE ; PHI-S = -40 DEGREE ; PHI = -40 DEGREE

EPEAK = 11.6 MVOLT/METER

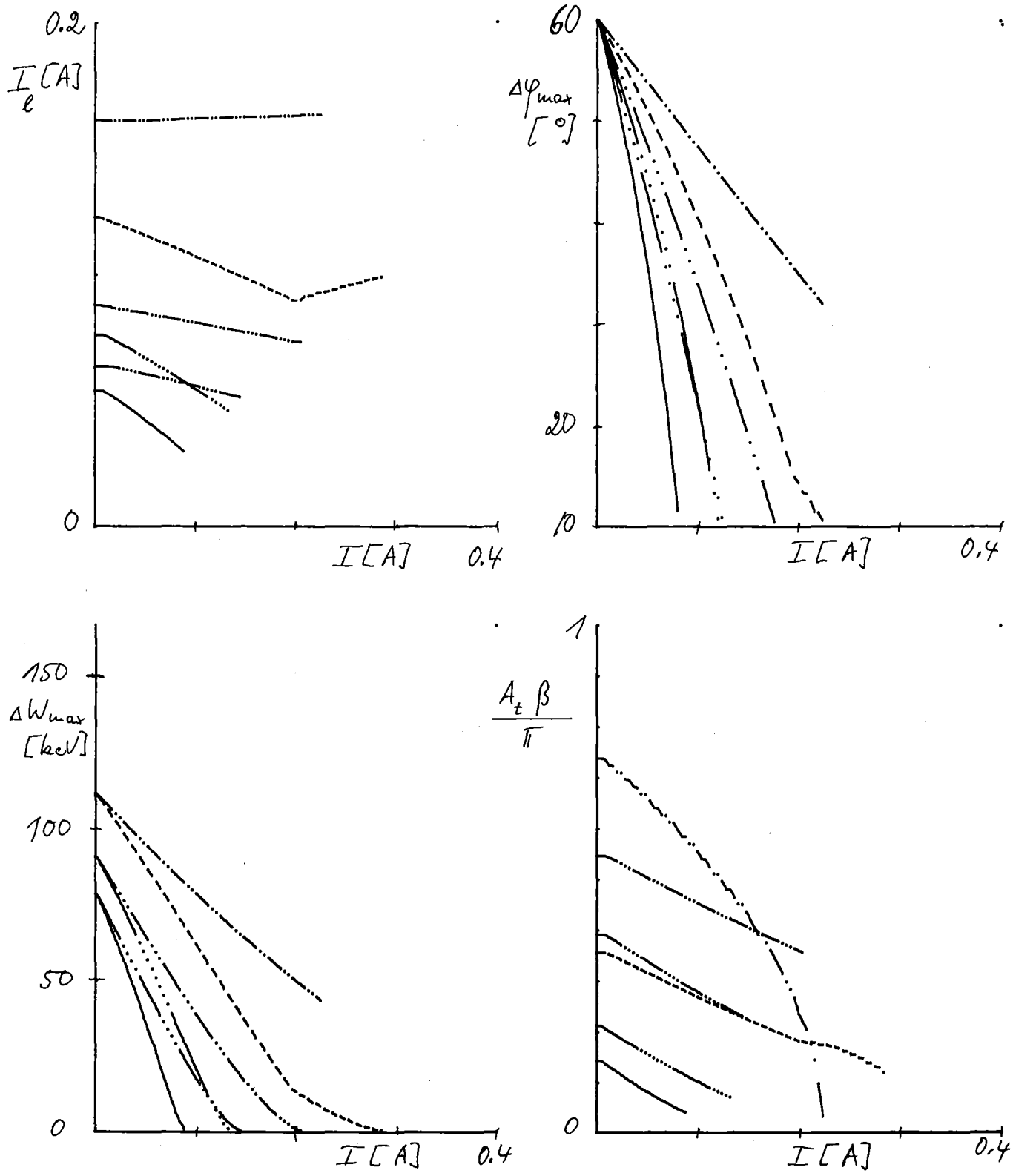

fig. 29

BETA = 0.0283 ; LAMBDA = 2.78 METER ; SIGMA = 0.75 ; MASS = 2

MUE(I=0) = 90 DEGREE ; PHI-S = -40 DEGREE ; PHI = -40 DEGREE

EPEAK = 11.6 MVOLT/METER

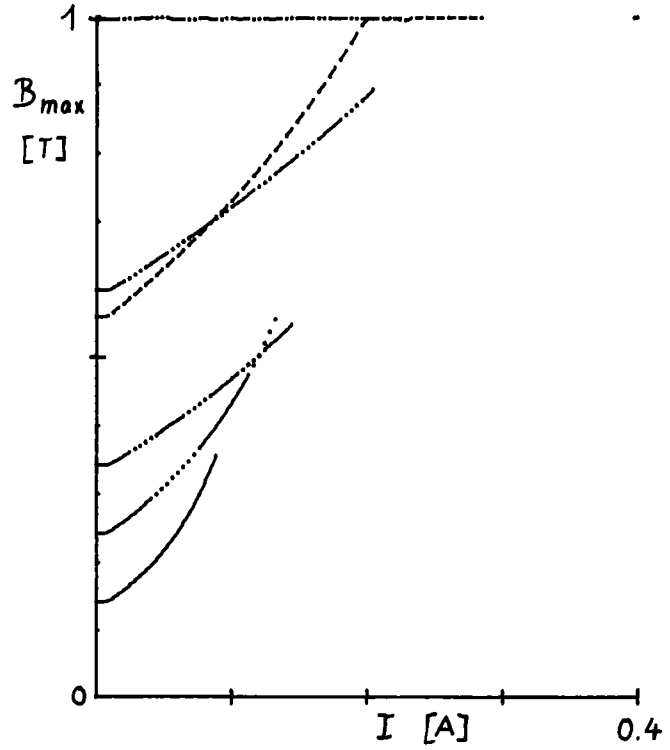

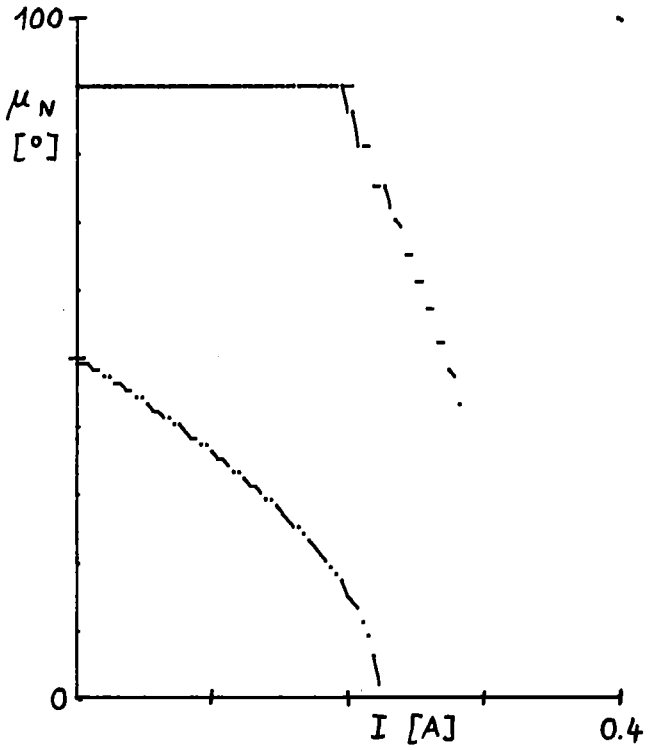

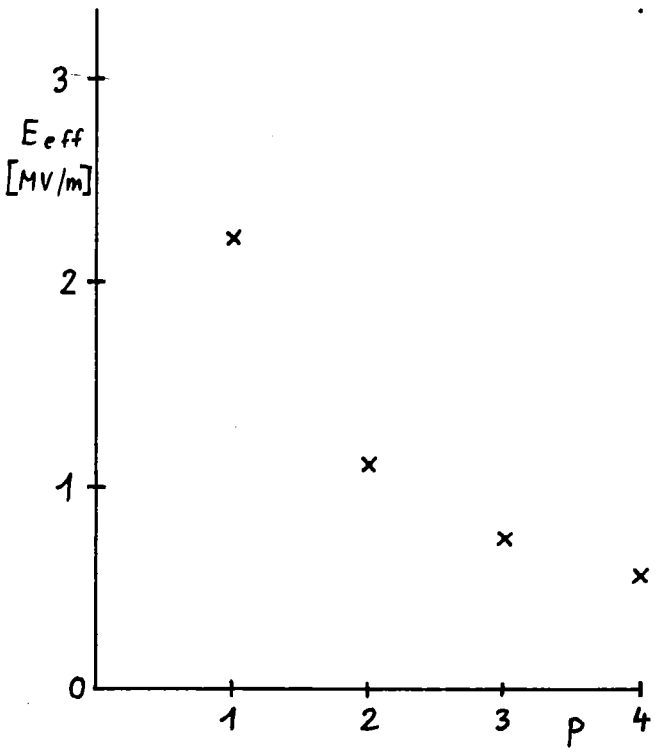

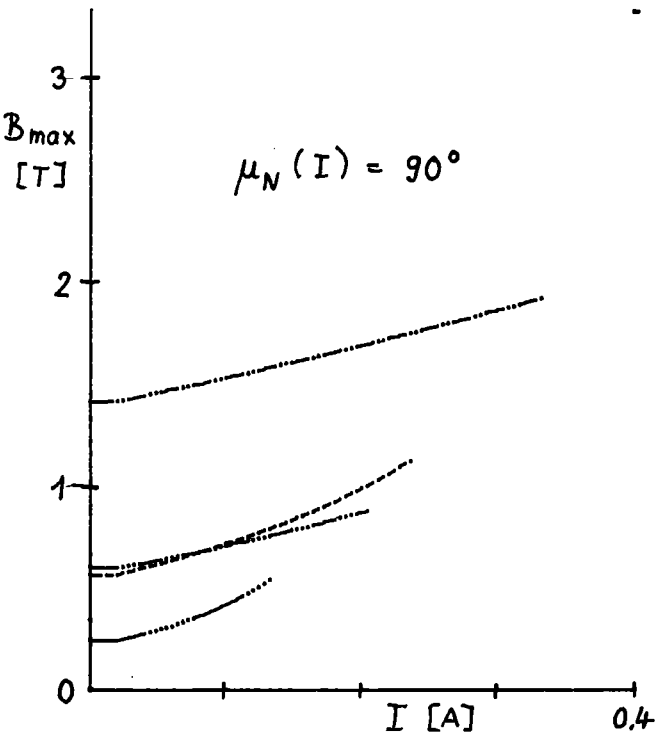

fig. 30

BETA = 0.0283 ; LAMBDA = 2.78 METER ; SIGMA = 0.75 ; MASS = 2

MUE(I=0) = 90 DEGREE ; PHI-S = -40 DEGREE ; PHI = -40 DEGREE

EPEAK = 11.6 MVOLT/METER

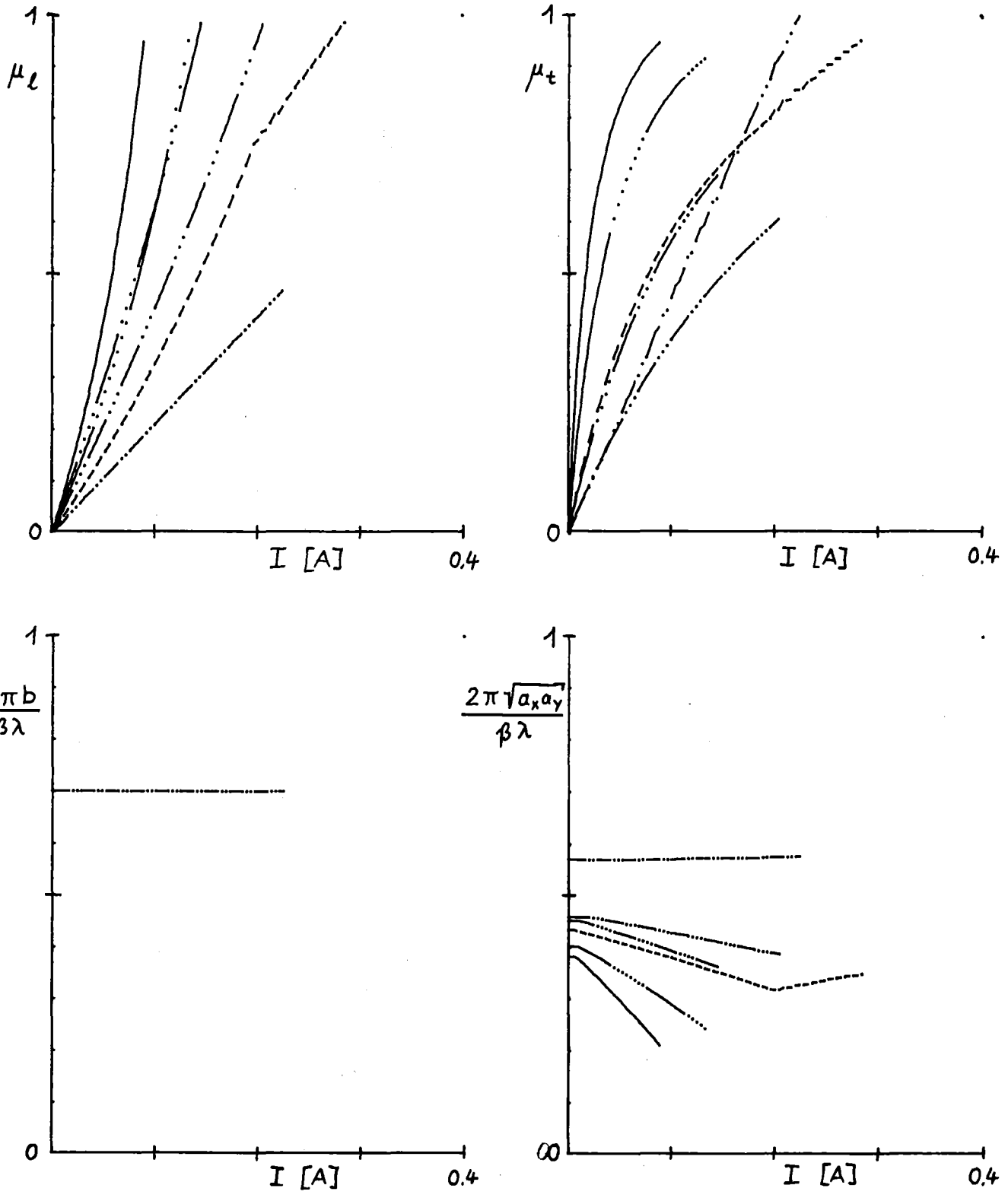

fig. 31

BETA = 0.0400 ; LAMBDA = 1.50 METER ; SIGMA = 0.75 ; MASS = 1

MUE(I=0) = 39 DEGREE ; PHI-S = -35 DEGREE ; PHI = -35 DEGREE

EPEAK = 10.0 MVOLT/METER

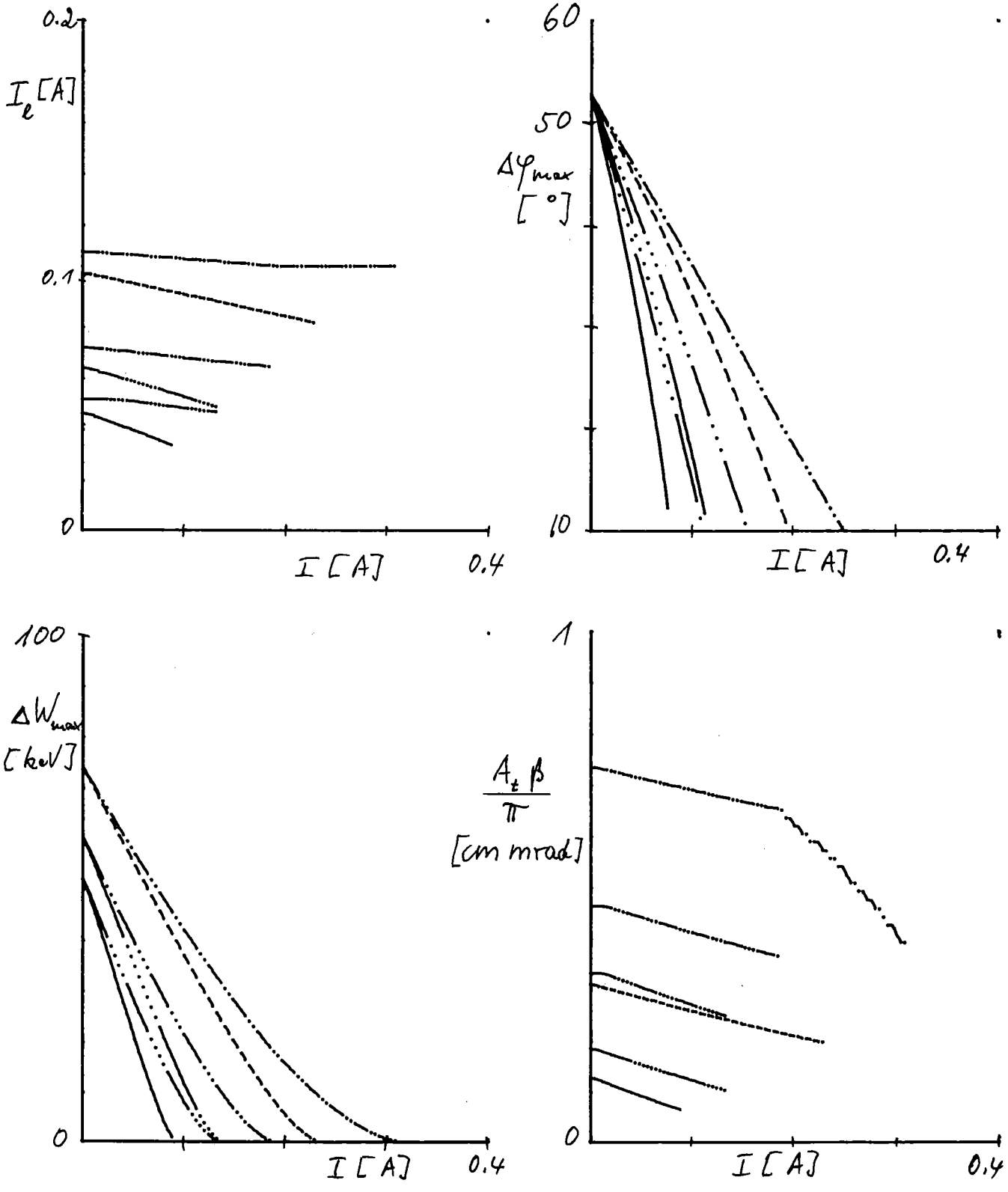

fig. 32

BETA = 0.0400 ; LAMBDA = 1.50 METER ; SIGMA = 0.75 ; MASS = 1

MUE(I=0) = 39 DEGREE ; PHI-S = -35 DEGREE ; PHI = -35 DEGREE

EPEAK = 10.0 MVOLT/METER

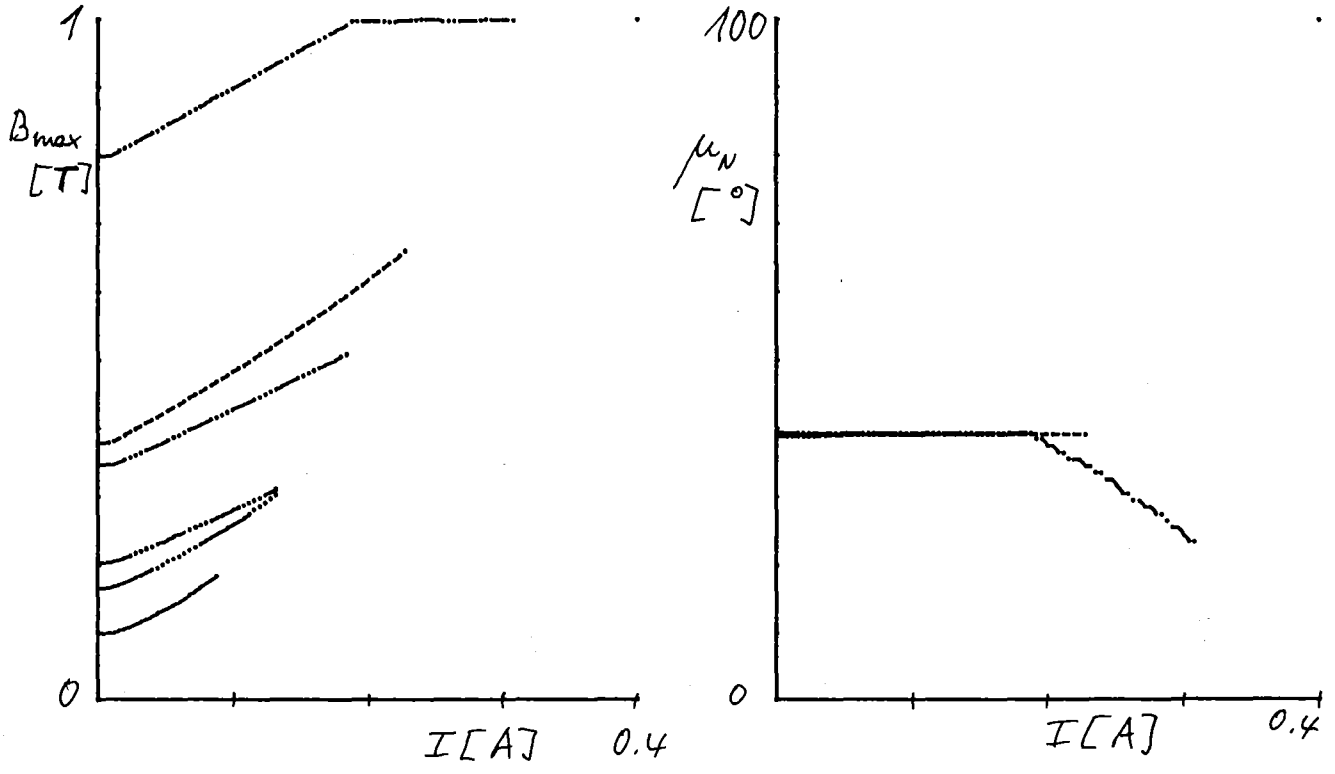

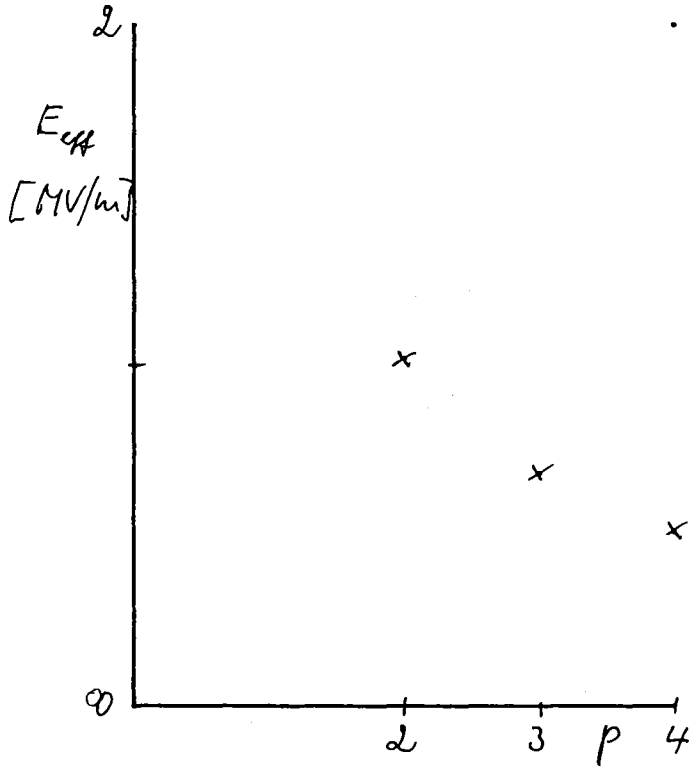

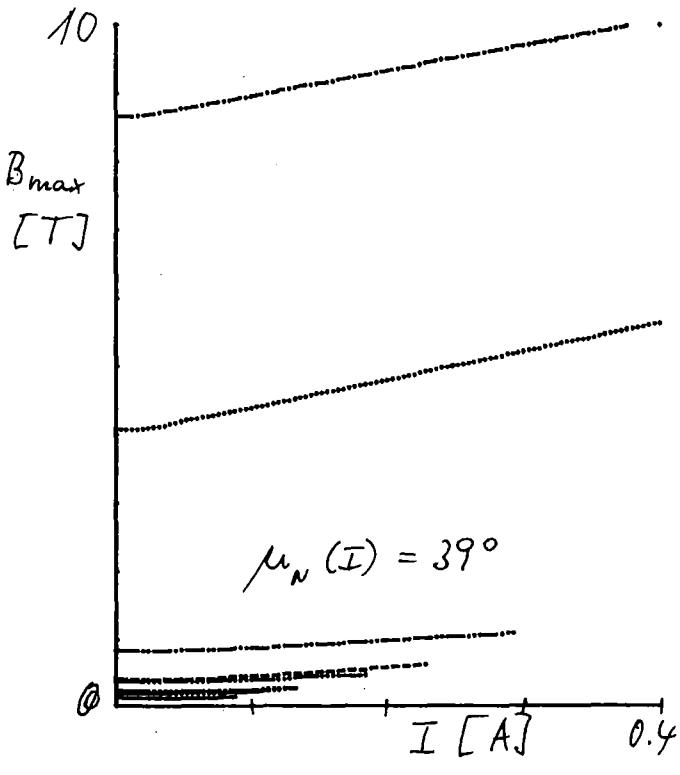

fig. 33

BETA = 0.0400 ; LAMBDA = 1.50 METER ; SIGMA = 0.75 ; MASS = 1

MUE(I=0) = 39 DEGREE ; PHI-S = -35 DEGREE ; PHI = -35 DEGREE

EPEAK = 10.0 MVOLT/METER

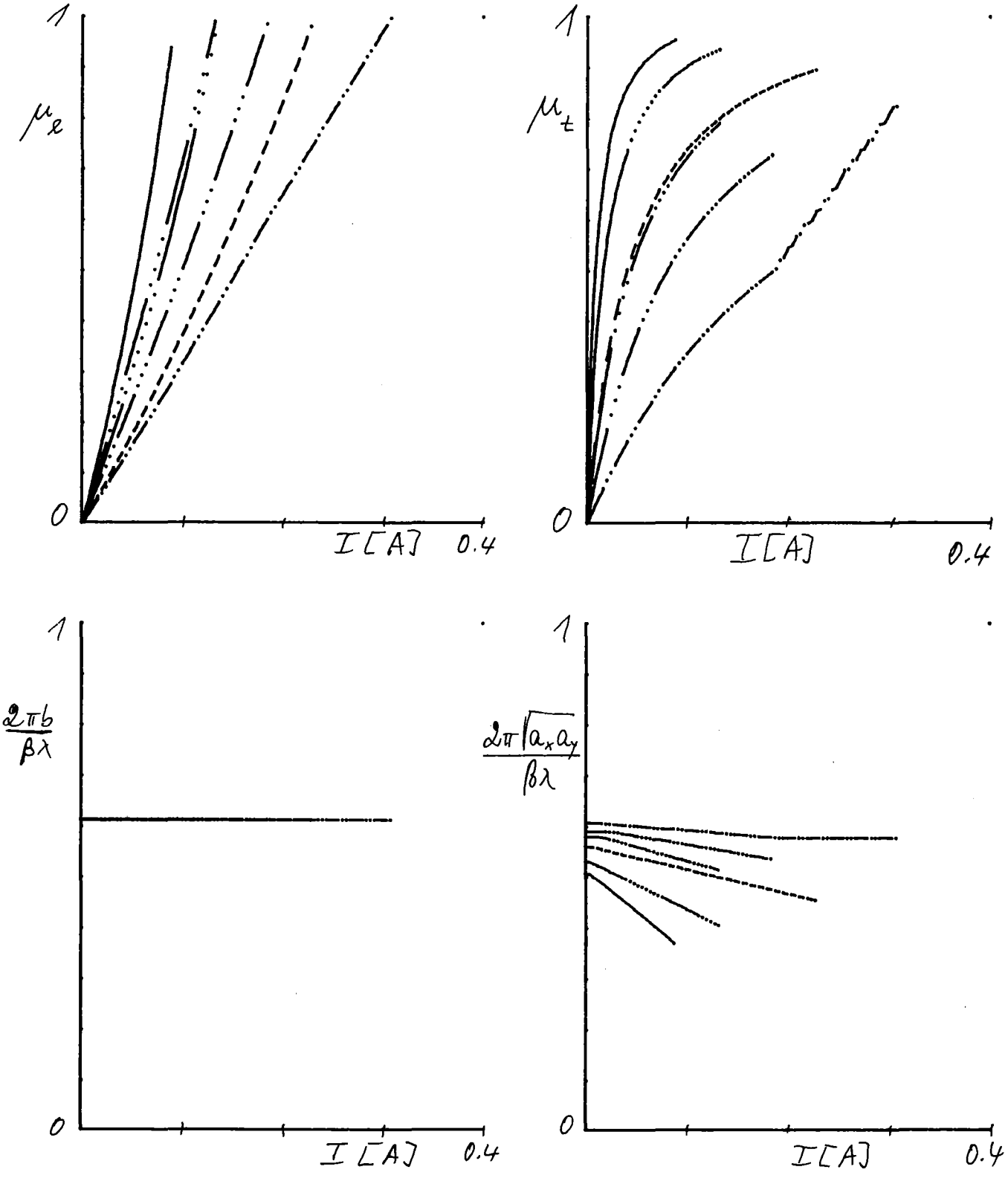

fig. 34

BETA = 0.0400 ; LAMBDA = 1.50 METER ; SIGMA = 0.75 ; MASS = 1

MUE(I=0) = 39 DEGREE ; PHI-S = -35 DEGREE ; PHI = -35 DEGREE

EPEAK = 14.3 MVOLT/METER

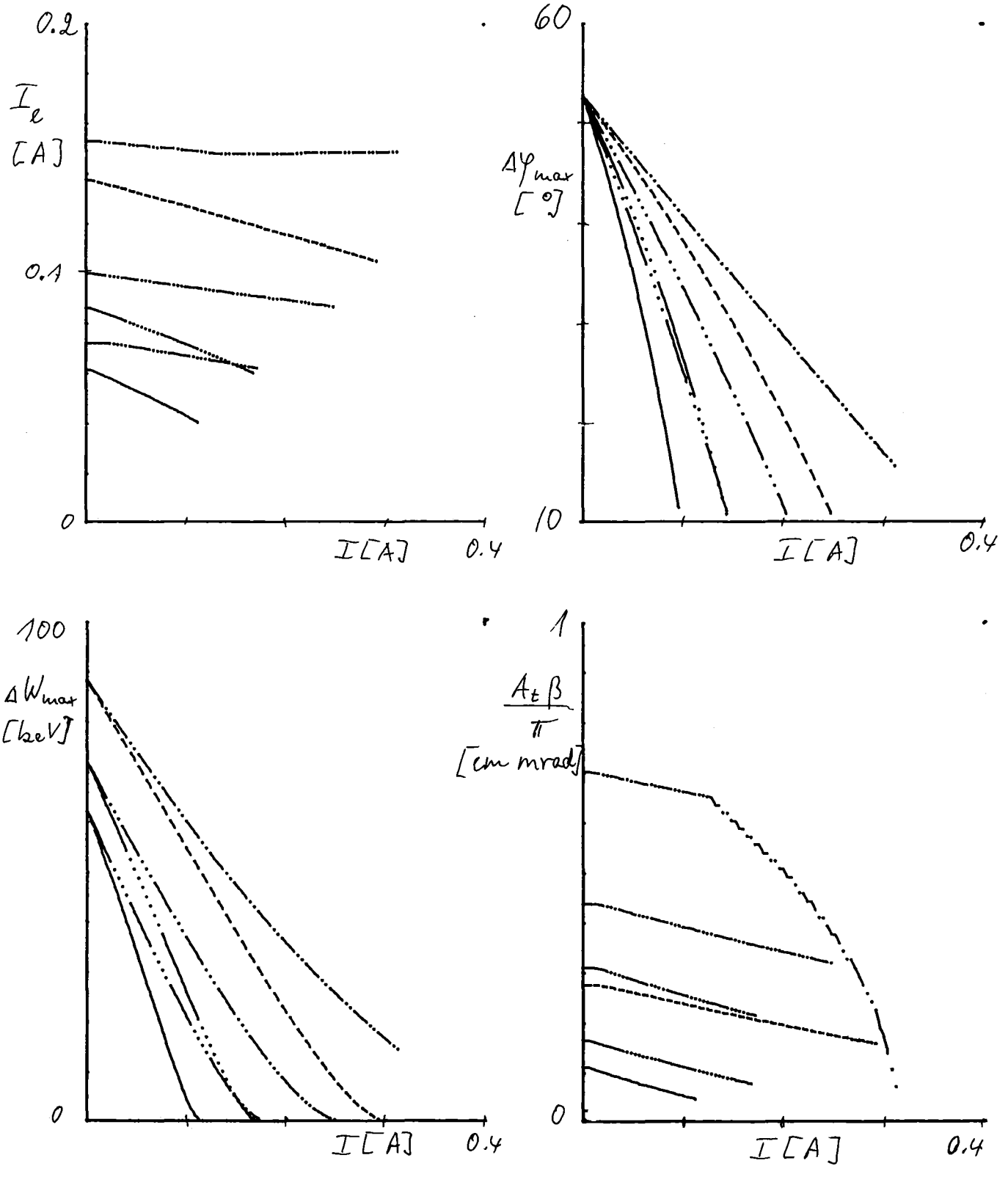

fig. 35

BETA = 0.0400 ; LAMBDA = 1.50 METER ; SIGMA = 0.75 ; MASS = 1

MUE(I=0) = 39 DEGREE ; PHI-S = -35 DEGREE ; PHI = -35 DEGREE

EPEAK = 14.3 MVOLT/METER

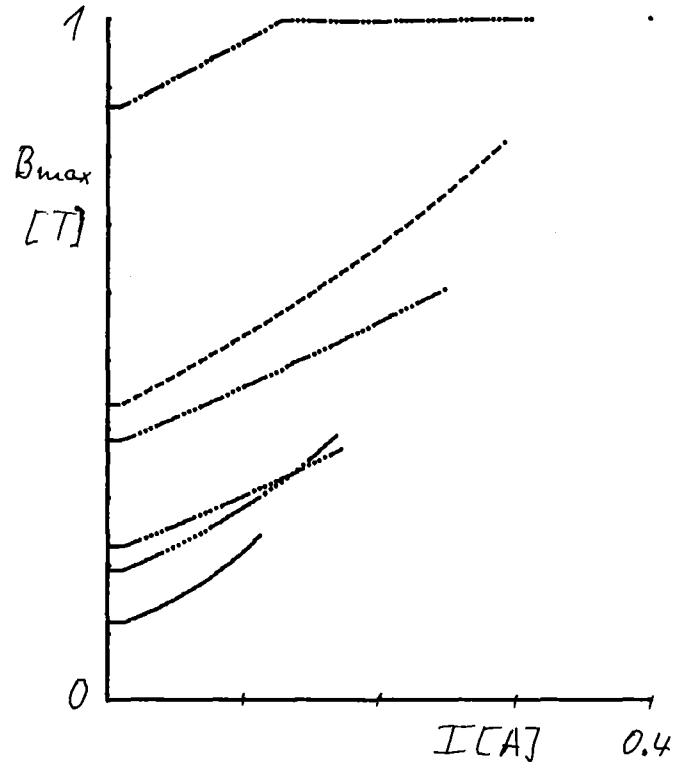

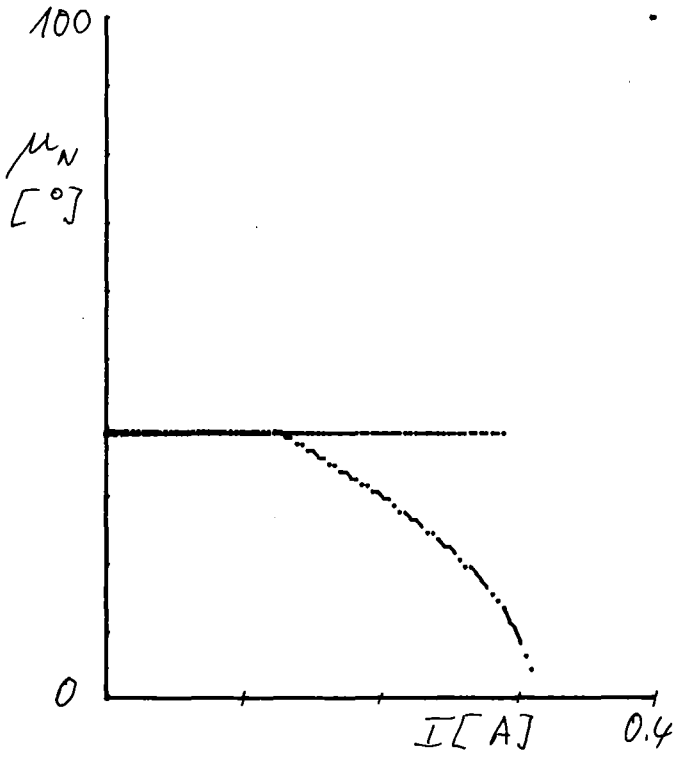

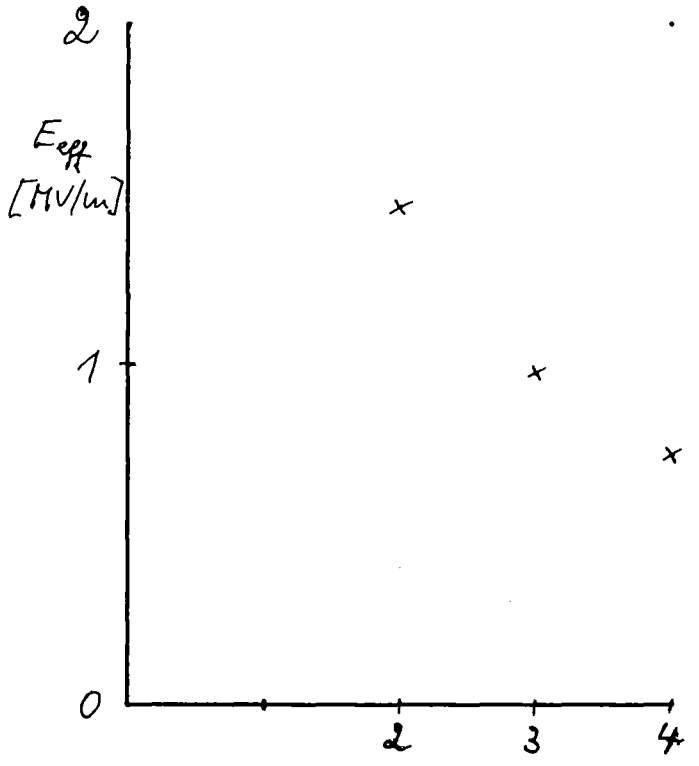

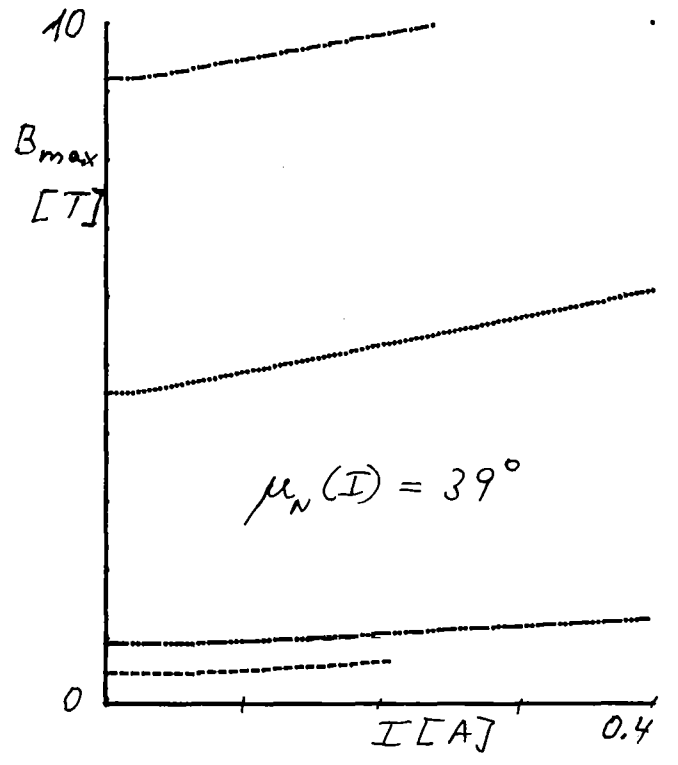

fig. 36

BETA = 0.0400 ; LAMBDA = 1.50 METER ; SIGMA = 0.75 ; MASS = 1

MUE(I=0) = 39 DEGREE ; PHI-S = -35 DEGREE ; PHI = -35 DEGREE

EPEAK = 14.3 MVOLT/METER

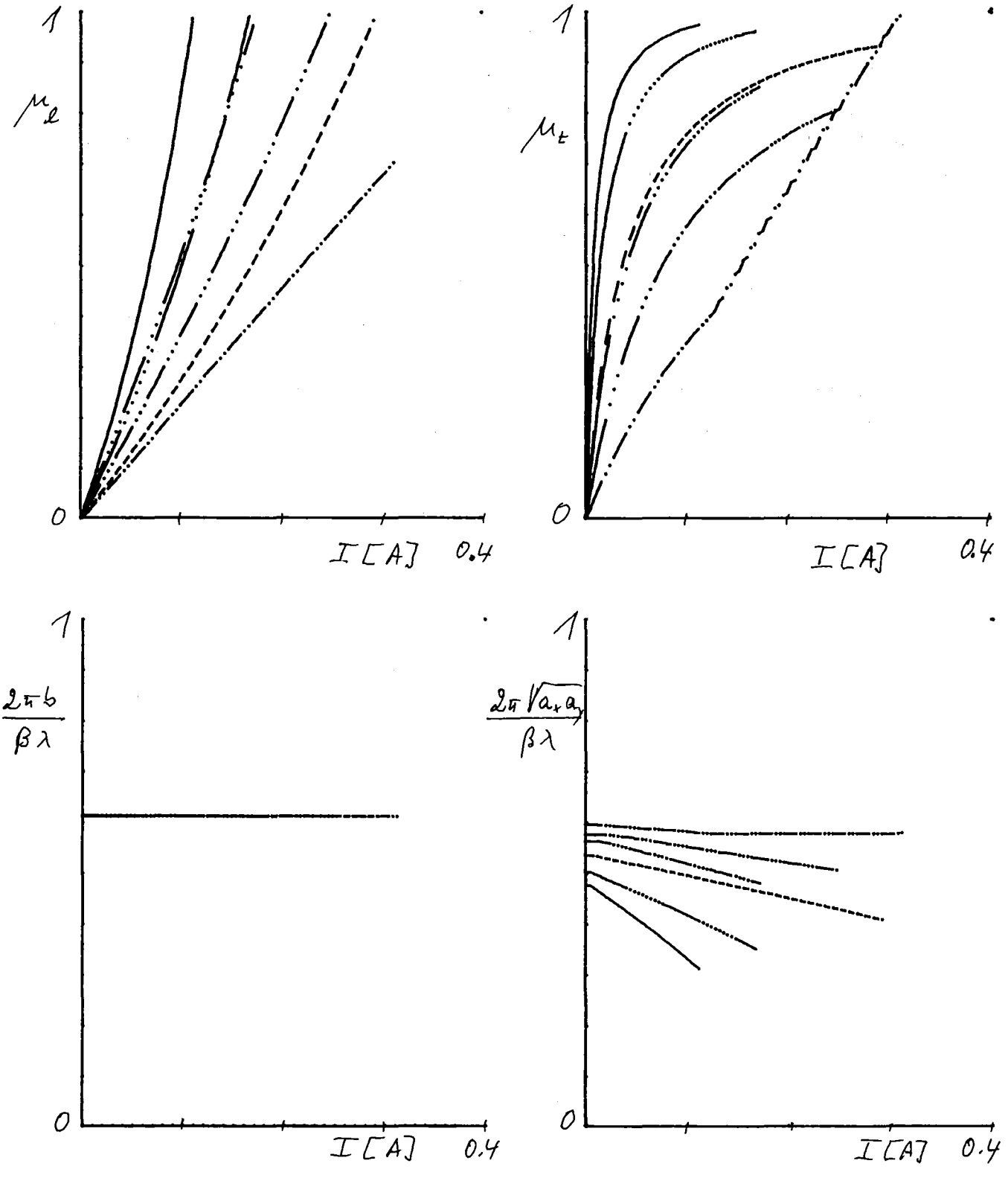

Appendix 1 Space charge form factors

In fig. 1 are shown the formfactors of a uniformly charged ellipsoid, calculated numerically according to formulas (44), (47) and (82). Formula (45) can be used to check the accuray in performing the integrals (44). The error is at most 2%.

The approximation of the transverse bunch cross section by a circular one effects M_z only sligthly. The approximation $a = \sqrt{a_x a_y}$ results in sligthly too large longitudinal space charge for $a_x/a_y > 1$. Taking on the other hand $2/a = 1/a_y + 1/a_y$ gives sligthly too small longitudinal space charge forces.

In the transverse direction the values of M_x and M_y differ appreciably from their average value, the more the larger a_x/a_y is. The transverse space charge forces are stronger than given by the approximation at a focussing plane, and weaker at a defocussing plane. In the accelerating gap the transverse bunch cross section will be about circular, and then the approximation is good.

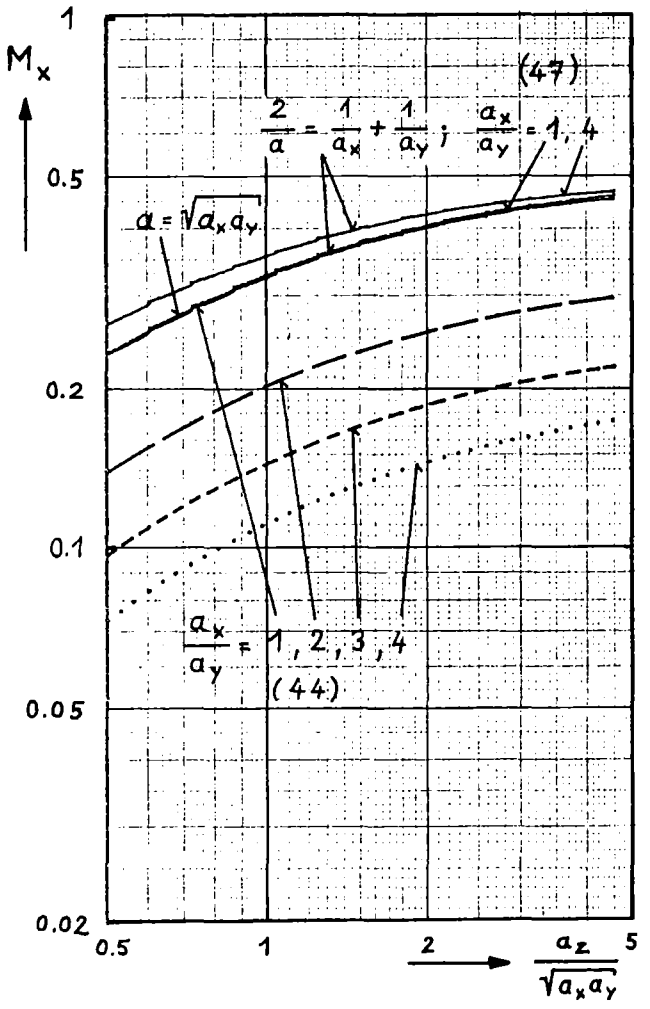

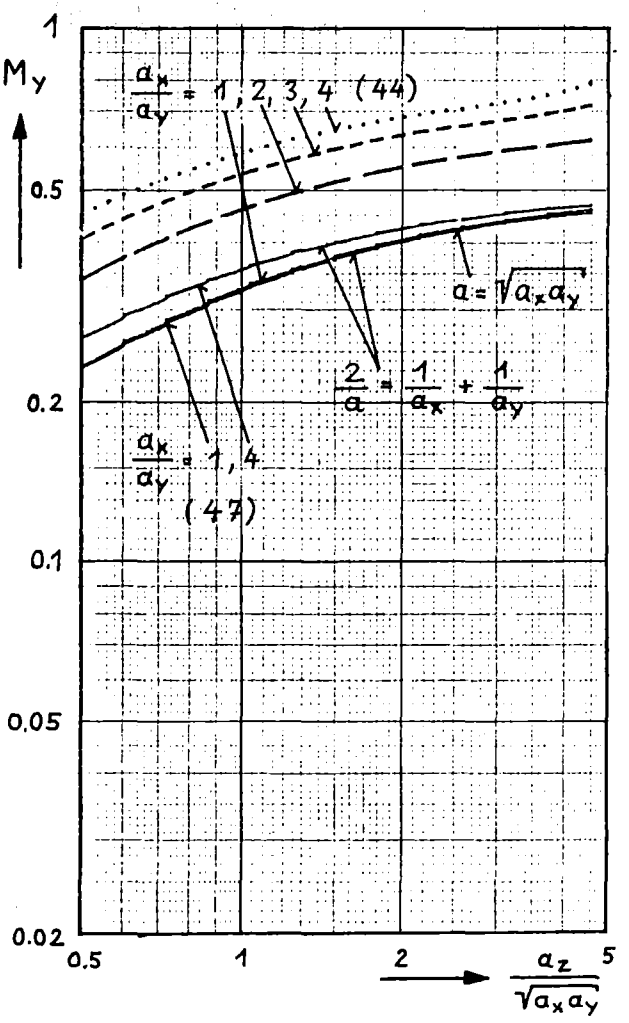

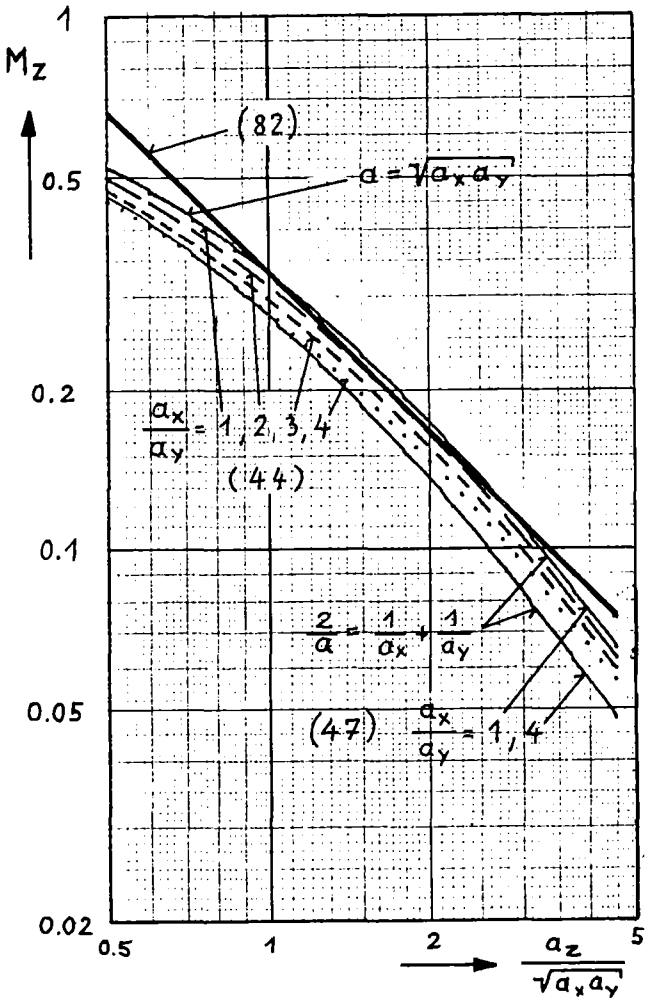

fig. 1

Form factors of a uniformely charged ellipsoid according to formulas (44), (47) and (82)

Appendix 2 Program "akzept"

```
0: "akzept":
1: flt 2
2: ent "massenza
 hl=1;2;3;...";
 M,"beta",B,"lam
 bda",r22
3: M*9.38256e8→r
 20
4: ent "sollphas
 e/grad <0",F,
 "teilchenphase/
 grad",H
5: ent "stay
 clear factor
 sigma",S,"mue
 der QP-Fokussie
 rung/grad",0
6: 1→r60;ent
 "Anzahl der
 Rechenwerte",
 r50
7: "plot1":
8: dsp "1→r57
 exe; falls plot
  Eeff(P)";stp
9: dsp "plot-
 variable in
 Nr.61 aendern";
 stp
10: dsp "plotter
  vorbereiten";
 stp
11: ent "Imax/
 A",r45,"Ymin",
 r46,"Ymax",r47,
 "dI",r48,"dY",
 r49
12: scl 0,r45,
 r46,r47
13: axe 0,r46,
 r48,r49
14: 1→r59
15: "plot2":
16: 0→U;0→r51
17: if r59=1;
 1→P;1→N;2→r52;
 gto +8
18: if r59=2;
 1→P;2→N;0→r52;
 gto +7
19: if r59=3;
 2→P;1→N;3→r52;
 gto +6
20: if r59=4;
 2→P;2→N;1→r52;
 gto +5
21: if r59=5;
 3→P;1→N;4→r52;
 gto +4
22: if r59=6;
 3→P;2→N;9→r52;
 gto +3
23: if r59=7;
 4→P;1→N;5→r52;
 gto +2
24: if r59=8;
 4→P;2→N;r50→r52
25: 1/r(1-B↑2)→r
 21
26: B*r22/(2*
 π)→D
27: S*D→A;D+.002
 →Q;B*r22/4.5→G;
 P*B*r22/2→L;(L-
 G-.012)/L→W;F*
 π/180→r40
28: π*G/B/r22→r4
 1;abs(r40)*D→r2
 4;9.23e6*(5.56/
 r22)↑(1/3)→r26
29: r26*r22↑2/
 G→r25;if r25>1.
 4e10;7.55e6→r26
 ;dsp "Kilpatric
 k 7.55e6→r26";
 stp
30: G*r26/1.3/
 L→E;sin(r41*
 180/π)/r41/1.26
 6→T;-π*E*T/r20/
 B↑3/r21↑3/r22→r
 1
31: E*T*cos(F)→r
 56;if r57=1;
 plt P,r56;pen;
 gto "plot3"
32: r1*sin(H)*
 L↑2→r27;r1*2*
 sin(F)→K;2.9979
 25e8→C;2*π*r24/
 B/r22→r54
33: 90*r22/r20/
 B↑2/r21↑3→r3
34: if N=1;2→r6;
 (.5-W/3)*W↑2→r7
 ;(2-W)*W/4→r8;
 .5→r9;.75→r11;
 gto "next1"
35: if N=2;8→r6;
 (4-4/3*W)*W↑2→r
 7;W→r8;2→r9;
 2.5→r11
36: if N=2;gto
 "next1"
37: dsp "N#1,2";
 stp
38: "next1":
39: r20/C*r21*B*
 Q/L↑2→r12;S↑2*
 r22/2/π↑2/P*
 B↑2→r13
40: B*E*T*r40↑2*
 sin(abs(F))/
 180/π→r14;1.5*
 abs(F)→r15
41: -2/3/π*r22*
 E*T*r20*(B*r21*
 r40)↑3→r16;L↑2→
 r17;A↑2→r18
42: -r27→V
```

Program "akzept" to estimate the acceptances, the accelerating gradient, and the quadrupole gradient of a high current linear accelerator, written for a HP9825A.

```
43: for I=0 to
 r45 by r45/r50
44: "mue":
45: U*π/180→r39;
 1-cos(U)→r4;
 cos(U/2)→r5;if
 U=0;pen;sto
 "plot3"
46: if N=1;2/
 sin(U)→r10;(2/
 r39)↑2→r19;sto
 +2
47: if N=2;4/
 sin(U)→r10;(4/
 r39)↑2→r19
48: Γ((r4-r6*V)/
 r7)→r42;(1+r8*
 r42-r9*V)/r5→X;
 r10*(1+r8*r42-
 r11*V)→R
49: r12*r42→r23;
 if r23>1;U-1→U;
 sto "mue"
50: A↑2/X→r30;
 Γr30→r53;2*π*
 r53/B/r22→r55
51: 1-r30/r24↑2→
 r2
52: if r2>0;Γr2→
 r2;(1-r2↑2)/
 r2↑3*(.5*ln((1+
 r2)/(1-r2))-
 r2)→r29;sto +3
53: if r2<0;Γ(-
 r2)→r2;(1+r2↑2)
 /r2↑3*(r2-π/
 180*atn(r2))→r2
 9;sto +2
54: 1/3→r29
55: .5*(1-r29)→r
 28
56: r3*I→r31;
 r31*r29/r30/
 r24/K→r32;r31*
 r28*r17/r30/
 r24→r33
57: r33/(r33+1/
 r19)→r34;r14*
 Γr30→r35;r15*
 (1-r32)→r36
58: if r36<0;
 pen;sto "plot3"
59: Γ(r16*(1-
 r32)↑3)→r37
60: r13/R→r38;-
 (r27+r33)→V
61: r35→r58
62: if r51<=r52;
 plt I,r58;sto +
 3
63: if r51<2*
 r52;plt I,r58;
 pen;sto +2
64: plt I,r58;
 pen;0→r51
65: r51+1→r51
66: next I
67: pen
68: "plot3":
69: r59+1→r59;
 if r59<9;sto
 "plot2"
70: r60+1→r60;
 if r60<5;sto
 "plot1"
71: dsp "Uebersc
 hrift-Plot vorb
 ereiten";stp
72: scl 0,18,0,
 26;csiz ;fxd 4;
 plt 0,25.5,1
73: lbl "beta =
 ",B;fxd 2
74: lbl " ;
 lambda = ",r22,
 " meter ;  siam
 a = ",S
75: fxd 0;lbl "
 ;  mass = ",M;
 plt 0,24.5,1
76: lbl "mue(I=0
 ) = ",O," degre
 e ;  ","phi-s
 = ",F," degree
 ;  "
77: lbl "phi =
 ",H," degree"
78: fxd 2;plt 0,
 23.5,1;lbl "epe
 ak = "
79: fxd 1;lbl
 r26/1e6," mvolt
 /meter"
80: sto "akzept"
81: end
*21317
```

List of variables used in "akzept

"akzept"	report
A	a
B	β
C	c
D	d
E	E_o
F	φ_s
G	g
H	φ
I	I
K	k_ℓ^2
L	L
M	m/m_p
N	N
U	$\mu_N(I)$
P	p
Q	d_q
R	γ_N
S	σ
T	T
O	$\mu_N(I=o)$
V	Δ

"akzept"	report
W	Λ
X	ψ_N
r1	(150)
r2	(47)
r3	(65)
r4 to r11, r19	(160)
r12	(161)
r13	(180)
r14	(84)
r15	(80)
r16	(77)
r17	L^2
r18	a^2
r20	mc^2/q
r21	γ
r22	λ
r23	B_{max}
r24	b
r25	(191)
r26	E_p
r27	Θ_r^2

"akzept"	report
r28	M_x
r29	M_z
r30	$a_x a_y$
r31	$\tilde{\mu}$
r32	μ_ℓ
r33	Θ_ς^2
r34	μ_t
r35	I_ℓ
r36	$\Delta\varphi_{max}$
r37	$\Delta W_{max}/q$
r38	$A_t\beta/\pi$
r39	$\mu_N\pi/180$
r40	$\varphi_s\pi/180$
r41	(36)
r42	Θ_0^2
r45 to r52, r57 to r60	used for plotting
r53	$\sqrt{a_x a_y}$
r54	$2\pi b/\beta\lambda$
r55	$2\pi\sqrt{a_x a_y}/\beta\lambda$
r56	E_{eff}

Appendix 3 Nomenclature

Number in parenthesis refer to the equation which defines the symbol

a average bunch radius (49)

a_x, a_y, a_z semi axis of ellipsoid (bunch) in the rest system (44)

b longitudinal semi axis of ellipsoid (bunch) in the laboratory system (44)

c velocity of light

d inner drift tube radius (fig. 1), (26)

f frequency of linac

g accelerating gap (fig. 1), 26)

k_l, $k_{t,rf}$ longitudinal and transverse rf force constants (63), (101)

$k_{t,q}$ force constant due to quadrupole focussing (102)

k_m, k_p radial wave number (20), (34), (40)

l period of transverse focussing (107), (fig. 2)

m particle rest mass

$\vec{p}$ particle momentum; p mode number (26)

q particle charge

r radius of polar coordinates; r_m transverse beam envelope radius (114)

s index referring to the synchronons particle

t time

$\vec{v}$ particle velocity

w index referring to properties of the travelling wave

x transverse cartesian coordinate

y transverse cartesian coordinate

z longitudinal cartesian coordinate, accelerator axis

A_l, A_t longitudinal and transverse acceptance (78), (113)

A_m of E_z for r = o amplitude of Fourier expansion (18), (35)

$\vec{B}$ magnetic flux density

B' quadrupole gradient

E beam emittance (115)

E_{kin} kinetic energy; $\vec{E}$ electric field strength; E_o amplitude of the electric field in the accelerating gap (26), (40);
E_p peak electric surface field (26), (194)
E_{eff} effective accelerating field (198)

F force

H Hamiltonian (85)

I beam current

I_o (x), I_1(x) modified Bessel functions

L length of accelerator cell (fig. 1, 2), (41)

L_q quadrupole length

M transfer matrix for one focussing period (132)

M_h, $M_{h'}$ transfer matrices for half a focussing period (132)

M_x, M_y, M_z form factors of charged ellipsoid (44)

N number of quadrupoles of the same polarity per focussing period (118)

T transit time factor (36), (41)

W relativistic particle energy

X transverse cartesian coordinate of bunch (43)

Y transverse cartesian coordinate of bunch (43)

Z longitudinal cartesian coordinate of bunch (43)

α related to the derivative of β_r (124)

β normalized particle velocity v/c

β_r betatron function (108)

β_{max}, β_{min} maximum and minimum of β_r (z) (112)

γ normalized relativistic particle mass

γ_N normalized betatron amplitude (158)

ϑ angle of polar coordinates

λ wavelength

μ betatron phase shift per period (111)

μ_l, μ_t longitudinal and transverse space charge parameters (64), (104)

$\tilde{\mu}$ space charge constant (65)

π 3.1415 ...

ρ charge density; as index indicating that space charge effects are included (71), (105)

σ drift tube clearance factor (166)

τ safety factor (80)

φ phase of particle relative to the electric field (42), (57)

ψ modulation ratio of beam cross section (146)

$\psi(z)$ phase shift of betatron oscillations (110)

$\omega = 2\pi f$

Δ thin lens defocussing parameter (152)

$\Delta\varphi, \Delta W$ deviations from values for synchronous particle (62)

Θ_o quadrupole focussing parameter (156)

Θ_r, Θ_ρ defocussing parameters for the rf field and for the space charge (150), (151)

Λ quadrupole filling factor (156)

References

1) J. D. Jackson, Classical Electrodynamics. J. Wiley, Inc., New York (1962)

2) H. G. Hereward, The General Theory of Linear Accelerators, in Linear Accelerators by P.N. Lapostolle and A. L. Septier, North-Holland Publ. Co., Amsterdam (1969)

3) L. Smith, Linear Accelerators, in Handbuch der Physik, Band XLIV, Springer Verlag, Berlin (1959)

4) A. D. Vlasov, Theory of Linear Accelerators (1968)

5) R. M. Bevensee, Electromagnetic Slow Wave Systems, J. Wiley, Inc., New York (1964)

6) H. Klein, Die Beschleunigung schwerer Ionen mit der Wendelstruktur, Habilitationsschrift, Universität Frankfurt am Main, Institut für Angewandte Physik (1968)

7) G. Dome, Review and Survey of Accelerating Structures, in **ref.2)**

8) H. C. Hoyt, D. D. Simmmons, W. F. Rich, Rev. Sci. Instr. 37, 755 (1966)

9) D. Warner, AECL-5677, 49 (1976)

10) K. Halbach, R. F. Holsinger, W. E. Jule, D. A. Swenson, ibid, 122

11) M. Martini, D. J. Warner, CERN Report No 68-11 (1968)

12) D. Boehne, IEEE Trans. Nucl. Sci., NS-16, No. 3, 380 (1969)

13) R. L. Gluckstern, Space Charge Effects, in **ref.2)**

14) D. J. Warner, M. Weiss, Proc. of the 1976 Prot. Lin. Acc. Conf., Chalk River, Ontario, AECL-5677, 245 (1976)

15) K. Batchelor, ibid, 160

16) J. Staples et al., ibid, 148

17) P. Tanguy, Proc., of the 1970 Prot. Lin. Acc. Conf., Batavia, Illinois, 771 (1970)

18) B. Bru, M. Weiss , ibid, 851

19) I. M. Kapchinskij, V. V. Vladimirskij, Proc. of the Conf. on High Energy Accelerators and Instrumentation, CERN, Geneva, 274 (1959)

20) S. Ohnuma, J. N. Vitale, IEEE Trans. Nucl. Sci., NS 14, No. 3 594 (1967)

21) O. D. Kellog, Foundations of Potential Theory, Dover, New York (1953)

22) E. Regenstreif, in Focussing of Charged Particles by A. Septier, Academic Press, New York and London (1967)

23) D. A. Swenson, AECL-5677, 234 (1976)

24) H. Deitinghoff, P. Junior, H. Klein, ibid, 238

25) E. D. Courant, H. S. Snyder, Ann. Phys. 3, 1 (1958)

26) M. Promé, Focussing, in: ref. 2

27) L. Smith, R. L. Gluckstern, Rev. Sci. Inst. 26, 220 (1955)

28) R. Friemelt, Unilac report No. 5-67, GSI, Darmstadt (1967)

29) W. D. Kilpatrick, Rev. Sci. Inst. 28, 824 (1957)

30) D. Böhne, W. Karger, E. Miersch, W. Röske, B. Stadler IEEE Trans. Nucl. Sci., NS 18, No. 3, 569 (1971)

31) D. Warner, private communication

32) J. E. Vetter, editor, KFK 2542, Kernforschungszentrum Karlsruhe, (1977)

33) K. Kaspar, AECL - 5677, (1976)

34) K. G. Steffen, High Energy Beam Optics, Interscience Publishers, New York (1965)

Acknowledgement

The many valuable discussions with C. Passow and J. E. Vetter are appreciated.